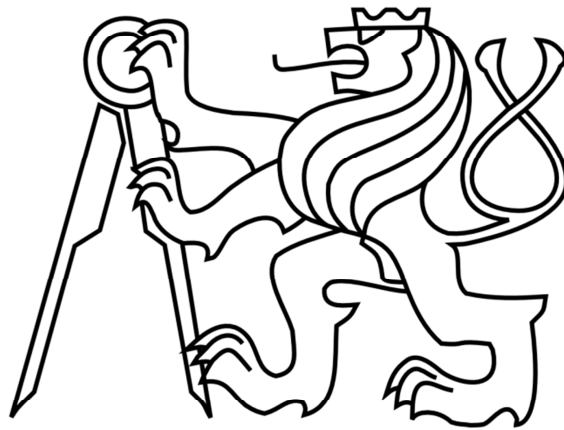


ČESKÉ VYSOKÉ UČENÍ TECHNICKÉ V PRAZE
FAKULTA STAVEBNÍ

Katedra konstrukcí pozemních staveb
Obor Budovy a prostředí



MASTER THESIS

Living Tree Structures
Analýza živé přírodní konstrukce

Supervisor from ČVUT:	Ing. Jan Růžička, Ph.D.
Supervisors from TU Delft:	Drs. W.F. Gard Prof. dr.ir. J.W.G. van de Kuilen
Student:	Helena Borská



ZADÁNÍ DIPLOMOVÉ PRÁCE

I. OSOBNÍ A STUDIJNÍ ÚDAJE

Příjmení: Borská Jméno: Helena Osobní číslo: 395717

Zadávací katedra: Katedra pozemních staveb

Studijní program: Budovy a prostředí

Studijní obor: Budovy a prostředí

II. ÚDAJE K DIPLOMOVÉ PRÁCI

Název diplomové práce: Analýza živé přírodní konstrukce

Název diplomové práce anglicky: Living Tree Pavilion

Pokyny pro vypracování:

Hlavním cílem diplomové práce je výzkum přírodní konstrukce tvořené živými stromy a stanovení její nosné kapacity. Tato kapacita bude vypočítána na základě zmapování konstrukce a měření provedených studentkou.

Seznam doporučené literatury:


Design in the Nature, Learning from the Trees - Claus Mattheck

Jméno vedoucího diplomové práce: Ing. Jan Růžička, Ph.D.

Datum zadání diplomové práce: 18.8.2017

Termín odevzdání diplomové práce: 7.1.2018

Údaj uveďte v souladu s datem v časovém plánu příslušného ak. roku


Podpis vedoucího práce


Podpis vedoucího katedry

III. PŘEVZETÍ ZADÁNÍ

Beru na vědomí, že jsem povinen vypracovat diplomovou práci samostatně, bez cizí pomoci, s výjimkou poskytnutých konzultací. Seznam použité literatury, jiných pramenů a jmen konzultantů je nutné uvést v diplomové práci a při citování postupovat v souladu s metodickou příručkou ČVUT „Jak psát vysokoškolské závěrečné práce“ a metodickým pokynem ČVUT „O dodržování etických principů při přípravě vysokoškolských závěrečných prací“.

H. B. 2017

Datum převzetí zadání


Podpis studenta(ky)

AFFIDAVIT

I hereby declare that this master thesis has been written only by the undersigned and without any assistance from third parties. Furthermore, I confirm that no sources have been used in the preparation of the thesis than those indicated in the thesis itself.

Prague, 18.2.2018

A solid black rectangular box redacting the signature of the author.

.....
Helena Borská

ACKNOWLEDGEMENTS

I would like to thank my thesis supervisors from TU Delft, Drs. W.F. Gard and Prof. dr.ir. J.W.G. van de Kuilen, for guiding and supporting me over past few months. Their door was always open for me and I really appreciate their professional advice but also their personal approach and support in hard times.

I would like to also thank Ruben Kunz and Jan Moraal for help with creation and transport of the setup for the pulling test and employees of Botanical Garden of TU Delft for their help when necessary.

Finally, I must express my very profound gratitude to my parents for providing me with unfailing support and continuous encouragement throughout my years of study and through the process of researching and writing this thesis. This accomplishment would not have been possible without them.

Last but not least, I would like to thank all my friends for their infinite support and namely to Noemi Barone who was helping me with the measuring but mainly, who was my immense support over past few months.

ABSTRACT

This master thesis is dedicated to the living tree structures, therefore load-bearing structures which are formed by living trees. The thesis is basically divided into two parts. First part is dedicated to general description of the main principle of these structures, including biomechanics of trees with emphasis on their self-optimization ability. Also comparison to other tree structures can be found within this part.

Second part of the thesis is focused on analysis of Living Tree Pavilion, structure located in the Botanical Garden of TU Delft. Description of investigation of the structure which was performed is stated in this part, specifically measuring of the geometry, performing the pulling test and others. Whereas the main goal of this structure is to use trees as a load-bearing system for the platform, calculation of the current load-bearing capacity of the structure is performed, and thereafter also estimation of time when the load-bearing capacity is sufficient.

KEY WORDS

Tree, load-bearing capacity, self-optimization, living structure, connection, pulling test, growth, failure, inspiration, axial weld, cross weld, support.

ABSTRAKT

Tato diplomová práce se zabývá živými stromovými konstrukcemi, respektive nosnými konstrukcemi tvořenými živými stromy. Práce je rozdělena na dvě části. První část je věnována obecnému popisu hlavního principu těchto konstrukcí, včetně biomechaniky stromů s důrazem na jejich schopnost samooptimalizace. Také porovnání s dalšími typy stromových konstrukcí se nachází v této části.

Druhá část práce je zaměřena na analýzu Živého stromového pavilonu, konstrukce umístěné v botanické zahradě TU Delft. Popis provedeného průzkumu konstrukce je uveden v této části, konkrétně se jedná o měření geometrie, provedení tahové zkoušky a další. Vzhledem k tomu, že hlavním cílem této konstrukce je použití stromů jako nosného systému pro plošinu tvořící rozhlednu, je proveden výpočet současné nosné kapacity konstrukce a následně i odhad doby, kdy je nosná kapacita pro podepření platformy dostatečná.

KLÍČOVÁ SLOVA

Strom, nosná kapacita, samooptimalizace, živá konstrukce, spoj, tahová zkouška, růst, porucha, inspirace, osový spoj, křížový spoj, podpora.

LIST OF CONTENTS

1.	Introduction	8
2.	Biomechanics of trees	10
2.1.	Tree growth	10
2.2.	Response to loads	12
2.3.	Failure possibilities	17
2.3.1.	Tree damage by abiotic sources	17
2.3.2.	Tree damage by biotic sources	21
2.4.	Tree behaviour as an inspiration for mechanical design	23
3.	Connection of trees	24
3.1.	Axial welds	25
3.2.	Cross welds	25
3.3.	Grafts	26
4.	Living and non-living tree structures	28
4.1.	Non-living tree structures	28
4.2.	Living tree structures	29
4.3.	Difference between living and non-living structures	32
5.	Living Tree Pavilion	33
5.1.	General description of the structure	33
5.1.1.	Description of the non-living structure	34
5.1.2.	Description of the original living structure	36
5.2.	Mapping of the existing tree structure	37
5.2.1.	Description of the supports	39
5.2.2.	Description of the natural joints	46
5.2.3.	Pulling test	55

6.	Calculation of the load-bearing capacity of the Pavilion	71
6.1.	Description of the previous calculations	71
6.2.	Calculation of permanent and variable loads	72
6.3.	Combinations of actions	77
6.4.	Calculation of the current load-bearing capacity	79
6.5.	Estimation of time when the load-bearing capacity is sufficient	88
8.	Conclusion	91
9.	References	93
10.	Appendixes	
	Appendix A Preliminary calculations for the pulling test	
	Appendix B Results of the pulling test	
	Appendix C Calculation of permanent and variable loads	
	Appendix D Calculation of the current load-bearing capacity	
	Appendix E Calculation of the load-bearing capacity over time	

1. INTRODUCTION

The most important feature of each structure and goal of each civil engineer is the efficiency. That means a structure which uses the material effectively, therefore all material is used where it should be used and no extra material is included. However, good structural design can fulfil this requirement and an efficient structure can be built based on the designed loads. But what common structure cannot do, is to change its efficiently designed shape when this load changes.

There is no other material, respectively structure, used in the structural engineering world which can be built so efficiently as a tree. While a structure, built from common building material, collapses in the moment when the value of internal stresses is higher than the strength limit, a tree has an option to prevent this moment by its response to the increasing stresses. Trees have the unique ability of an active reaction to loads and adaptation to them. This mechanical self-optimization of trees guarantees a high stability at minimum material, an optimal material usage and prevention of early failure by avoiding of weak spots.

Moreover, this feature of trees, the effort to ensure the equal load distribution all over their structures, can result into creation of the connections with other elements or other trees. This behaviour can cause formation of a complex framework structure consisting from many trees. When this manner is applied in the field of civil engineering, the living tree structure is created. This structure uses all advantage of tree features and thus has nearly flawless mechanical properties.

Trees belong to the oldest and the most massive organisms in the world. They have been always used as a refuge, protection against sun, wind and frost. The fact that trees have been always part of our life is proved by countless number of myths, legends and religions where trees play major role. A tree has been always associated with wisdom. To this day, a tree is still used as its symbol and there is still a lot to learn from it.

There are several points of view how trees can inspire us in the field of the structural engineering. It is not only the technical site where we look at a tree as at structural, load-bearing, element but also aesthetic, ecological and economical aspect.

Structural aspect

A tree can be easily compared to structure of a building. The root system works as foundations, it must also ensure stability of whole construction. Main load-bearing element is presented by a trunk which is the only element at the beginning but with aging is completed by branches. Tree crown can be compared to a roof of a building for its protection function. It protects the rest of the structure from sunshine, wind, snow and other external conditions.

Although, the trees can be compared to the construction of the building, there is one

big difference. Trees from the beginning of their life adapt to the surrounding environment, both underground and aboveground. Their trunks create every year new annual ring which shape depends on the load that trees had to resist the previous year. Generally said, trees have the ability of reaction to the load, they create new material where necessary. Professor Clause Mattheck, who invented CAO method that serves as a graphic model for shape optimization according to trees, summarised his research as follows: "Throughout many millions of years of evolution, trees have learned to adapt their shape to resist external influences such as wind or snow pressure. Each tree grows in such a way as to achieve a uniform distribution of mechanical stress on its surface. Through the strategic growth of wood, the tree is able to minimize this stress at the point of the greatest mechanical strain (for example cracks) without wasting the material." [1]

This self-optimization is the main reason why the living trees should be used for the civil structures.

Ecological aspect

Recently, there is an unsustainable growth in construction of the cities where nature is often missed. Trees have a beneficial influence on human health. Not only because of photosynthesis which is necessary for life on the planet but also because trees serve as a natural air filter and they even create balance in CO₂ level. Generally said, trees can offer beneficial environment that is in structural engineering industry lacking. Comparing a tree to a building, tree acquires the energy necessary for its life and growth by itself, building is dependent on the energy of man.

Nowadays sustainable development becomes more and more important in the field of civil engineering. Emphasis is put on energy savings, recyclability of the construction after its lifetime, also on use of materials and their effect on the environment. This approach can motivate us to explore the possibilities the living tree structures offer.

This master thesis is devoted to the living tree structures which are still rare and unexplored topic in the world, but topic that can bring really new light into the field of the structural engineering. The main goal of the project is to analyse Living Tree Pavilion, the structure located in the Botanical Garden of TU Delft.

Main research questions are following:

- *Estimation of the time when the load-bearing capacity is sufficient to be able to take over the load of the structure, therefore estimation of the current state*

The sub questions are following:

- *How the connections effect the structure?*
- *How to evaluate, respectively measure, the structure and its properties?*
- *How does a tree react to loads?*

2. BIOMECHANICS OF TREES

In order to use trees as a load bearing structure, it is necessary to understand well their biomechanical principals. All the important properties mentioned bellow, are described in the following chapter.

- tree growth
- response to loads
- failure possibilities

Last part of the chapter is devoted to application of tree behaviour in the structural design.

2.1. TREE GROWTH

Whereas trees appear in the changing environment, they are constantly influenced by many factors. Therefore there are several tree growth regulators which determine the shape of a tree. Phototropism, negative geotropism and apical dominance can be considered as the main 3 factors effecting the tree growth (*Figure 1*). [1]

Geotropism or more accurately negative geotropism is generally said the ability of a tree to grow up against gravity. Many branches on trees tend to grow away from the trunk. They receive the command to grow more steeply from the leading shoot which is the main stem or branch of a tree. Stronger growth can be found on the upper part of the branch and that is also the reason why branches bend downwards. This mechanism is called apical dominance. In case the leading shoot for some reason falls sick or even breaks off, the strongest from the other branches takes over the leading position. That in reality means that in the moment of the failure of the old leader, the other branches start to grow fast towards the sky to become the new leader of the tree. They accomplish sometimes incredible feats of bending themselves in order to become a leading shoot itself. They are even able to totally change the direction of their growth as you can see in *Figure 3*. This ability is based on forming the reaction wood. This reaction wood is created on the upper side of the branch in broad-leaved trees and on the lower side in conifers (*Figure 2*). That means that it works in tension for the broad-leaved trees and compression for conifers. [1]

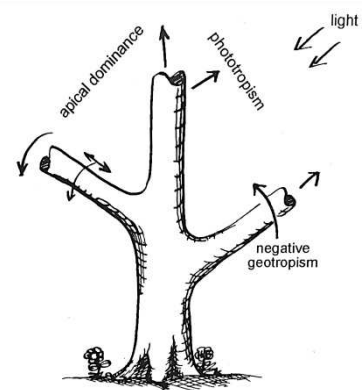


Figure 1. Growth regulators and their effect on tree shape [1].

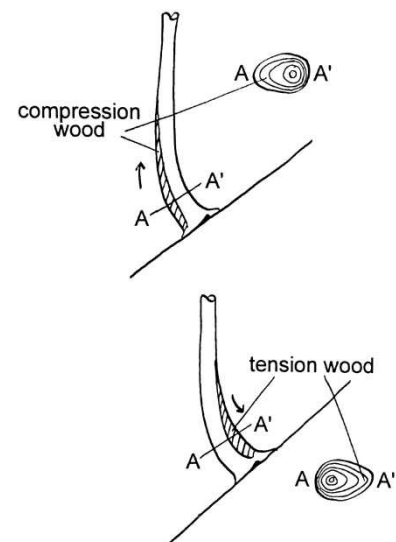


Figure 2. Schema explaining the difference between tension and compression reaction wood [1].

And finally the phototropism, the quest for the light, has the dominant role over the two previous regulators because the optimal shape is worthless without light. Generally said, phototropism is the tendency of trees to grow towards the light. As you can see in *Figure 4*, trees try to catch as much light as possible with outstretched branches or stem even though they create mechanically more complex structure. Whereas trees cannot live without light, they have to trap this extra bending by creating new, secondary wood to limit the stresses. [1]

To sum up the mechanism of tree growth, the simplified description of the regulators is:

- negative geotropism allows trees to grow vertically by forming reaction wood
- apical dominance is the dominance of the main stem or branch which suppresses the others from growing up too steeply
- phototropism is the tendency of trees to grow toward the light

All the mentioned regulators are for better picture also shown in *Figure 5*. These three mechanisms can act in unison but also against each other. This natural competition is their advantage because each single one acting just for itself could become a big handicap for the tree (also *Figure 5*). Together, they react to environmental influences such as for example temperature, soil moisture and chemistry and adapt the tree to new circumstances. [1]

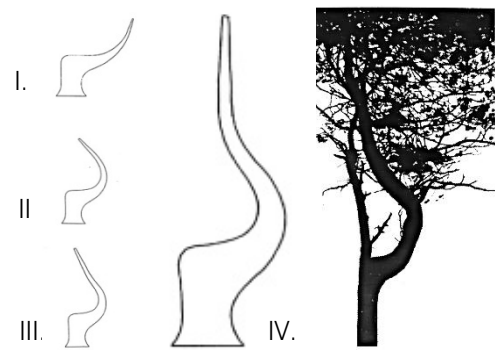


Figure 3. Schemas and picture showing a side branch taking over leadership [1].

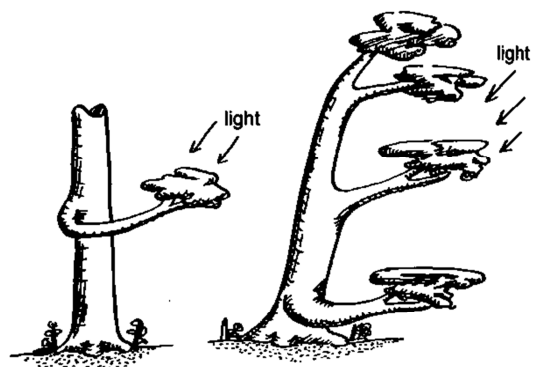


Figure 4. Example of phototropic growth and thus caused bending [1].

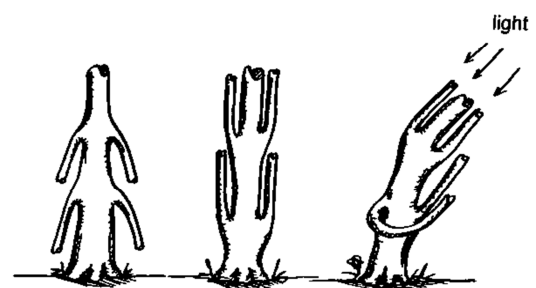


Figure 5. Growth regulators acting alone (from left): apical dominance, geotropism, phototropism [1].

2.2. RESPONSE TO LOADS

First of all, it should be mentioned that wood is an anisotropic material which means that the material has different characteristics in the longitudinal and radial or tangential direction (Figure 6). It is caused by the sophisticated growth of trees and the way they create wooden fibres.

There are many types of external loads that a tree can be exposed to. Simple division can be due to caused stresses, thus compressive, tensile and shear stresses caused by forces, bending moments, torsional moments, and also thermal stresses. These mechanical effects are recalled in relation to the trees in the following paragraph.

The basic axial force such as own weight is the simplest example of normal force. It causes pure compression (Figure 6) and this compressive stress is determined by formula:

$$\sigma = F / A$$

σ ...stress

F ... force

A ... area

This is also the reason why shape of trees is mostly conical. The top of tree trunk does not carry as much weight as bottom, therefore, according to above mentioned formula, the cross-sectional area can be smaller on the top and grow downwards under about constant tension (Figure 8). This shows the ability of trees to actively react to external loads and reduce the caused internal stresses, mainly by increasing the area of a tree trunk by secondary growth.

Another type of external strain is an eccentric loading which causes the bending moment (Figure 9). In that case following formula can be applied:

$$\sigma = M * r / I$$

M ... bending moment

r ... distance from the axis

I ... moment of inertia

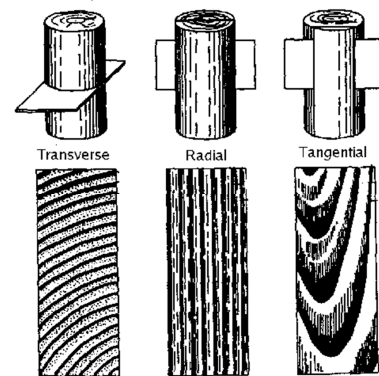


Figure 6. Different directions and their cross-sections [2].

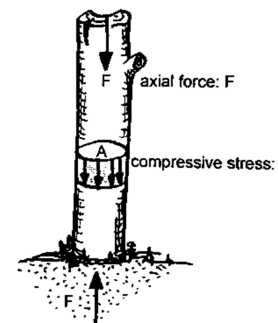


Figure 7. Normal compressive stress in a tree trunk [1].

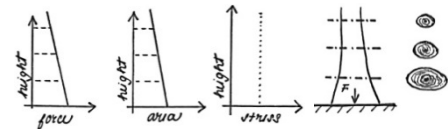


Figure 8. Shape of a tree trunk adapted to forces.

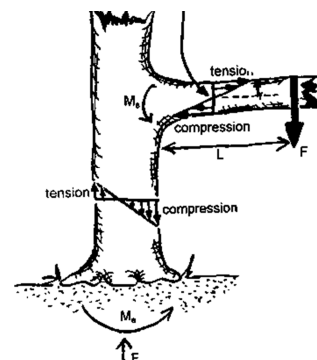


Figure 9. Bending moment in a tree trunk [1].

Except for an extra eccentric loading, the bending can be caused by an irregular shape of a tree but also by wind load which is actually one of the most important load cases of a tree due to big tensile stresses caused especially above the ground. In reality, a tree is exposed to all the types of loads at the same time (*Figure 10*), also to torsion which can be caused by an irregular shape of a tree as well. This leads to a twisting of a trunk or branches and thus to the shear stresses inside the cross-section. Last but not least, the thermal forces have also their effect on trees, like on other materials. The difference between commonly used materials and wood within a tree structure is a reaction to loads.

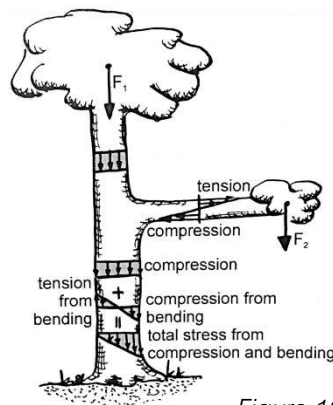


Figure 10. Combination of load cases [1].

Trees have the unique ability of an active reaction to loads and adaptation to them. As with other materials, when the value of internal stresses is higher than the strength limit, than the material collapses. There are always many options how to prevent the material from the failure but two main principles are to improve the strength of the material or to reduce the internal stresses. Whereas the stresses in commonly used non-living materials cannot be reduced just by themselves, a tree has this self-optimization ability. It adapts its outer shape, internal structure and thus the mechanical behaviour.

Trees create an almost uniform stresses over their entire volume for the most common load situations. They create an extra wood in places with higher undesirable stresses. This self-repairing technique is very efficient because the material is used effectively, in the places where it is necessary and without creating a superfluous material. This mechanical self-optimization of trees guarantees a high stability at minimum material, an optimal material usage and prevention of early failure by avoiding of weak spots. [1]

There are basically five principals how trees reduce the stresses:

- minimisation of lever arms
- axiom of uniform stress
- adaptation of the strength
- minimization of critical shear stresses
- growth stresses

These above mentioned principals are briefly described in the following part of this chapter.

Minimisation of lever arms

Trees minimise stresses by reducing the length of the loaded lever arm. The length can be reduced by active self-bending in the stiff parts thanks to creation of above mentioned reaction wood. More flexible parts are simply passively bended. [1]

Axiom of uniform stresses

Axiom of uniform stresses says that trees are characterized by a homogeneous stress distribution on the tree surface. They grow in a way that local high stresses, potential points of rupture, as well as locally small stresses are avoided. This theory was demonstrated by Metzger and later verified by Mattheck on several examples which are mentioned further. To keep a homogeneous state of stress on a tree surface, the outer annual ring always tries to adapt the external loading by locally increasing or reducing growth (Figure 11). [1]

One of the above mentioned examples verifying this universal design rule for biological structures is creation of wind braces. They grow towards the ground to transfer the wind forces to the ground and thus to minimize strain of a tree. Mattheck describes an experiment in which a wind-exposed site of a tree has been rigidly supported by a tripod of thick sticks (Figure 12 up). This support basically forms man-made wind braces. The reaction of a tree after six years is shown down in Figure 12 (down). A tree evaluated that it is not necessary to put on much wood in the supported part because the stresses from bending were minimized thanks to the tripod. As a result, the annual rings in this part were thinner than the ones above the point of attachment where the tree was exposed to the wind load just on its own (Figure 12 down). [1]

Another nice example of this efficient use of material is a shape of junction of branches on a tree trunk. A tree efficiently adjusts a shape of junction according to an importance of a branch. The strong branches on the top which are exposed the most to the wind load have a strong junction which allows smooth force flow towards the roots. The braces below, around middle of the height, are not as strained as the ones above so these junctions are not as

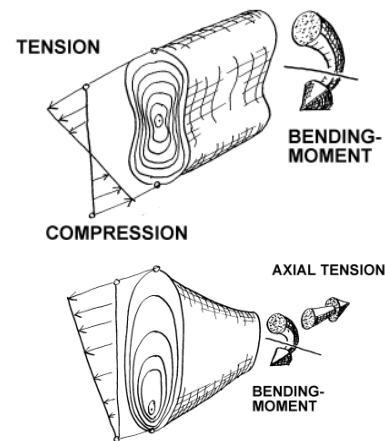


Figure 11. Examples of creation of annual rings according to type of loading [3].

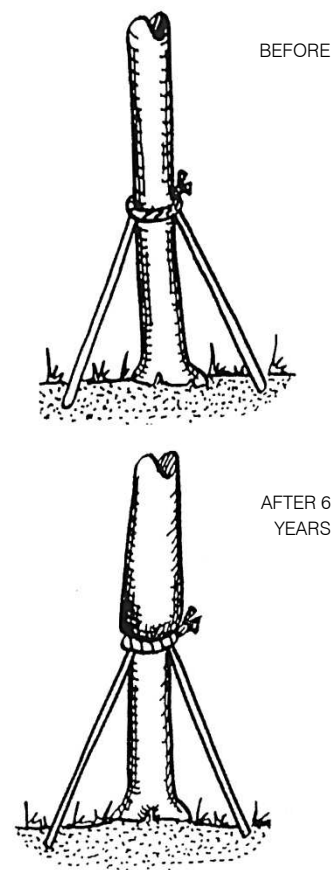


Figure 12. An example of tree reaction to stresses [1].

strong. Also other wood fibres are formed around a junction to transfer load from the top without straining these junctions. Lastly the lower branches are not really loaded and they are basically just ballast for a tree so a tree does not have any need to create a new material in a junction to preserve them. Whole principal is for better picture shown in *Figure 13*. [1]

These experiments are an outstanding example of biological shape optimization of material of which one could wish for in the field of civil engineering.

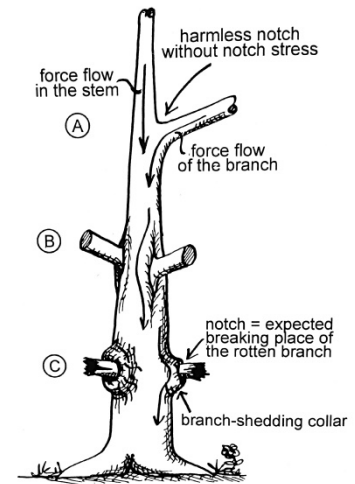


Figure 13. Force flow in a tree [1].

Adaptation of the strength

Also wood quality depends on type of loading. There were made measurements proving that wood on the bottom sides of branches reacts to permanent pressure by developing high compressive strength profile [3]. This mechanism is also associated with creation of annual rings. When the branch is compressed on the bottom side, an annual increment is maximal on the top of the branch to create an oval shape which is more preferable for that kind of strain. As a result of that, the top of a branch has lower compressive strength and the bottom side has it clearly higher (*Figure 14*). [1]

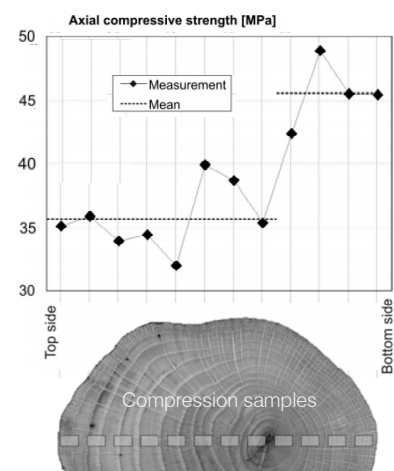


Figure 14. Compressive strength profile of a branch [1].

Minimization of critical shear stresses

As already mentioned above, wood is an anisotropic material which is formed by fibres. A tree tries to form this fibrous pattern along the force flow and thereby the stiffest material direction is located along the direction of the maximum stresses. Therefore the modulus of elasticity of wood is different in longitudinal and transverse direction, specifically much higher in the direction of fibre growth and lower in the perpendicular direction. Layout of fibres also influences shear stresses in the structure. Depending on a shape of fibre growth, shear stresses can be either minimised or got a higher value. Fibre growth around decay of wood can be used as an example. Generally said, spindle shaped fibres around a decay minimises shear stress unlike uniaxial fibre arrangements. [1]

Growth stresses

There are axial stresses inside the structure of a tree which are caused by growth [4, 5]. The distribution of these stresses is shown in *Figure 15*, the area of a cross-section is basically longitudinally pre-stressed by tension while its outer part is compressed. As a result of that, a tree can resist higher bending moment (*Figure 16*) because the compressed side

of a tree has a support which is given by the axial growth. The principle of this kind of support is minimization of the hazardous compressive stresses on the compressed side by the longitudinally tensile pre-stressing. On the other hand, this principle also works on the other side of a branch where this pre-stressing contrariwise increases the tensile stresses which are however less critical. Also the tensile strength is from two to four times higher than the compressive. [1]

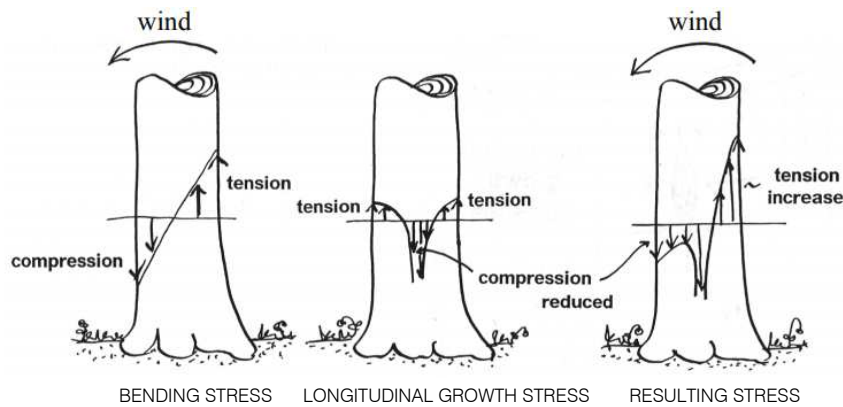


Figure 16. The assistance of growth stresses in bending [6].

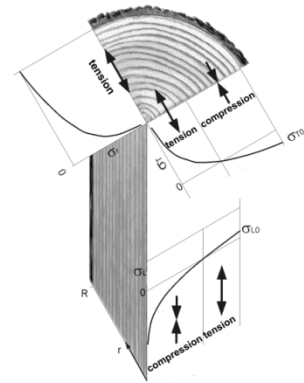


Figure 15. Distribution of the growth stresses [1].

Besides the mechanical character of tree response to loads, the reaction, mainly the production of new wood, depends also on physiological and morphological conditions. It is dependent on species, health, energy reserves and available resources such as water, light, nutrients and others.

To highlight what leads us to an idea of usage of trees in the field of civil engineering, brief summary of tree response to loads follows. What should be emphasized from tree mechanics is the shape optimization. New wood is produced in response to damage or change of loading. This so-called reaction wood reduces higher strain in marginal fibres in order to ensure constant stresses within a tree.

2.3. FAILURE POSSIBILITIES

As other structural elements or materials, also a tree has a risk of failure. However, it is in principle possible to make a tree safe against failure due to its self-optimization mentioned above. In this case, a tree would grow thicker in order to withstand heavy loads but then it would probably stay in the shade and die because of lack of nutrition because its growth upwards would be reduced. A tree grows towards the light, source of energy, and at the same time maintains its structure to keep it safe. In comparison to the first case, this tree would be thinner and thus a possibility of rupture exists here. But this balance between gaining energy and keeping a tree safe is the key of efficiency. [1]

This chapter is devoted to the possibilities of failure and divided into following parts:

- tree damage by abiotic sources
- tree damage by biotic sources

2.3.1. TREE DAMAGE BY ABIOTIC SOURCES

A failure is primarily defined by the load situation, the geometry and characteristics of a tree. As already mentioned in the previous chapter, there are different types of strain of a tree but the most striking loading is bending moment which causes considerable tensile and compressive stresses inside a tree. The critical stress under which a tree collapses is almost always compressive stress because as already described, wood can withstand much higher tensile loading than compressive. The resulting failure of a structure is in this case caused by buckling of fibres on the compressed side (*Figure 17*). In case that collapse of a tree or its part is caused by tension, then it is because of fibre tear.

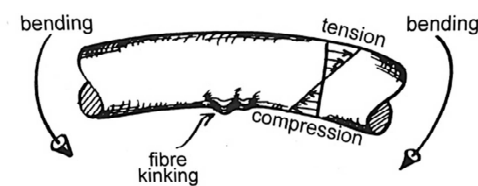


Figure 17. Example of a trunk failure in bending showing a fibre kinking on the compressed side [1].

The calculation of the critical stress can be provided on the simplified shape of a trunk, solid wooden cylinder having a round or oval cross-section. This calculation is based on the classical mechanical equation where the caused strain must be smaller than the material strength. But in this case, the strength of wood must be reduced or determined by experiment because of imperfections of a tree. So the basic calculation looks as follows:

$$f_{red} > \sigma_{cr}$$
$$f_{red} > M_{cr} / W$$

f_{red} ... reduced strength
 σ_{cr} ... critical stress
 M_{cr} ... critical moment
 W ... section modulus

In the previous example, a solid cylinder was considered and so a cross-section of a tree. But a section can be also hollow due to for example biological attack. In that case, the failure scenario depends on the size of hole inside a trunk. For small holes, the behaviour is the same as for solid cylinder. If the hole is big and cross-section of a trunk or branch is therefore thick-walled wooden tube, the reason for failure is flattening of a section. This flattening is caused by transverse inwards-directed force. Result of this flattening is an oval form of section which can lead to failure even without big rising of strain. Whole process is illustrated in Figure 18. [1]

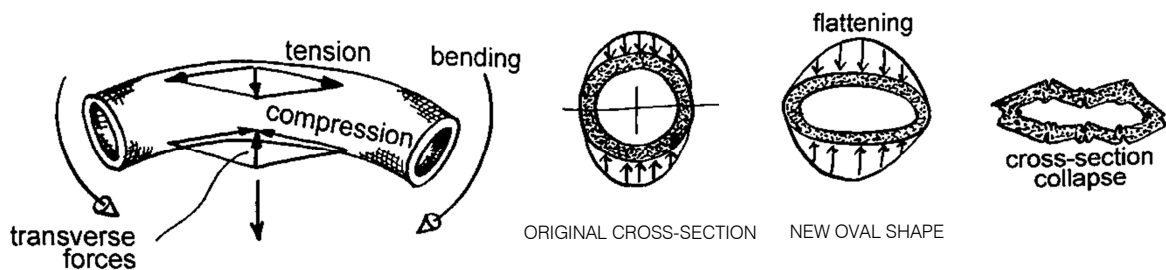


Figure 18. Process of failure of hollow cross-sections [1].

If a wall of hollow section is really thin, the oval shape does not have to be created and a structure can straight collapse without warning. This really dangerous behaviour is caused by buckling.

Next stage of cross-section reduction is an open cross-section which can be caused f.e. by mechanical rupture of hollow structure. This shape is naturally dangerous because it is much more strained by wind, on all sides. Therefore, there are many different possible ways of failure. A tree can buckle forward, backward or flatten to the side (Figure 19). [1]

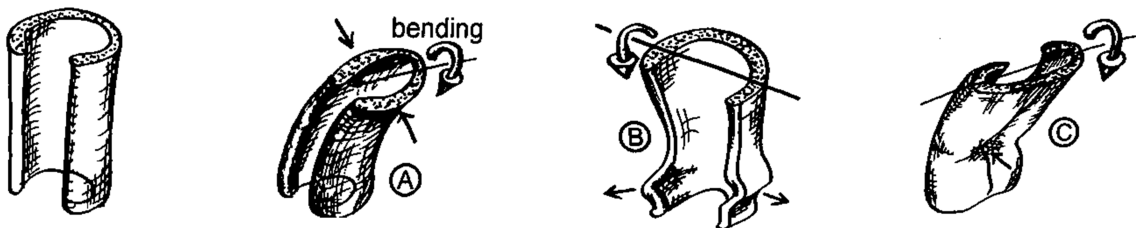


Figure 19. Possibilities of failure of an open cross-section: A-forward buckling, B-backward buckling, C-flattening [1].

If a big decay is located above the ground but a tree trunk is solid, a hinge effect can occur. Whereas a trunk is stiff but it does not have so stiff support, it rotates under the wind pressure as in hinge over a large decay. Result of this situation is a trunk collapse while

sides of a trunk around a decay stay squeezed into the air (Figure 20). This part of a tree does not tear off because of the neutral line going through this part of the cross-section. Therefore fibres are not strained at this point and they do not tear off. [1]

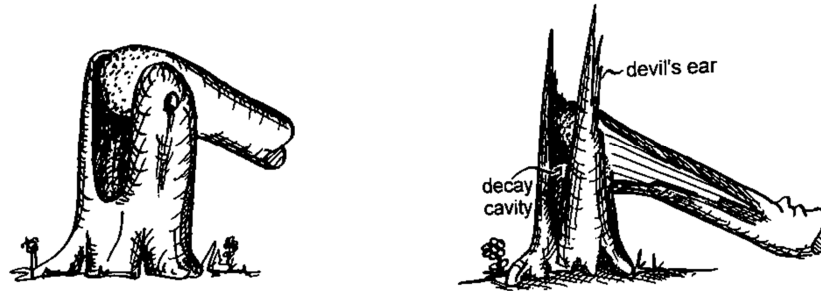


Figure 20. Tree failure caused by flipping over decay and its representation as a rotation in a hinge [1].

Above mentioned types of failure, hollow and open cross-section and trunks with cavities above the ground, are caused by decays inside a tree which weakens a structure. In principle, these weak spots are detectable and thus failure can be predicted or better be avoided. In the following paragraph, less predictable example of failure is presented.

If a branch or a trunk is crooked and bent up or straightened, its cross-section experiences tensile stresses in the transverse direction. As already mentioned, a tree has much lower tensile strength in perpendicular direction to the fibres, therefore this strain can lead to an explosive collapse. The dangerous situation is mainly caused by the unusual inner stresses which are equal to nil at the surface and have their maximum inside a trunk. Although, it can be expected that a tree is not able to react at all to such stresses, it is capable of mechanical self-defence even in this case. There was an experiment provided by Dr. Wolfgang Albrecht supporting this theory [6]. According to this experiment, it can be said that a tree creates more and thicker rays in the zone of the strength maximum and also their shape is optimized for tension, it is more round. Rays are always located in transverse direction to ensure that fibres hold together. In this case, they create stronger connection between these longitudinal fibres and thus increase their transverse strength. [1]

However, not each tree is capable of formation of such strong rays and if it is, the bond is not eternal so these crooked branches are still considered as dangerous for a structure and can be resembled to hazardous beams. First step of the failure procedure is longitudinal splitting due above mentioned transverse stresses and low strength tolerance in this direction. There are two possible subsequent scenarios, the transverse stress is extinguished in the upper part of a branch and the lower delaminated part is transversally compressed so it has no tendency to split again. In the other scenario, the upper part is still strained by the transverse tension and thus the splitting continues and a secondary crack is formed. This process can be repeated again and again until the transverse stress gradually disappears. For both cases, these cracks naturally weaken cross-sections and they are an open gate for decay pathogens. Also a tree optimized shape is suddenly useless because a damaged branch created completely new formation. [1]

However this failure may appear unstoppable, a tree has a special way how to deal with this problem and prevent a sudden failure or at least postpone it to form another substitute branches. The fibres in tension act like a rope connecting the beneath located fibres in compression (*Figure 21*). In the moment when the angle is bent up, these fibres creating the rope effect are fully taut and use the rest of tensile strength they have. At the same time, these fibres naturally tear off the rest of the branch. However this massive fracture might sound like a big price to be paid for improving the structure, a tree gets a time reserve in this manner. During this process, substitute branches can be formed or even new stream of assimilates along the damaged place can be created so the branch still can function to some extent. [1]

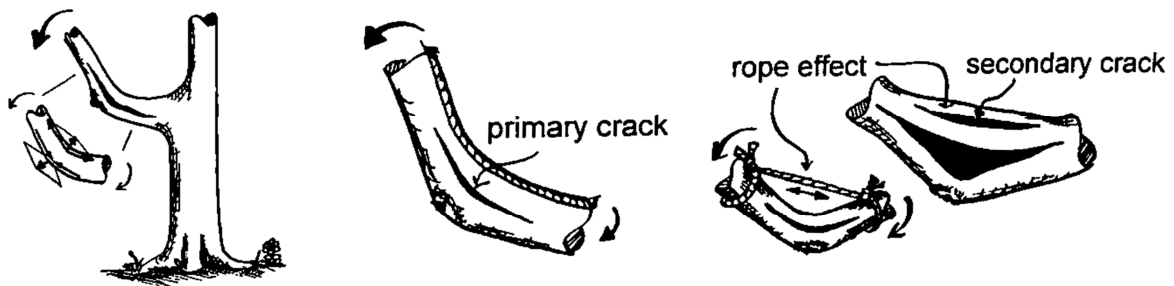


Figure 21. Longitudinal crack caused by transverse tension and its development [1].

There is an infinite number of tree failures, as with standard structures. Basically, all other failures are based on the principals mentioned in the preceding paragraph . However there is one exception when whole tree flips over because of roots and their interaction with soil. This problematics is very complex because there is suddenly another element influencing tree stability. Although roots and their effect are another point of interest of living structures, this problematics is not the main subject of this master thesis and therefore is not described in more detail.

Considering all above mentioned behaviour, a tree shows an ability of preserving itself in a moment of despair even at the cost of a big damage of its structure. But still, a branch with longitudinal crack is of more use to a tree than a branch completely broken off.

2.3.2. TREE DAMAGE BY BIOTIC SOURCES

There are several biotic pests which can attack a tree. The rate of attack depends on different aspects but mainly on the temperature, moisture, presence of oxygen and existence of heartwood within a tree. Generally said, a tree which contains heartwood is more durable than a tree with sapwood only, however the strength characteristics are nearly equal. The difference between these wood is mainly the age. Sapwood is formed in the youth phase of most trees and after several years, heartwood is formed (*Figure 22*). Unlike sapwood, heartwood contains waste material in which cells are located. These cells transform proteins inside of them into resins, natural gums and tannic acids which preserve the material. That is also why heartwood has very often darker colour but it is not a rule. Heartwood trees with colour change are for example oaks, cherry trees, elm and chestnuts. On the contrary, those without colour change are lime and pear trees, spruces and beeches. Also trees entirely without heartwood occur, some of them are for example willows, poplars, alders, maples and birches. [6, 7]

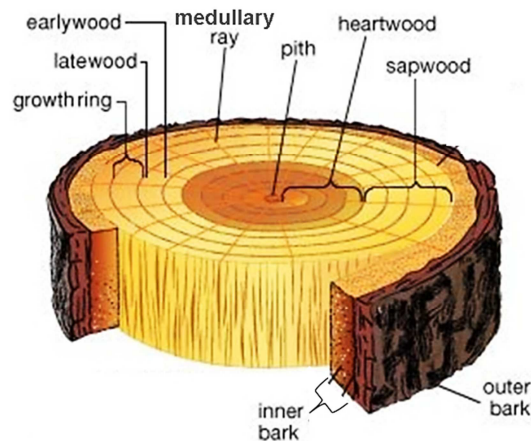


Figure 22. Schema of a tree trunk showing its single elements [11].

Main decomposers of wood are fungi, insects or bacteria and virus. These biotic sources damage the main elements in wood as cellulose, hemicellulose and lignin and the extent of their damage depends on the above mentioned parameters. [2]

Presence of fungi within a tree and its growth is strongly influenced by amount of oxygen, water and their preferable temperature is between 19 and 31 °C. Also the most suitable moisture content for fungi growth is from 20 to 80%. The same applies to bacteria impact. But on the contrary, bacteria are able to grow even in not that convenient environment like for example in wood with low concentration of oxygen. And this is the main difference between these two pests. Bacteria can degrade wood even without special conditions unlike fungi but if fungi have their optimal condition, they can cause extensive damage in short time. With regard to living wood, it has much higher moisture content which can imply suitable conditions for fungi and bacteria. On the other side, in wet wood, there is

not enough oxygen. For dry wood, exactly the contrary applies. Therefore it cannot be clearly stated that living wood, thus wet wood is more prone to biotic attack. [2, 6]

Next biotic source of damage are insects. A tree must be infected to be attacked by insects but then, insects lay their eggs inside the structure, in cracks inside wood. Last but not least, a tree can be damaged by mites, especially by spider mites, large mammals and also human beings. All the main biotic sources of damage are shown in *Figure 23*. [10]

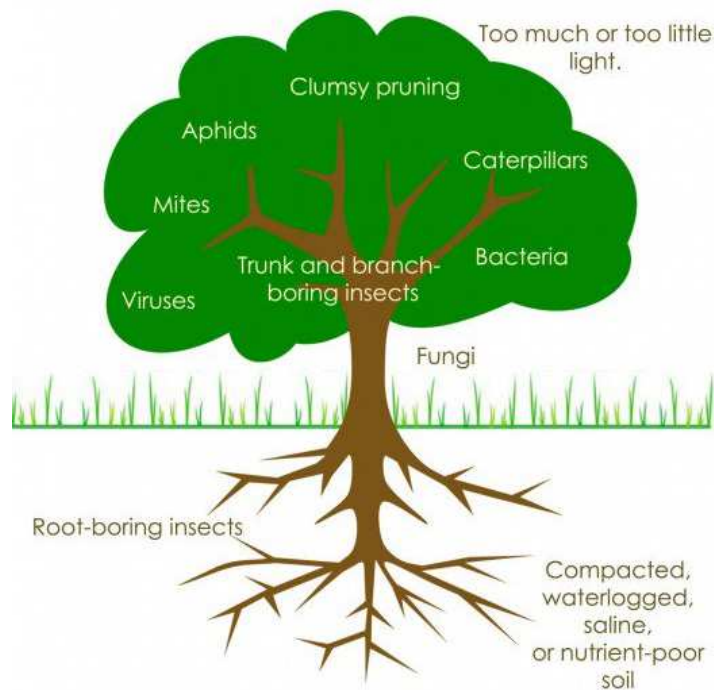


Figure 23. Main examples of sources of biotic tree damage [10].

A tree reacts to all the kinds of biotic damage by regeneration of its cells. There is a special mechanism inside a tree structure which reacts to rotting. This rotting process exudes humid acids, interrupts the sap flow within a tree and thus a tree responds to this change by forming new material. [7]

2.4. TREE BEHAVIOUR AS AN INSPIRATION FOR MECHANICAL DESIGN

The ideal mechanical design is a design without any weak places but on the other side without wasting of material. To achieve this state, efficient use of material must be ensured and thus the stresses distribution all over the component of a structure must be ideally uniform. Only in this case each cross-section of a structure is fully utilized without surplus material.

One thing is to design a structure to specific loading and the other thing is its response over time to this loading which naturally alters during the life of a structure. Good example in practise is wind load. This kind of load is very variable and its real behaviour is always uncertain. Wind blowing only from one side can be used as a model situation. And this is the moment when a tree should serve as an example of ideal structural behaviour. Unlike common building materials, a tree can adapt its shape, and specifically in this situation, create an ideal cross-section which has the long side along the wind direction (*Figure 24*). Thereby an optimal shape ensuring great stiffness is formed.

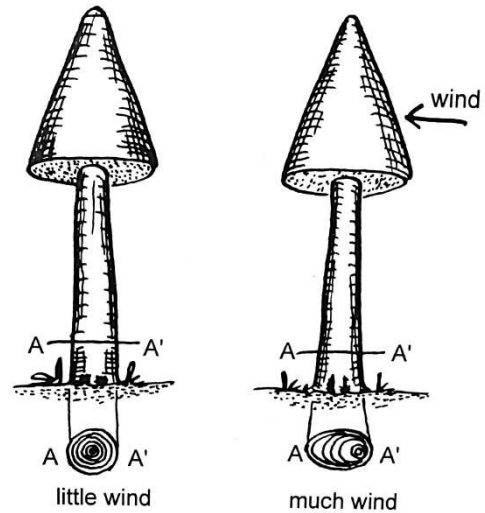


Figure 24. Adaptation of a tree shape over time according to load change [1].

As already mentioned above, this tree mechanism is stated and described in the axiom of uniform stress and is of special interest for designing of structures. [1]

To sum up tree behaviour and state the simple reason why a tree should be used in the field of civil engineering, it should be emphasized that there is no other material, respectively structure, used in the structural engineering world which can be built so efficiently. For many years, a tree serves as an inspiration in structural design for its optimal shape but only a tree itself has the extraordinary ability of self-optimization, an eternal reaction to changing environment.

3. CONNECTION OF TREES

A tree as a living organism can also grow around other objects as for example stone or different structure, another tree is not the exception. One of the reasons why a tree does not avoid contact with other structures but rather seeks a connection is again to reduce the inner stresses. [1]

Main difference between connection of two trees and tree in contact with other structure is that in this case, both partners envelop each other and thus enlarge the contact area. But not all the trees can grow together. The ability of growing together depends on the type of a tree. Generally, not really suitable trees for forming connections are needled-leaved trees. These trees contain lot of resin which makes creation of the connection between them more difficult. When there is a wound, a tree balm flows out of it and creates a hard layer of resin, and thus trees are not able to form any connection between them at this point because of this resin layer. Also trees containing toxic substances are not suitable for tree connections. These trees are for example Eucalyptus tree or Taxus.

Unlike needled-leaved trees, most of broad-leaved trees are able to form connections between each other, within one species but also with other tree types. Approximately same speed of growth is essential for creation of quality joints. But the speed is not the only influencing characteristic of a tree, for example type of tree bark also plays its role. Whereas some types of bark crack horizontally, others crack vertically. This difference makes the connection between different types of trees with different bark more difficult, sometimes even impossible.

Generally said, the ability of making connection between the trees depends on many aspects and therefore the best connection are between the trees of the same specie or exceptionally between different species but with very similar characteristics. Connection between more species or even between broad-leaved and needled-leaved trees should be avoided because it can cause more damage than benefit.

Next paragraphs are devoted to description of different types of welds. These tree welds can be generally divided into three types:

- axial welds
- cross welds
- grafts

3.1. AXIAL WELDS

Due to the changing load, two tree trunks can get closer to each other and even come to mechanical contact. This approach is mostly caused by wind movement. When trees are in contact, which by the way even does not have to be permanent, they start to form new material at the point of contact. This creation of new wood is simply response to new introduced load to a tree and its effort to reduce the stresses. Whereas the trees lean on each other, they also burden each other. In first phase of this process, spurs facing each other are formed at the point of contact (*Figure 25, up*). Over time, trees naturally grow, diameter of their trunks gets bigger and thus the distance between trees is reduced. Therefore the contact becomes more permanent and intense which leads to intensification of local growth in order to enlarge contact area and thus ensure uniform stress distribution. Next phase of the coalescence is the state when the contact becomes really permanent. In this phase, mutual enveloping occurs and also the area grows in size in general (*Figure 25, middle*). At this time, trees largely share their mechanical problems while their biological system and its needs are still separated. Resulting phase is a state when new annual ring is formed around whole circumference without disruption by bark (*Figure 25, down*). This connection ensures mutual exchange of water and nutrients which is biological gain for the trees. Because of the new created framework, shape of trees is optimized. Especially material below the connections is reduced and on the contrary trunks or branches above the connection tend to be thicker because unlike the lower part, they still act separately and on their own in terms of mechanics. [1]

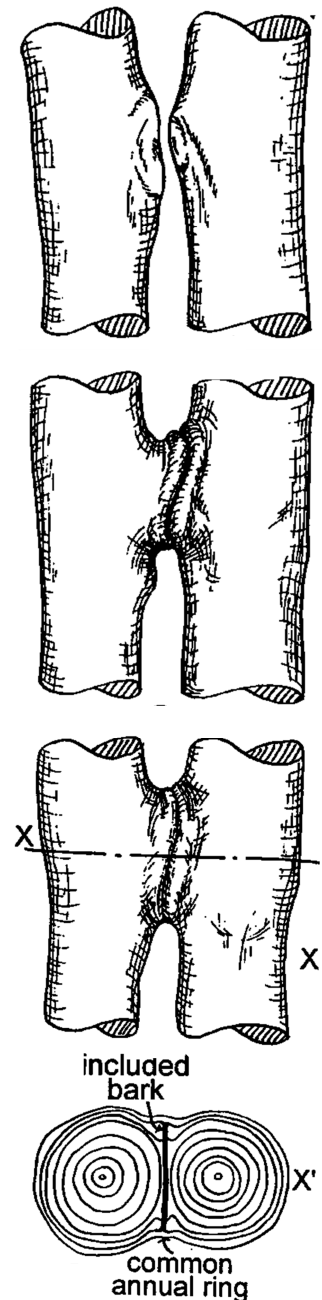


Figure 25. Individual stages of the development of the connection [1].

3.2. CROSS WELDS

Besides axial welds, trees can form also cross-welds (*Figure 26*). This connection represents the peak of adaptability of trees and is one of the greatest biomechanical interests due to the special arrangement of annual rings.

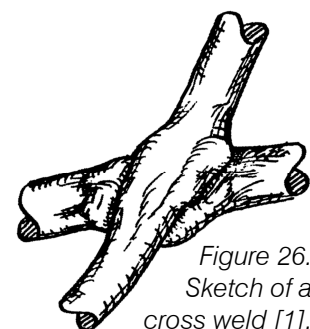


Figure 26. Sketch of a cross weld [1].

The beginning of creation of cross welds is the same as for axial welds. The trees get to contact due to the changing load, for example wind. Over time, this contact is more frequent and more intense so it causes creation of abrasion wood and later on enlargement of the contact area in order to limit new introduced stresses. But in this case, trees cross each other so the mutual enveloping works differently than with axial welds. The thinner transverse branch or trunk usually enlarges its area more than its thicker partner, on the contrary, thicker element flattens its shape so its cross-section becomes approximately an oval (*Figure 27, middle*). [1]

Unlike axial welds, in cross welds the fibres run in both directions which make the connection more sophisticated. There are two requirements for this weld union, first one is that the thinner element's annual rings flow without kinking into the flattened annual ring of the thicker element. This element outer part is flattened largely in the direction of the force flow of the crossing branch or trunk. When these two conditions are fulfilled, new annual ring can be formed in the direction of the dominant element, thus simply said in the direction of the thicker branch (*Figure 27, down*). [1]

The result of the cross weld is creation of frameworks within one or more trees due to which trees can work more effectively with loading, mainly wind load blowing in the direction of framework. Connected stems cooperate, they can support each other and thus relieve each other of load, respectively caused stresses. Also the growth can slow down in comparison to the rest of a tree above the connection which still works only on its own. [1]

3.3. GRAFTS

Unlike the previous two types of welds which are purely natural, grafts are always man-made. Part of a tree is removed in order to reveal cambium layer which is responsible for tree growth. Then two trees modified in this way are connected together. Their layers of cambium should touch each other in order to create strong connection between them.

Due to initial large area of contact, a graft can transfer larger compressive forces immediately after creation of the connection in comparison to axial welds. On the contrary, there is always a risk of infection of a tree because of an opened wound which is always very susceptible to pest infestation. Also grafting can be applied within one species only, moreover not all the trees can be grafted unlike axial and cross welds which are not so limited.

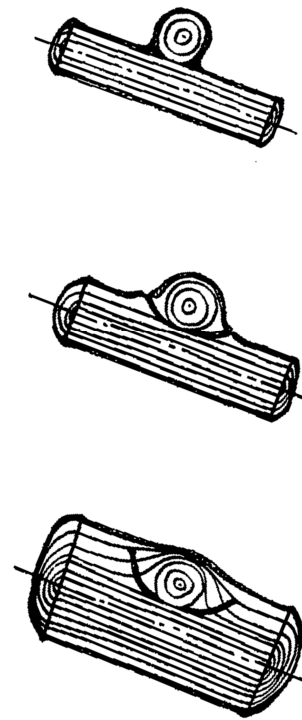


Figure 27. Individual stages of the development of the connection [1].

As could be apparent from the previous chapter, contact behaviour of trees is their great benefit, it brings lot of advantages. The most important ones are once more summarized below:

- minimization of stresses by enlargement of area
- minimization of stresses by reduction of rubbing movements
- creation of stiffer structure leading to material savings

Generally said, in the first phase, a tree has to create more material to form a connection but then this extra material can be compensated by reduced diameter growth in the parts of a tree relieved of load. In the end, this behaviour is again another proof of an optimal material use of trees dependant on stresses distribution.

4. LIVING AND NON-LIVING TREE STRUCTURES

Living tree structures can be easily confused for non-living structures. Next chapter is devoted to description of both types of structures and pointing out the main differences between them.

4.1. NON-LIVING TREE STRUCTURES

This type of structure is not so rare in the world. Tree structures have been built all over the world from small to great dimensions. Majority of the structures are made of common construction material and attached to a strong and tall trunk of a slow growing tree (*Figure 28*). These trees are for example a walnut tree, an oak, a cedar, a beech or a cherry.



Figure 28. The Orcas Island treehouse built by Nelson Treehouse as an example of a non-living tree structure [15].

They can be attached to just one but also to more trees at a time. The difference is in the method of attachment which can be following:

- by cables
- by beams
- by braces

Single methods are designed according to requirements of a structure because each type of attachment naturally has different mechanical behaviour and thus affects a tree differently.

Individual methods are also very often combined together. One thing, which is common for all the types, is interference into a tree structure by bolts, nails, screws or ropes.

The main reaction of a tree to this intervention in its structure is an attempt to repair the injured spot and reduce the spread of an eventual disease. A tree tries to insulate this spot by growing around it instead of healing it and thereby creates a solid connection with a bolt by strong squeeze. A large and healthy tree can deal with this intervention without any bigger damage. On the contrary, if a tree is young and weak or even shows signs of decay, such intervention can cause big damage. Especially for young trees, introduced bolt, nail or another object can get to the sapwood due to growth of a tree and interrupt water and nutrients supply. This situation can result in longer healing process of a tree and therefore make it more susceptible to diseases. [8]

Also rope tightened strongly around a tree trunk or branch can cause damage of the outer and inner bark or even of the cambium layer. Inner and outer bark layer is responsible for water and nutrients supply and for protection of a tree against frost damage and other kinds of damages. If the inner bark layer is damaged, the nutrient supply to the roots is reduced and therefore some roots can die. The cambium layer is responsible for the production of new cells within a tree so its damage can lead in the worst case scenario to the death of a tree or its part. [7]

As could be apparent, trees carrying the structure have to face basically always human intervention within their structure. Moreover, a structure of a tree itself, distribution of the stresses and the tree reaction, is not a subject of the design of non-living structures.

4.2. LIVING TREE STRUCTURES

Unlike non-living structures, living structures are not so common in the world or rather they are really rare. Some of them are built in Germany, in the Netherlands, there are no structures like these yet except for Living Tree Pavilion which is located in Botanical Garden of TU Delft and which is the main subject of this master thesis. However, this project is still in its beginnings because the trees are not an integral part of the structure yet due to their load bearing capacity which is still not sufficient.

As already mentioned, the main principle of living tree structures lies in the fact that the structure itself consist of trees, therefore a tree is an integral part of a structure. These structures use all the tree properties which have been mentioned in the previous chapters. Also, the ability of growing together with another tree or non-living material and thereby creation of stiff connections is one of the key principles of this type of structures.

One of the most known examples of living tree structures is Baubotanik Tower (*Figure 29*) which was designed by architect, Dr. Ferdinand Ludwig, the founder of Baubotanik, or Living Plant Constructions alliance. An inspiration for the structures comes from ancient

history, from art of tree shaping. Examples can be found already in ancient Meghalaya in India, living root bridges, or the pleached hedge fences in medieval Europe. [13, 14]

However, Ludwig's Baubotanik goes one step further by incorporating metal scaffolding and other construction materials in a living structure. The same applies to the already mentioned Baubotanik tower. The whole construction is supported by a temporary steel tube scaffold, which is anchored in the ground by a screw base, which can be removed. The living part of a structure is formed by the plant containers which are constantly kept wet to ensure the necessary watering of the plants. Willow trees are used for their fast growth and easy propagation. The structure has the footprint of about eight square meters, the height of barely nine meters and consists of three walkable levels. [13, 14]

Over time, as the trees age, they completely intergrow, their joints strengthen and thereby provide further load bearing support. As soon as the living structure is stable enough and can take over the loading capacity to support the floors, the scaffold will be removed. However, the structure fell behind growth expectations after six years, due to non-predictable factors such as an infection, a frost etc., Ludwig and his team were able to solve occurred problems and thus the structure still stands. Moreover, they have developed a system to cut back and replant certain trees without affecting the overall vitality of the structure. [13, 14]

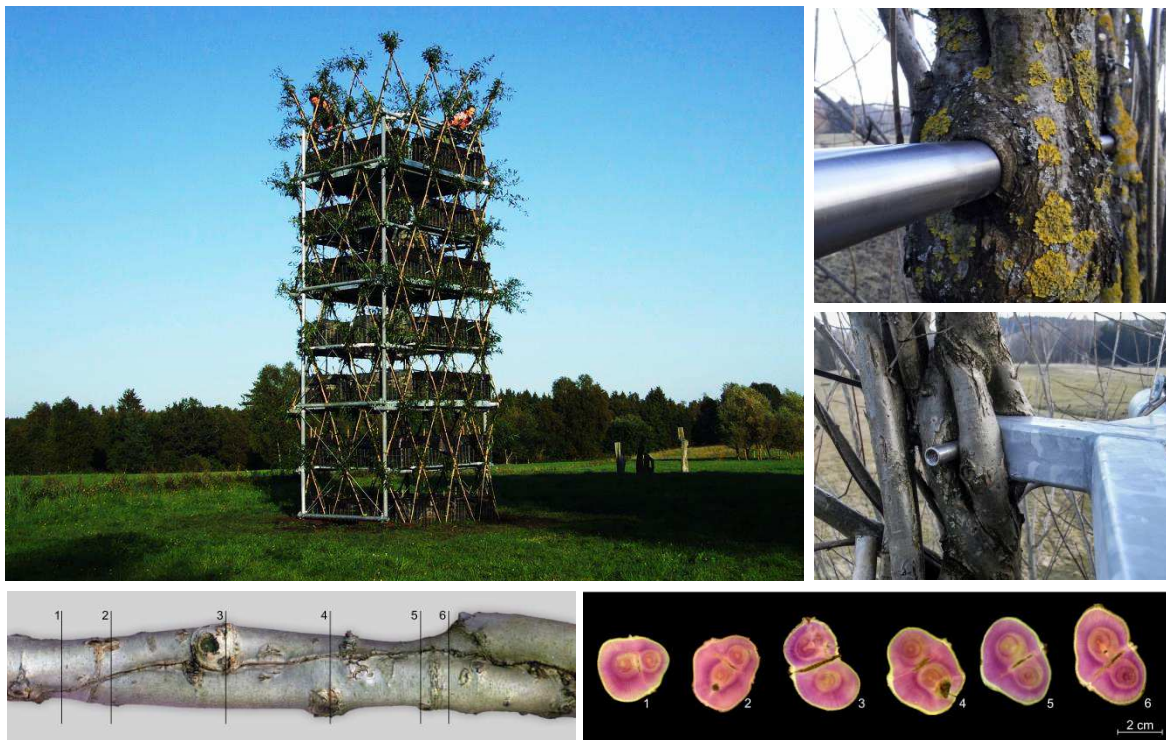


Figure 29. Pictures of Baubotanik Tower showing its structure and connections, both live and man-made [14].

Another example of living structures is the Plane-Tree-Cube which is the largest baubotanikal structure so far (Figure 30). The Cube was even awarded the Special Prize for

Innovation for Holzbaupreis Baden-Württemberg, a contest that judges unique buildings made from wood. [16]

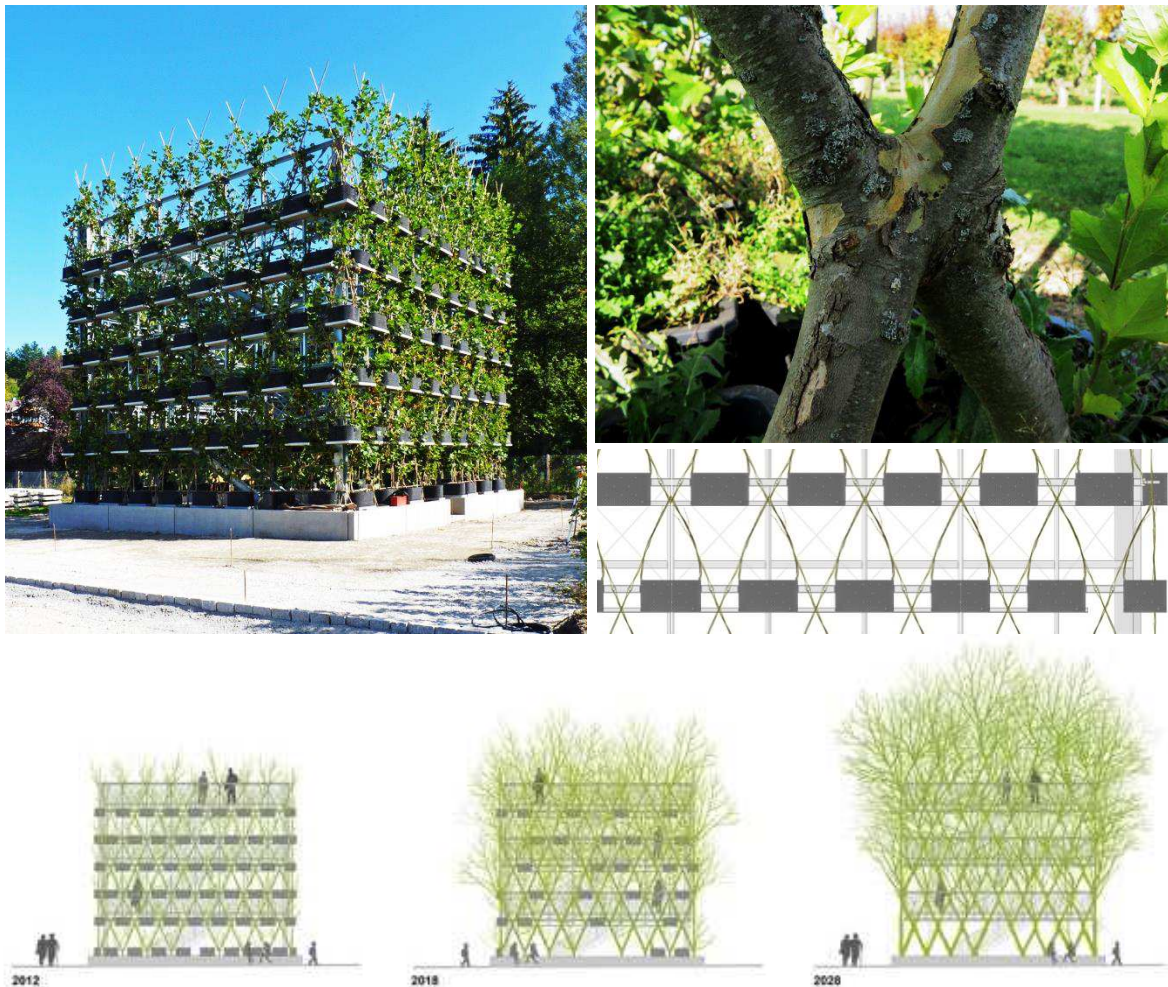


Figure 30. Pictures of Plane-Tree-Cube showing the structure, its connections and development over time [13].

Living tree structures are a big contribution to the field of civil engineering, respectively to urban world for their abilities which greatly affect their surroundings. Baubotanik structures combat soil erosion, they can also reduce storm water runoff and improve water quality through their roots. Moreover, they provide oxygen, sustenance, shelter and habitation. Due to their cooling shade, they can even reduce energy costs which can lead to greenhouse gas emissions cut down. Naturally, despite all these benefits, trees are still living structures and thus must be treated accordingly. As architect Dr. Ferdinand Ludwig said: “If you do not respect the rules of growth in your design, the plant structure will not grow as you want it to and may even die.” [14]

4.3. DIFFERENCE BETWEEN LIVING AND NON-LIVING TREE STRUCTURES

In both, living and non-living structures, a tree or group of trees play their load-bearing role within a structure. The main difference between these two types of structure lies in use of trees. Unlike living structures, non-living structures use trees just to carry the structure which is essentially made of common construction material. Basically, the structure itself is only attached to a tree. Therefore a tree itself is not the main part of the structure, thus not the main subject of the design, and the structure does not use its full advantage. On the contrary, talking about living tree structures, trees are an integral part of their structure. That means that the structure is not only attached to a tree but trees themselves basically form a structure.

As a result of that, living tree structures fully use the advantage of trees, their self-optimization ability and therefore their durability can be much higher. This ability is to some extent used even within non-living structures but really only very gently.

In terms of sustainable development, however non-living structures could be considered as eco-friendly, the production of emission is still higher in comparison with living structures. As an example, production of CO₂ can be used. Whereas the main part of non-living structure is simply said common house, for which construction lot of extra material is needed, more CO₂ is produced to build this structure. However, living structures also need extra material at the beginning, the amount is smaller. Moreover, in the moment when the trees creating the structure have sufficient load-bearing capacity to support the structure, this extra material can be removed and reused.

On the other hand, there are still lot of points of interest of living structures. Unlike non-living structures, these structures have not been built as water and wind tight structures yet. While it is possible to talk about non-living structures as about houses, living structures are really only structures for now. But this is also a reason why we should pay more attention to them because they have great potential which have not been fully used yet.



Figure 31. Pappenheim, an examples of living structures [17].

Figure 32. Yellow Treehouse Restaurant, an example of non-living structures [18].

5. LIVING TREE PAVILION

This chapter is devoted to the description of Living Tree Pavilion, from the general information to the detailed description of the single elements of the structure. Finally, the calculation and the overall evaluation of the structure are made.

Living Tree Pavilion is situated in Botanical Garden of TU Delft. The structure was designed by a former student of TU Delft A.D.W. Nuijten. The structure was built in November 2010 according to her design and during the spring 2011 opened for the public.

The Pavilion is an open dome-shaped structure that serves as a small lookout tower, or simply an elevated platform, on which people can walk. The structure consists of the non-living temporary structure and the living part, trees. Nowadays the platform is supported by the non-living load-bearing structure but the main idea of The Pavilion is that this structure will be removed and the platform will be borne only by the trees which surround it. This leads us to the task of the thesis, to evaluate the living structure and estimate when the trees are able to carry the platform. In order to make this calculation, the structure has to be mapped first.

5.1. GENERAL DESCRIPTION OF THE STRUCTURE

As already mentioned above, the structure is an open dome-shaped construction with the diameter of approximately 6 meters. The living part of the structure is created by the group of trees which are planted in the circle of the mentioned diameter of 6 meters. The central part is created by the non-living structure, the spiral staircase and the wooden braces which carry the platform. This platform is located in the height of 4 meters and its circumference is 3,7 m.

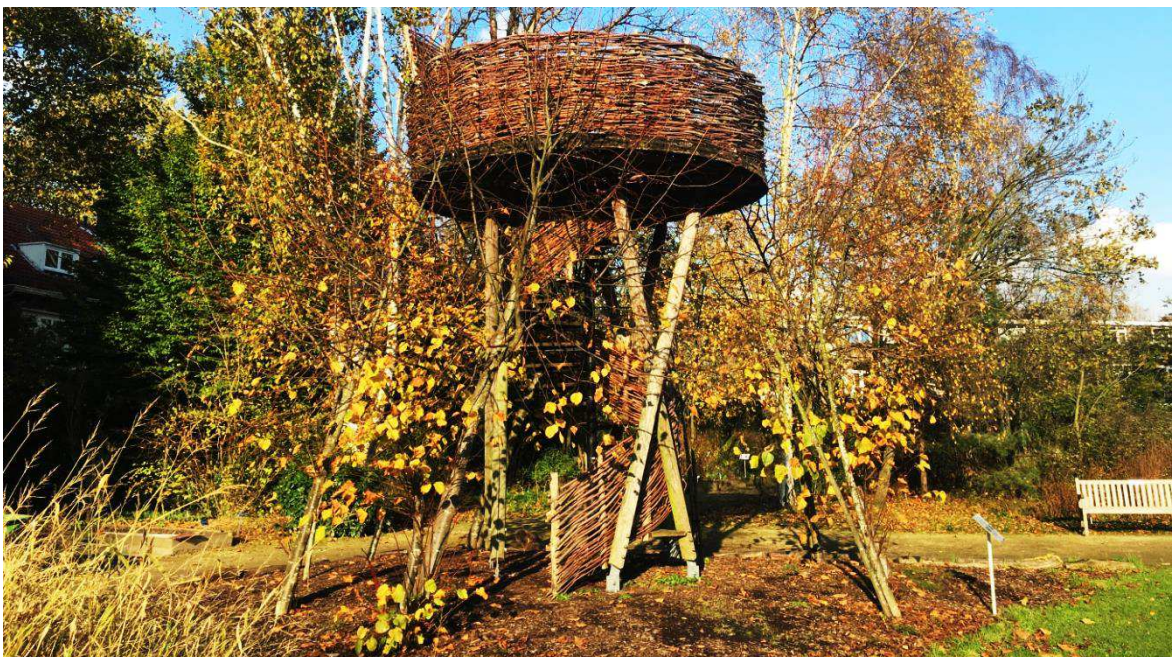


Figure 33. Picture of the Living Tree Pavilion.

5.1.1. DESCRIPTION OF THE NON-LIVING STRUCTURE

The non-living structure is created by the stable part and temporary part that is meant to be removed when the trees are strong enough to carry the platform. All the elements are described further.

The platform

The platform is a stiff flat element with the diameter of 3,7 meters and with a hole for the staircase in the middle part of the diameter of 1,75 meters. Around the circumference, the small holes can be found. These small holes were projected for the connection with the trees when they reach the platform.

The material used for the platform is robinia wood for its durability and endurance. Specifically, it is made of 6 layers of 20 mm thick boards, so the total thickness of the platform is 120 mm. These boards are formed by the 135 mm wide planks which are connected together by the screws. Each of these 6 layers is laid with the 60 degrees rotation (*Figure 34*). This system allows the planks to be oriented to the 3 main directions, to the braces which support the structure. While designing the platform, also the fact that it is supported now from the inner side by the braces, but in future, it will be on contrary supported from the outer side by the trees, was taken into account.

Finally, the water output is solved by the system of gaps and holes in the platform.

The temporary load-bearing structure

As already mentioned, the structure is temporary supported by the wooden braces, specifically 6. Two braces are always crossing each other in the height of 2 meters so they create 3 X-shape supports (*Figure 35*). Each of these braces has a circular cross-section of the diameter of 140 mm. And the material used for them is larch wood.

Whereas the temporary load bearing structure must enable to be removed, it is attached to the platform on the inner side so it leaves trees free to grow on the outer.

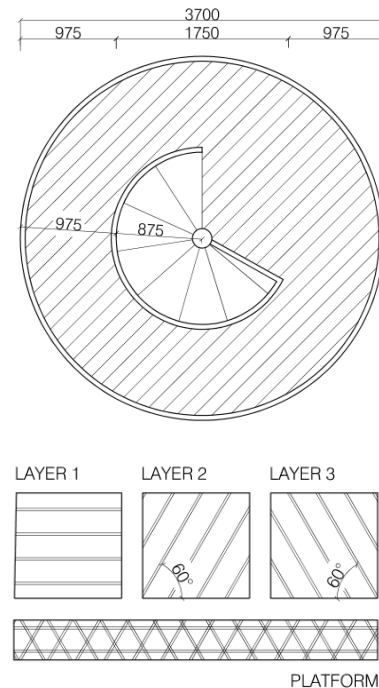


Figure 34. Geometry of the platform and its composition.

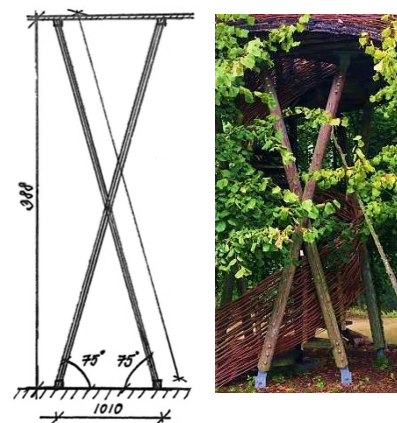


Figure 35. Picture of the wooden braces supporting the platform.

The braces are based on the foundation which is formed by the concrete baseplate, common for the staircase and these 6 columns.

The staircase

In the middle of the structure, the spiral staircase is located. Its radiance is 850 mm and the material used for the steps is hardwood with a high durability class. The individual steps are connected to the steel pole which creates the axis of the structure. The connection between the steps and the pole is created by the steel rings which clutch the pole. Similar ring is used also for the connection between the pole and the platform.

Whole structure of the staircase is carried by the baseplate as already mentioned in the previous chapter.



Figure 36. Pictures of the staircase.

The railings

The railings along the platform and the staircase are made from woven willow-twigs that are wrapped around poles from robinia wood. The height of the railing is 1 m.



Figure 37. Pictures of the railing.

Description of the living structure

The main thought of the Living Tree Pavilion is placing the platform and whole its load on the living trees which create the living element of the load-bearing structure. The specie of the trees has been chosen as an ash tree (*Fraxinus Excelsior L*). There were lot of choice criteria for this decision. In order to fulfil the goal of the project, the tree has to have a moderate or fast growing rate, durability and has to fit in Dutch ecosystem. Also not all the trees can grow together naturally or even to be grafted. Due to the fact that all types of the connections; axial welds, cross welds (Figure 40) and grafts, should have appeared within the structure, the ash tree has been chosen because it fulfils all the mentioned requirements.

There were originally 24 trees which were planted in the circle with the diameter of 6 m. Young ash trees of the diameter of 30 mm were used then in 2010. These 24 trees created basically 12 supports of the structure because two trees were always planted close to each other (Figure 39). In order to test the different connection methods, three different types were used. Two close trees creating one support were tightened together, above the ground and in the height of 1,3 meter, in order to make an axial weld. Then later, when trees grew bit more, another connection was made. In this case, the connection was made in the bigger height, around 2,8 meters. The trees were also tightened but this time with the tree standing nearby, not the one from the same support (Figure 39). These connections should have created the cross welds or grafts. Last designed connection was in the height of 4 m, again an axial weld. Trunks should have been bent again and interconnected and tighten to the platform.

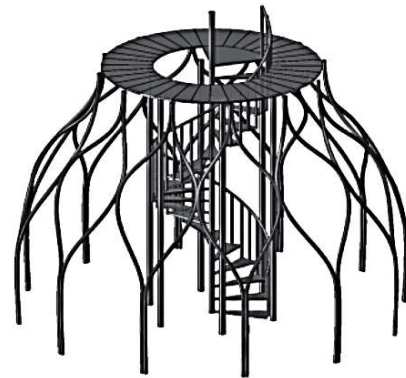


Figure 39. 3D model of the designed structure [9].

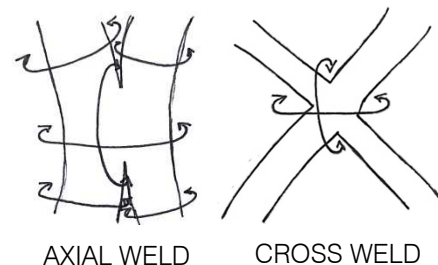


Figure 38. Sketches showing the axial weld and the cross weld.

From year 2010 till now, the trees were maintained and tangled together by the workers of Botanical Garden of TU Delft, according to the design. Unfortunately, some trees had to be removed and on contrary, others were planted. Therefore the current living structure is different than the original design.

Nowadays, the structure consists of ten supports, some of them are created by one tree and some of two of them. The total amount of the trees is 17. The detailed description of the current state of the living structure is described in the following chapter.

5.2. MAPPING OF THE EXISTING TREE STRUCTURE

In order to determine the load-bearing capacity of the structure, it is necessary to describe the structure in detail first. The geometry of the structure was measured manually. The tree properties were obtained from the pulling test which was applied to several trees of the structure. Whole procedure of the measuring is described further in this chapter. Properties necessary for the evaluation of the structure are listed below:

Tree trunks

- circumference of the stems depending on the length
- length of the stems
- height of the stems
- tangential angle between the stems
 - between the stems creating one support
 - between the stems and the ground
- radial angle between the stem and the ground
- distance between the stems
 - between the stems creating one support
 - between the single supports
- distance of the stems from the axis of the structure

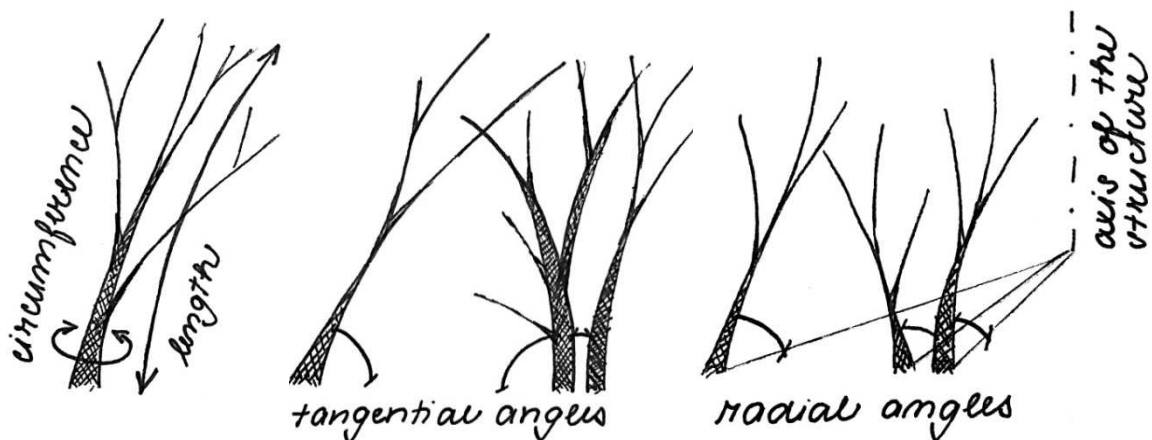
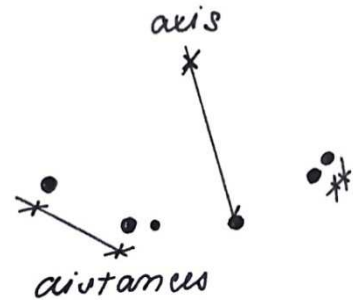


Figure 40. Sketches showing the measured characteristics of the stems.

Tree joints:

- width of the connection
- height of the connection
- circumference of the connection
- circumference of the stems below the connection
- circumference of the stems above the connection
- total circumference of the cross-section at this point

- angle between the stems at this point
- location of the joints
 - height of the joint above the ground
 - horizontal distance between the joint and the supports

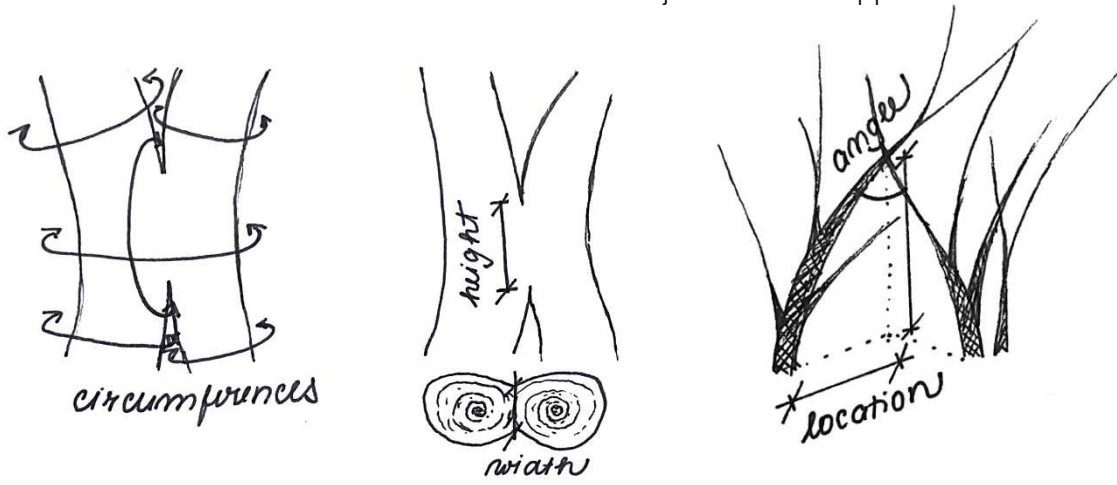


Figure 41. Sketches showing the measured characteristic of the connections.

5.2.1. DESCRIPTION OF THE SUPPORTS

This chapter describes the trees of the Pavilion, the properties of each single tree, organisation of the structure but also the procedure of measurement. Live structure of the Living Tree Pavilion consists of 10 supports. Some of these supports consist of two tree trunks, some only of one. Layout of the structure is visible in *Figure 42* and *Figure 43*.

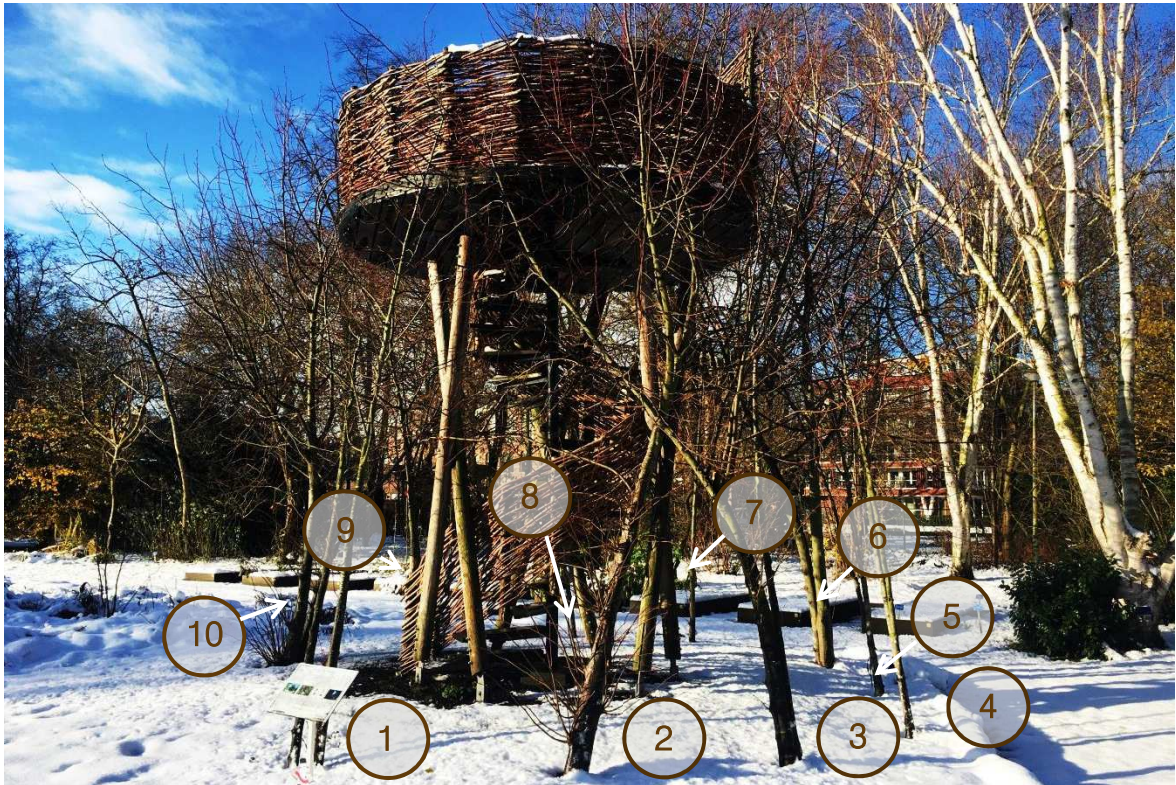


Figure 42. Picture of the structure with the indication of the supports.

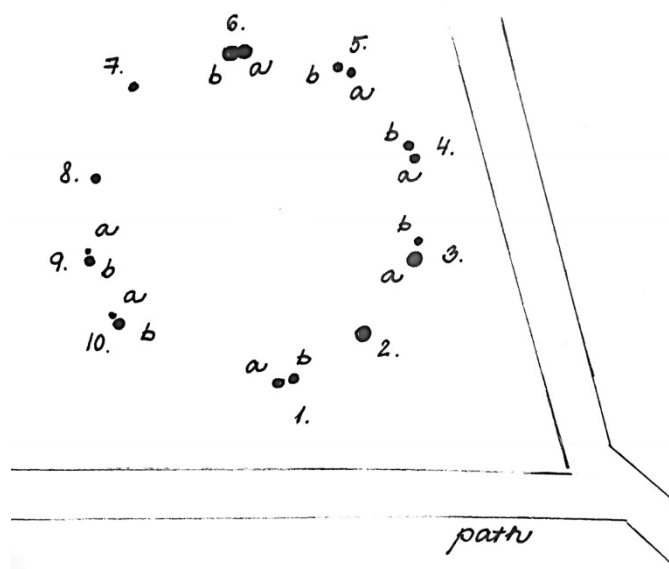


Figure 43. Schema showing the layout of the structure with the indication of the trees.

Measuring of the tree structure

As already mentioned above, the mapping of the structure was carried out by manual measurement. The following chapter describes the procedure of measuring, how the individual characteristics were obtained and their values are listed in following *Table 1* and *Table 2*.

At first, all the tools necessary for the measurement should be mentioned. They are also shown in *Figure 44* and their list follows:



Figure 44. Necessary measuring tools.

- steel retractable meter measuring tape
- sewing tailor measure ruler soft tape
- spirit level
- rope
- weight
- planks
- scissor
- ladder



Figure 45. Marking of 1 m of the length.

All the measurements were provided by one meter of the length of the stem, so the first step was to label each meter of the tree trunk for following easier work (*Figure 45*). The common jute string was used for the marking because it was only several days matter so the rope could not damage the trees. To provide as accurate results as possible, the distance between the ropes was checked every day of measuring.

Next, the circumferences were measured by the soft tape which can better adhere to the surface of the stem. Also the length of the stems was measured by the soft measuring tape. Other properties, such as height, distance between the supports and trees creating one support and distance between the trees and the centre of the structure were measured by the steel retractable tape.

Last step of the measurements was measuring the angles of the stems, tangential and radial. This measurement required more sophisticated approach. Due to the fact that the angles alter by the length of the tree, the angles were also measured in two places, in 1 and 2 meters of the length. First step was to place one wooden plank in the tangential direction and one in the radial direction from the tree. Whereas the terrain is not completely straight, both of these planks were supported to stay horizontally and the spirit level was used to ensure this horizontal plane. Then measuring tapes were put on the planks, starting from the stem. When everything was set, the measuring itself could start. From both spots of

the stem, rope with the weight was dropped down and the tangential and radial distance between the stem and the end of the rope with the weight was measured. Either was measured the vertical distance between the plank and the point where the rope was tangled. Simply said, the coordinates were obtained from this measurement and it was easy to count the angles in both directions according to Pythagoras' theorem. This procedure was performed for each tree. The measurement system can be seen in *Figure 46*.

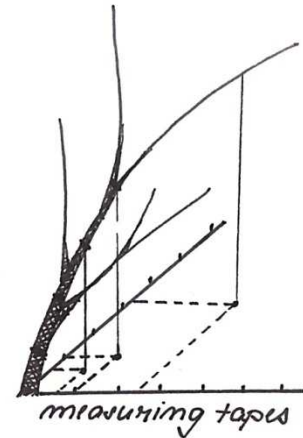


Figure 46. Sketch showing the measurement procedure.

The results of the measuring

The main properties obtained from the manual measurement can be found in following tables.

TREE	CIRCUMFERENCES OF THE TRUNKS IN THE LENGHT OF [mm]					LENGTH [m]	
	0 m	1 m	2 m	3 m	4 m		
1	A	211	154	123	95	-	3,04
	B	314	200	147	108	77	4,48
2		482	384	246	157	105	4,66
3	A	343	282	145	111	85	4,48
	B	188	157	125	99,5	71	4,07
4	A	178	129	103	79	-	3,23
	B	211	157	130	104	-	3,63
5	A	205	154	116	93	-	3,62
	B	161	125	93	72	-	3,62
6	A	513	380	326	272	217	5,91
	b	435	308	268	210	162	5,19
7		242	182	119	85	-	4,01
8		174	143	94	69	-	3,93
9	A	189	148	111	85	-	3,93
	B	386	326	198	139	107	5,09
10	A	305	214	127	82	-	4,27
	B	626	386	316	224	159	5,42

Table 1. Overview of the circumferences of the tree trunks according to the length.

SUPPORT	LENGTH [m]	HEIGHT [m]	DISTANCE BETWEEN [m]		
			TREE - CENTER	THE SUPPORTS	THE TREES
1 A	3,04	3,00	2,730	3,884	0,094
	b 4,48	4,40		1,492	
2	4,66	4,50	2,795	1,492	-
				1,213	
3 A	4,48	4,30	1,492	1,213	0,042
	B 4,07	4,00		1,489	
4 A	3,23	3,20	2,845	1,489	0,031
	B 3,63	3,60		1,213	
5 A	3,62	3,60	2,710	1,213	0,028
	B 3,62	3,50		1,255	
6 A	5,91	5,60	2,930	1,255	-
	b 5,19	5,00		1,461	
7	4,01	3,90	2,825	1,461	-
				1,281	
8	3,93	3,80	2,805	1,281	-
				1,638	
9 A	3,93	3,80	2,970	1,638	0,018
	B 5,09	4,90		1,369	
10 A	3,99	3,70	2,855	1,369	0,090
	B 5,42	5,20		3,884	

Table 2. Overview of the geometry of the tree trunks and the distances between them.

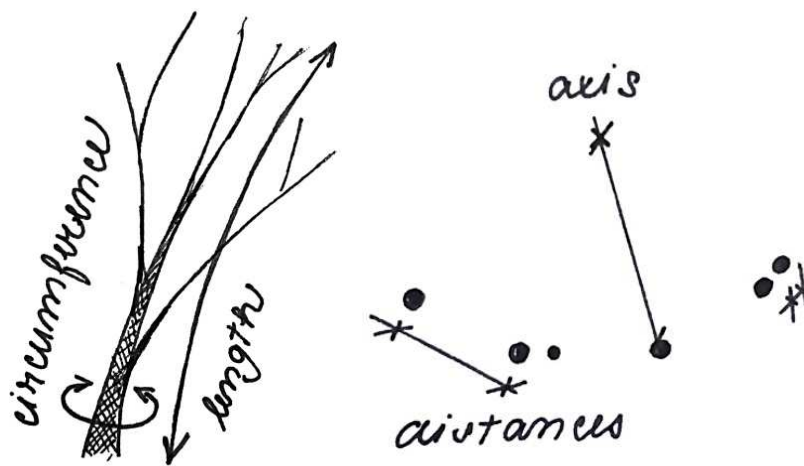


Figure 47. Schemas explaining the measured characteristics.

Following part of the chapter describes all the supports, their specific characteristics and mainly their appearance is shown in the figures. To give a general overview of the structure, also the existence of the connections is mentioned but their detailed description is given further, in the chapter dedicated to tree joints.

Support 1

This support consists of two trees, tree A on the left side and tree B on the right side as shown in *Figure 48*. These trees do not have any connections with other trees, nor between each other as visible in the same *Figure 48*.

During the measurements, it was found that the support 1A has a big crack above the ground that basically interferes with more than half of the cross-section of the stem. More and more cracks appeared over time also in vertical direction (*Figure 48*, down). The whole tree is dry and it can be said that it is basically dead and therefore should be replaced by a new tree in the future.

Tree 1B can reach the platform.



Figure 48. Pictures showing the support 1, its trees and location within the structure.

Support 2

This support consists of only one tree that is interconnected with the tree 3A as shown in *Figure 49*. Type of the connection is a cross weld and it is described in more detail in the next chapter under the name Connection 2-3.

At the beginning of December, big vertical crack of the stem appeared above the ground (*Figure 49, down*). The tree did not show any signs of dryness and the crack was monitored during all the analysis. At the end, in February, it was visible that the crack is just a matter of surface and the inner part is all right.

This support is tied to the platform because its height is sufficient to reach it.

Support 3

This support consists of two trees that are jointed together in two places above the ground, as visible on the *Figure 50*. Both connections are axial welds. There is also connection with the support 2 as mentioned above, and again visible in *Figure 50*. Type of the connection is a cross weld. Also other small connections can be found between the branches higher in the tree.

Height of both trees is sufficient to reach the platform so their branches are tied to it.

Figure 49. Pictures showing the support 2, its trees and location within the structure.



Figure 50. Pictures showing the support 3, its trees and location within the structure.

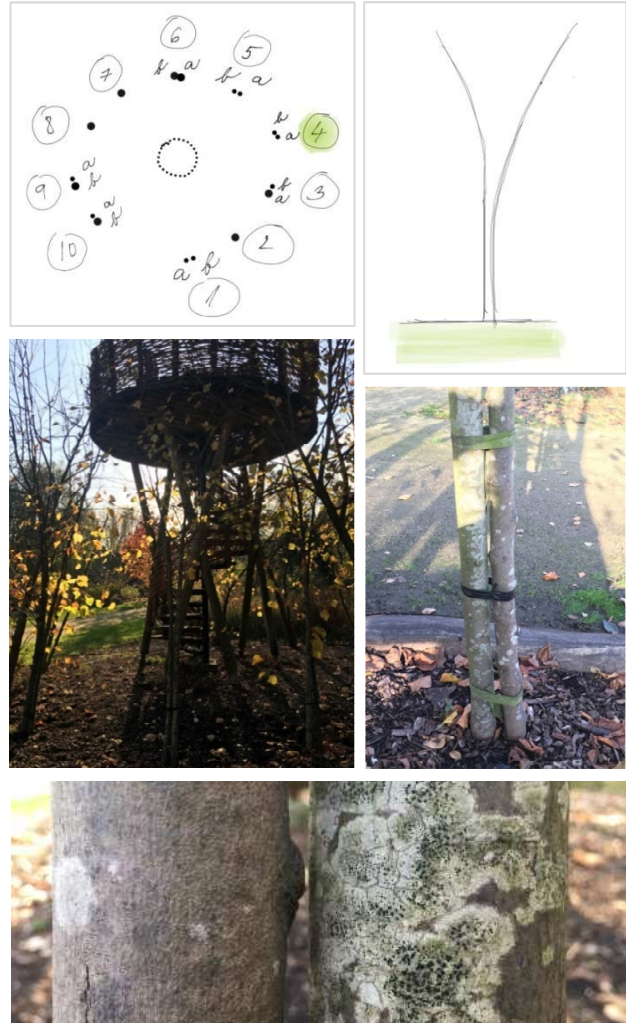


Support 4

This support consists of two slender trees that are very close to each other but not connected as you can see in *Figure 51*.

Height of both trees is sufficient to reach the platform but they are not attached yet.

Figure 51. Pictures showing the support 4, its trees and location within the structure.



Support 5

This support is very similar to the previous one, it also consists of two slender trees that are close to each other but not connected as visible in *Figure 52*. Tree 5B is in transverse contact with the tree 6, but it doesn't form any solid connection. Trees are in this spot only tied together. This place of contact is also shown in the schema in *Figure 52* by the orange colour. Again, small connections between the branches can be found higher in the tree.

Height of both trees is sufficient to reach the platform, they are tied to it and tree 5A even grows into the railing of the platform.

Figure 52. Pictures showing the support 5, its trees and location within th



Support 6

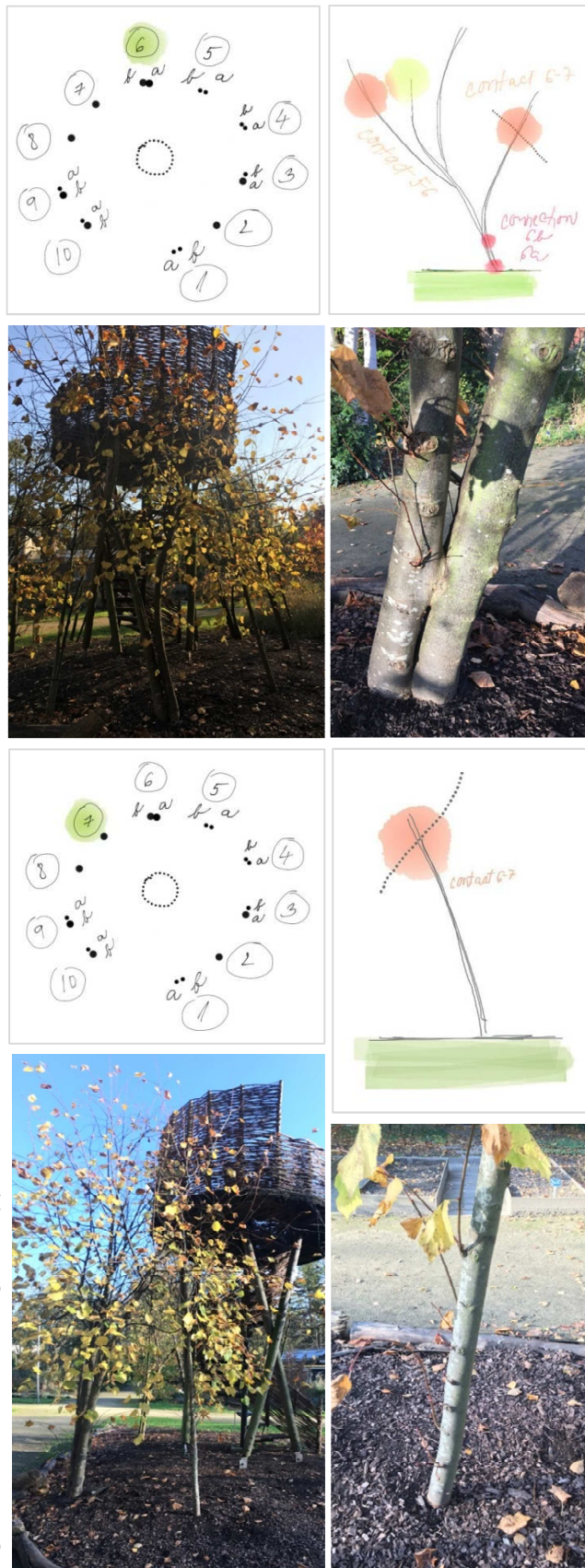
This support consists of two strong stems that are interconnected above the ground in two places. Both connections are axial welds and it is possible to say that these connections are the most massive axial welds which can be found within the structure. Their location is shown in *Figure 54*. As mentioned above, the tree is in tight contact with the support 5 but also with the support 7 as you can see in the same schema in *Figure 54*. Branches are only tied together in these places but do not create any solid connections. There is also one bigger interconnection between these two stems higher and other small connections between the branches can be found there as well.

This support seems as one of the strongest of the structure due to its big circumferences and strong connections. Height of both trees is bigger than the height of the non-living structure. Trees are tied to the platform and even grow through its railing.

Support 7

This support consists of one slender tree that is only in contact with the support 6. Also other small connections between the branches can be found higher in the tree (*Figure 53*). This support can reach the platform only by really fine branches which are not tied to it yet.

Figure 54. Pictures showing the support 6, its trees and location within the structure.

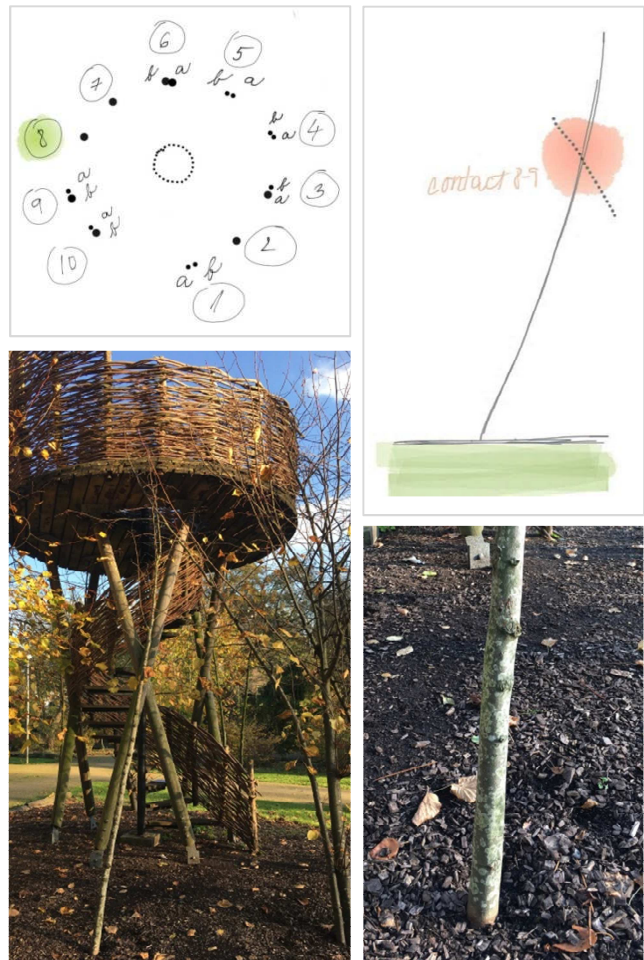


Support 8

This support is very similar to the previous one (Figure 55). It consists of the only one slender tree that is in contact with the support 9. Other small connections between the branches can be found higher in the tree as well.

This support reaches the platform only by fine branches as well as the previous support and they are also not tied to the platform yet.

Figure 55. Pictures showing the support 8, its trees and location.

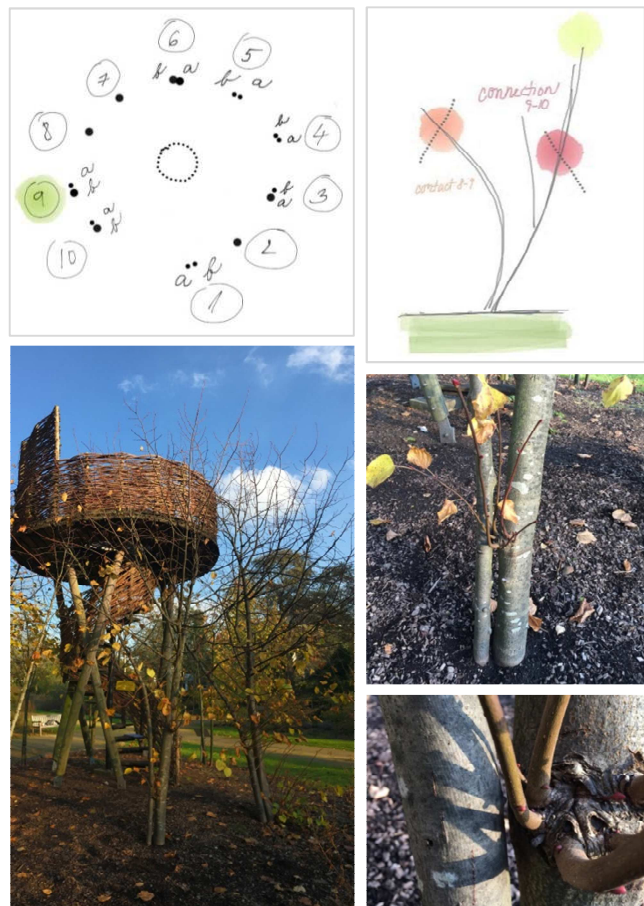


Support 9

This support consists of two trees that are not connected to each other but have connections with other trees (Figure 56). As mentioned above, tree 9A is in the transverse contact with the support 8. Tree 9B has a solid connection with tree 10A. This connection is a cross weld and it is the biggest joint of this type of the structure. Also other small connections between the branches can be found higher in the tree.

This support is tied to the platform and its height is bigger than the height of the non-living structure. As shown in the schema in Figure 56 by yellow colour, branches of tree 9B grow into the railing of the platform.

Figure 56. Pictures showing the support 9, its trees and location within the structure.

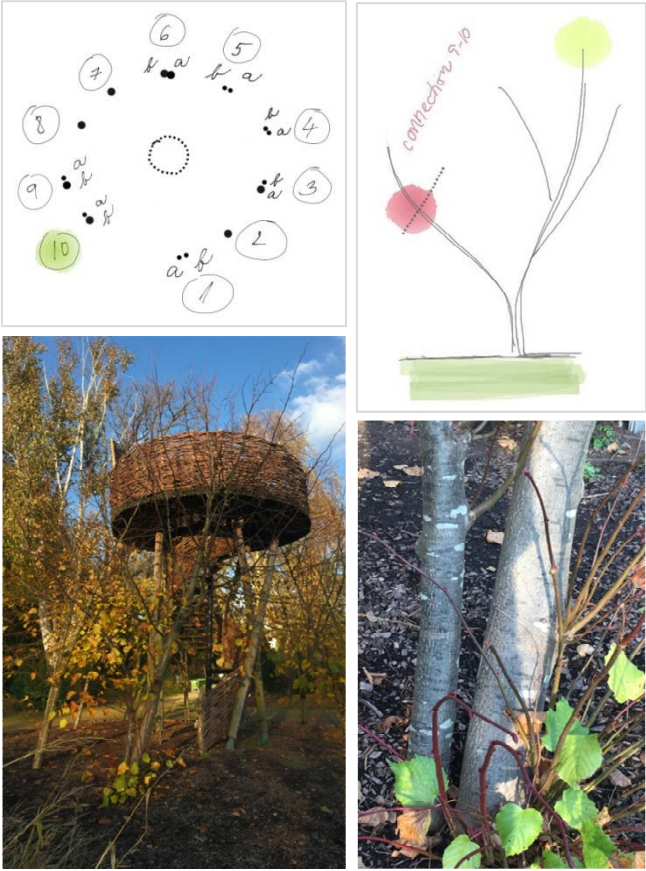


Support 10

This support consists of two trees that are not connected to each other. As mentioned above, tree 10A has solid cross weld with tree 9B. Also this support has other small connections between the branches that can be found higher in the tree.

Trees creating this support are very high and they are tied to the platform. Their branches heavily grow through the railing as indicated in Figure 57.

Figure 57. Pictures showing the support 10, its trees and location.



5.2.2. DESCRIPTION OF THE NATURAL JOINTS

This chapter is dedicated to the tree connections, it describes the major ones but also the measuring procedure. The following text describes how the individual characteristics of the joints were obtained and their values are listed in *Table 3* and *Table 4* below.

The tools that were necessary for the measurements are the similar to the ones that were used in previous chapter for the measurements of trunks, thus:



- steel retractable meter measuring tape
- sewing tailor measure ruler soft tape
- rope
- scissor
- weight

Figure 58. Necessary measuring tools.

Generally, it is hard to measure precisely the connections because of their complicated shape. Different methods of measuring were used for each connection depending on the shape and accessibility. Sometimes the steel tape was used but generally, mainly for the width and the height of the connections. The soft tape was used for all the circumferences, of the stems below, stems above and total circumference in the spot of the connection. For measuring the circumference of the place of contact the rope was used. It was wrapped around the connection and the place where both ends of the rope touched was marked by a pen. The distance between two dots was measured after unwinding the rope. The angle between the stems creating the connection is calculated from the measured vertical and horizontal distances between them. Location is determined by the horizontal distance between the vertical projection of this point to the ground and the center of the construction and vertical distance between the connection and the ground. This location was measured again with the help of rope and weight. The weight tangled to the rope was dropped down from the place of the connection and the vertical distance to the ground was measured. Then from the place where the weight touched the ground, the horizontal distance was measured. For both measurements, the steel measuring tape was used.

Due to all above mentioned about measuring the geometry of the natural joints but also generally the geometry of the trunks, another manner of measuring should be considered for the future researches. One possibility could be 3D scanning or photogrammetry. These methods could provide easier work and more precise results.

All the results from the manual measurement can be found in following *Table 3* and *Table 4*.

JOINT TYPE	CIRCUMFERENCE OF [mm]					
	CONNECTION	TOTAL CROSS-SECTION	STEMS BELOW		STEMS ABOVE	
			a	B	a	b
2 – 3 cross	32	397	245	147	275	159
3 – 3 a axial	70	435	311	178	303	174
3 – 3 b axial	172	509	371	202	342	190
6 – 6 a Axial	-	796	-	-	471	387
6 – 6 b Axial	383	694	461	369	411	339
9 – 10 cross	242	281	119	169	181	125

Table 3. Circumferences describing the connections.

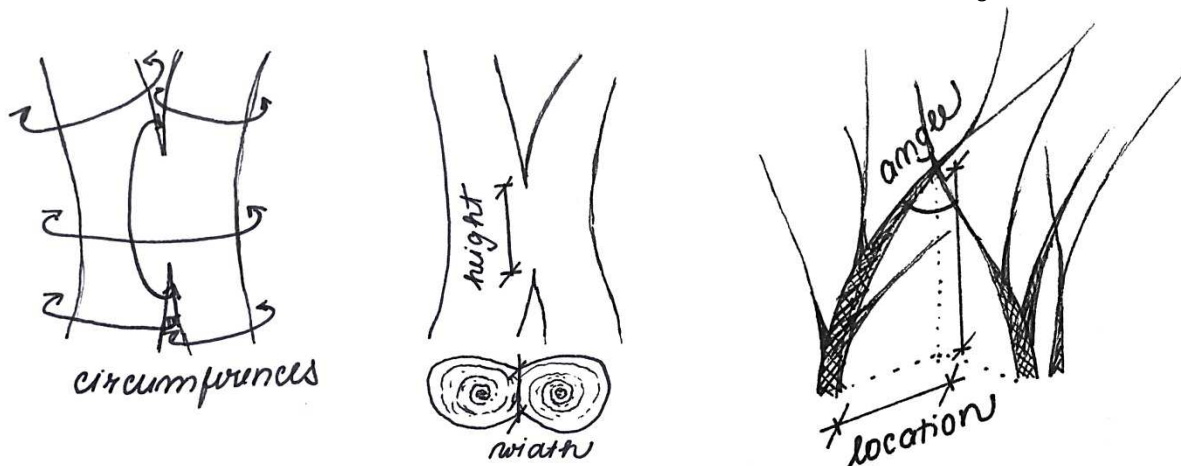


Figure 59. Sketches showing the measured characteristics.

JOINT TYPE	WIDTH [mm]	HEIGHT [mm]	LOCATION [mm]	
			DISTANCE VERTICAL	HORIZONTAL
2 – 3 Cross	13	12	2024	630 / 680
3 – 3 a Axial	32	51	0	0
3 – 3 b Axial	35	57	267	0
6 – 6 a Axial	75	210	0	0
6 – 6 b Axial	70	150	434	0
9 – 10 Cross	85	75	2060	580 / 950

Table 4. Characteristics describing the connections.

As already mentioned above, the trees creating the structure are interconnected by the joints; cross welds and axial welds. These connections can be generally divided into three levels (Figure 60). First level is joints between the stems just above the ground so they create one solid support of the structure. Next level is joints between the stems or main branches in the bigger height above the ground, connecting single supports together and basically creating structural framework. Last level is minor connections between the small branches also in the bigger height. There are also some contact places between the trees and their branches that do not create solid connections yet. They are tied together, tangled together or just simply lie on each other.

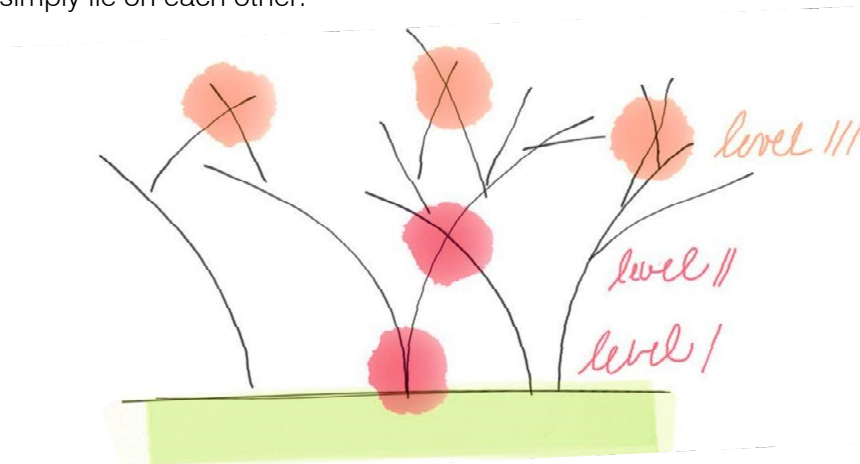


Figure 60. Schema showing the levels of the connections.

All the major connections of the structure were mentioned in the previous chapter and are described in detail below. The list of the joints can be divided as follows:

- level I, joints above the ground
 - axial weld A of the support 3 (Figure 61, left down)
 - axial weld B of the support 3 (Figure 61, left up)
 - axial weld A of the support 6 (Figure 61, right down)
 - axial weld B of the support 6 (Figure 61, right up)

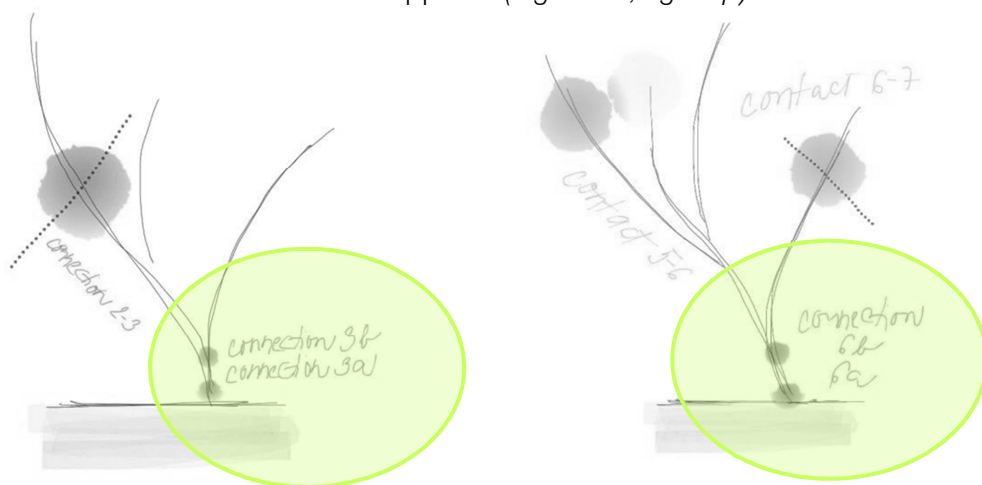


Figure 61. Schemas of the supports 3 and 6 with the highlighted connections above the ground (from the left).

- level II, joints creating the framework
 - cross weld between the supports 2 and 3 (Figure 62, left)
 - cross weld between the supports 9 and 10 (Figure 62, right)

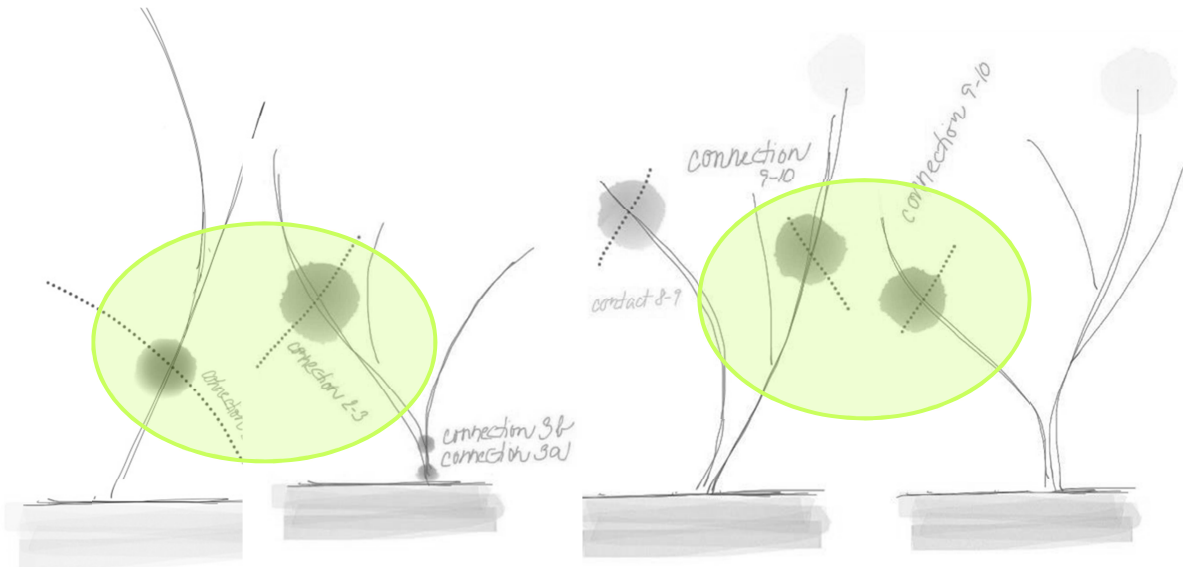


Figure 62. Schemas of the trees with the highlighted connections between the supports 2 and 3, 9 and 10 (from the left).

- level III, minor connections between the small branches
 - these connections can be found basically within whole structure in the bigger height

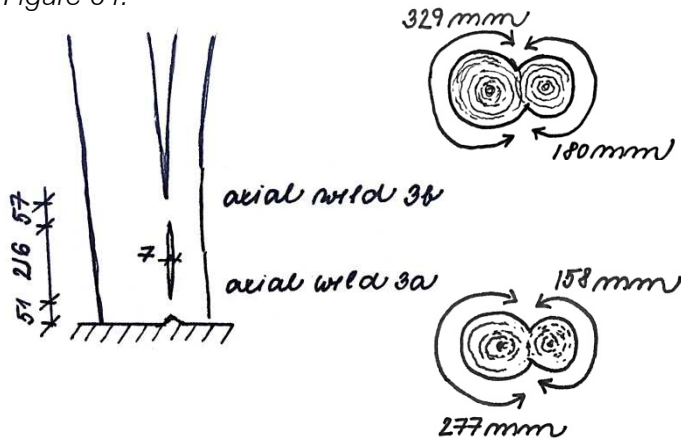


Figure 63. Minor connections between fine branches.

Axial welds of the support 3

Trees creating the support 3 are connected in two places above the ground as visible in Figure 64. Both connections are axial welds. One joint is located directly above the ground, 3a, but the bottom gap between the supports still can be found. The other one is in the height of 21,6 cm above 3a connection, 3b.

The geometry of these joints can be found in Figure 64.



Axial welds of the support 6

Trees creating the support 6 are, as the ones above, connected in two places above the ground as visible in Figure 65. Both connections are axial welds and they are the biggest axial welds of the structure. One joint, 6a, grows directly from the ground, so the separate stems below are not visible. The other one, 6b, is in the height of 224 mm above the connection 6a.

The geometry of these joints can be found in Figure 65.

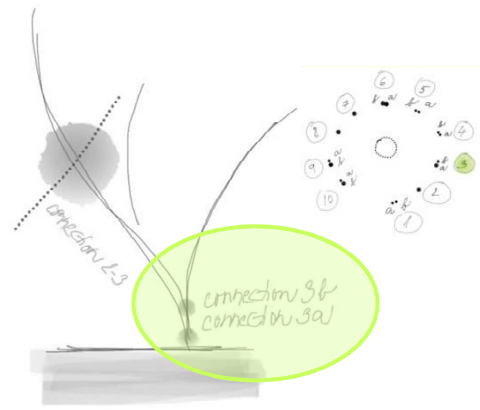
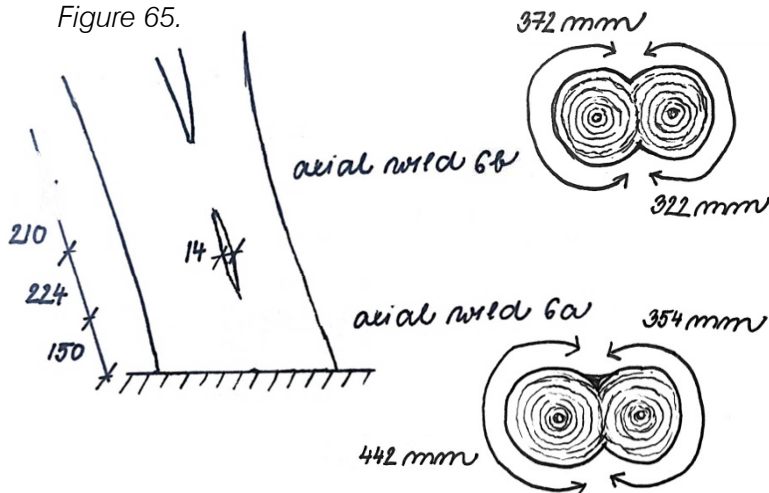


Figure 64. Axial welds 3a and 3b.

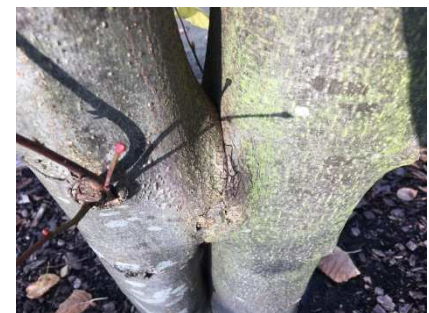
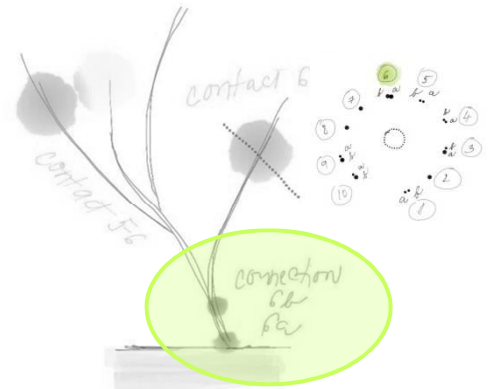


Figure 65. Axial welds 6a and 6b.

Cross weld between the support 2 & 3

The cross weld 2-3 is formed by the crossing of the trees 2 and 3A as visible in *Figure 66*. This connection is located approximately 1,9 m above the ground and the inner angle between the trees is 61 degrees. Since the trees 3A and 3B are also connected as mentioned above, the joint 2-3 basically forms a frame structure in which the trees 2, 3A and 3B cooperate. This connection is still tightened by a rope but it creates a solid joint.

The geometry of this joint can be found in *Figure 66*.

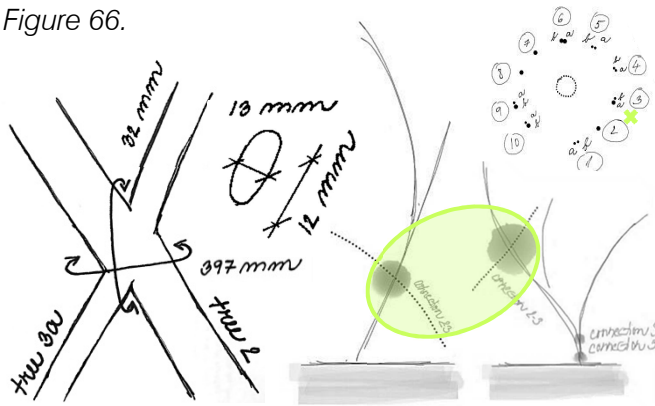


Figure 66. Cross weld between supports 2 & 3



Cross weld between the support 9 & 10

Trees 9B and 10A form the cross weld 9-10 which is located approximately 2,1 m above the ground. The inner angle of this connection is 98 degrees. Just as the joint above, also this joint is still tightened by a rope but it creates the solid joint, the biggest cross weld and one of the biggest welds of the structure at all.

The geometry of this joint can be found on the *Figure 67*.

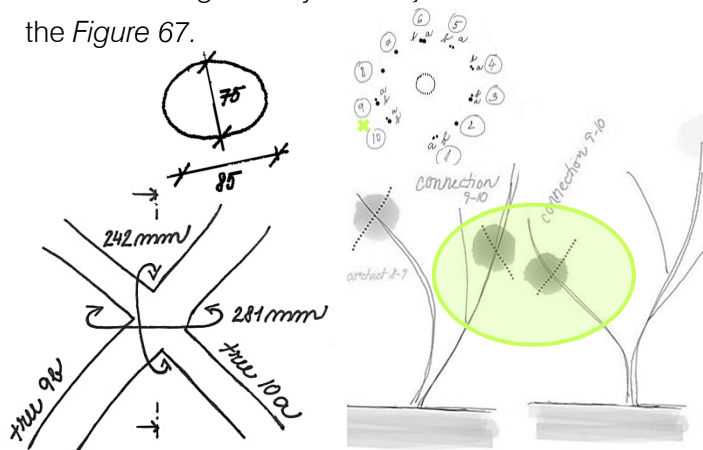


Figure 67. Cross weld between the support 9 & 10.



5.2.3. PULLING TEST

In order to gain real mechanical properties of trees creating the structure, pulling test was performed. The following chapter is devoted to description of the whole process, from preliminary calculations, through setup creation to testing itself. Individual steps can be divided as follows:

- step 1: preliminary calculations
- step 2: design, creation and transport of the setup
- step 3: pulling test
- step 4: calculations of the mechanical properties

Step 1: Preliminary calculations

Before the measurement itself, it was necessary to estimate the load-bearing capacity of trees in order to have an idea about the weights which can be used during the pulling test to see some reasonable deflection but on the other hand not to damage the trees. There were two approaches used during the calculation. First is the estimation of the maximal elastic deflection, respectively calculation of the maximal force which can be used to stay within the elastic behaviour of the material, thus get an idea about the maximal weight for the test. Second approach is the calculation of the weight necessary for 150 mm deflection. All the calculations are provided for each individual tree and can be found in detail in *Appendix A*. Both approaches and main outcomes are described below.

First step of the calculation is common for both approaches and it is the determination of wood strength. For this estimation, the value from strength qualities of ash stated in the *Houtvademecum* is used. Whereas these values are for treated wood without defects, it must be adjusted for live wood which has defects reducing this strength. Therefore the strength is reduced to only 25% according to research carried out by TU Delft.

$$f_{m,0,k} = 110 \text{ MPa}$$

$$f_{m,0,red} = 0,25 * 110 \\ = 27,5 \text{ MPa}$$

f_{m,0,k} ... bending strength for ash wood

f_{m,0,red} ... reduced bending strength

Now, it is necessary to find the strength class of wood which matches this result in order to use it as the representative class for the trees creating the Pavilion. Whereas the ash trees are deciduous, the searched class should be preferably for deciduous trees as well. The closest class is D30 which is the lowest class but it still exceeds the obtained value. In order to stay on the safe side during the pulling test, classes for coniferous trees are used. The most matching class is class C27 which values are slightly smaller than the calculated reduced strength and other properties of ash wood.

$$f_{m,0,rep} = 27 \text{ MPa}$$

$f_{m,0,rep}$... bending strength for class C27

Once the determination of class of wood is done, the first calculation can be performed. As already mentioned, first approach is based on the maximal bending strength of the trees within elastic area. This means that the caused deflection of a tree is elastic and thus a tree does not have any lasting damage after the testing. Main idea used for this calculation is following:

$$f_{m,d,rep} > \sigma_{m,d}$$

$f_{m,d,rep}$... 70% of $f_{m,d}$ – elastic area

$\sigma_{m,d}$... stress caused by the test

To stay within the elastic area, the stresses caused by pulling the trees must be smaller than maximal elastic bending strength which is approximately 70% of the total bending strength. From the above mentioned inequality, the bending moment can be easily calculated and thus force causing this moment.

$$\sigma_{m,d} = M_d / W$$

M_d ... bending moment

W ... section modulus

$$M_d = F_d * L$$

F_d ... pulling force

L ... lever arm

$$\text{Resulting inequality: } F_d < f_{m,d,rep} * W / L$$

To sum up, result of this calculation is the maximal force which can be theoretically used during the pulling test to see the maximal deflection without causing the lasting effect. The calculation was performed for each tree and all the resulting forces can be found in the summarizing *Table 5* below.

The second approach is based on the calculation of force needed for the deflection of 150 mm in the height of 2 m. This value was chosen as a suitable value for the test, mainly because it can be easily legible during the measuring. The calculation itself was based on the formula for deflection which is following:

$$\delta = \frac{1}{3} FL^3 / EI$$

δ ... caused deflection

F ... pulling force

L ... lever arm

E ... modulus of elasticity

I ... moment of inertia

Used elasticity modulus is a table value for above mentioned class C27 and the other values are calculated for each tree according to its geometry. From the above mentioned equation, the pulling force is given as follows:

$$F = (3 \cdot \delta \cdot E \cdot I) / L^3$$

All the resulting forces from the second approach can be also found in the summarizing *Table 5*.

Values from both methods are compared to check that any force which should cause the required deflection does not exceed the value of maximal force obtained from the first calculation. Therefore it is verified that all the trees allow the deflection of 15 cm within the elastic area.

TREES	FORCES [kN]		CONNECTION
	maximal elastic force	causing 150 mm deflection	
1A	0,15	0,05	-
1B	0,50	0,10	-
2	1,81	0,80	cross weld 2-3
3A	0,65	0,10	both types, 2-3 & 3-3
3B	0,11	0,05	axial welds 3-3
4A	0,09	0,02	-
4B	0,15	0,06	-
5A	0,14	0,04	-
5B	0,07	0,02	-
6A	2,18	2,47	axial welds 6-6
6B	1,33	1,13	axial welds 6-6
7	0,23	0,04	-
8	0,08	0,02	-
9A	0,11	0,03	-
9B	0,93	0,34	cross weld 9-10
10A	0,46	0,06	cross weld 9-10
10B	2,29	2,18	-

Table 5. Overview of the forces obtained from the calculations; maximal force which can be used for the pulling test and force causing the deflection of 150 mm. Also existence of the connections and their types are mentioned in the table.

However, the results from the calculations are based on the estimation and table values which can differ from the reality. Not only that the material characteristics can be different than the estimated ones but also the fact that the trees create connections between themselves can cause really different results of the test. Material can show better but also

worse mechanical properties caused by defects in wood for example, but on the other hand, the connection between trees makes the stiffness higher. Moreover, the choice of the strength class is underestimated. Therefore, also personal opinion based on the knowledge of the trees of the Pavilion was used as a final factor. This personal recommendation is included in the final *Table 6* for the pulling test.

Last step of the preparation for the pulling test is to select the trees which should be pulled. For easier comparison, always two trees of the similar geometry but one single standing and one with the connection are picked to be compared. Also one pair is created of two single standing trees just for comparison of the results obtained from the test. Following *Table 6* shows all the pairs of trees, the pulling forces obtained from the calculations and the personal recommendation.

TREES	RESULTS FROM TO THE CALCULATIONS				RECOMMENDED WEIGHT [kg]	JOINT
	force [kN] max elastic deflection	weight [kg]	force [kN] 150 mm deflection	weight [kg]		
1B 10A	0,50 0,46	50,9 46,9	0,10 0,06	10,2 6,1	20	single cross weld
9A 3B	0,11 0,11	11,2 11,2	0,03 0,05	3,1 5,1	10	single axial welds
7 4B	0,23 0,15	23,4 15,3	0,04 0,06	4,1 6,1	10	single single
10B 6A	2,29 2,18	233,4 222,2	2,18 2,47	222,2 251,8	50	single axial welds
1B 3A	0,50 0,65	50,9 66,2	0,10 0,10	10,2 10,2	20	single cross weld

Table 6. Overview of the tree pairs to be tested and compared. Table shows all the calculated forces including the personal recommendation.

Step 2: Design, creation and transport of setup

Whereas the idea is to pull the trees in the horizontal direction, parallel to the surface, the setup must be created. First thought was to create an arm which is attached to the ground so a rope tightened to a tree can go parallel to the ground over this arm and be loaded behind it (*Figure 68*). Therefore the setup is designed as a wooden board of dimensions approximately 1,2 x 1,2 metres to which a timber beam is attached. This beam's

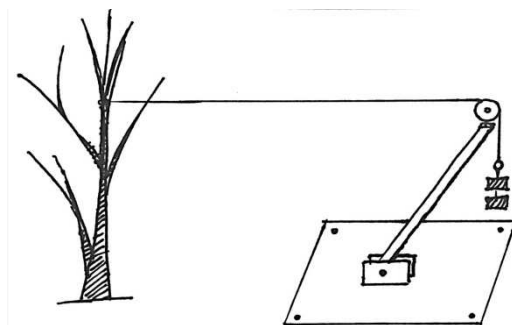


Figure 68. Setup concept.

cross-section is 50 x 120 mm and the length approximately 2,3 m. The beam is attached to the slab by joint which allows the movement and thus the angle between the beam and the ground can be always adjusted according to the requirements. This connection is formed by two wooden plates of 300 x 300 mm anchored to the slab which squeeze the beam, plus there is a hole drilled through so the connection can be tightened by the bolt (*Figure 69*). On the top of the beam, there is a rotating wheel attached, to allow an easy movement of a rope over the beam. To ensure that the setup is not sliding on the ground during the test, four holes in the corners are drilled through the board so it can be anchored to the ground by the bolts.

Dimension of the setup were estimated according to the preliminary calculations and thus according to the expected weights. Based on the above mentioned design, the setup was built by Ruben Kunz at the faculty of Civil Engineering and Geosciences at TU Delft and from there transported to the Botanical Garden of TU Delft with the help of Jan Moraal. The final setup and its transport can be found in *Figure 69*.



Figure 69. Pictures of the setup prepared for the pulling test and its transfer from the faculty of Civil Engineering and Geosciences to the Botanical Garden TU Delft.

Step 3: Pulling test

Pulling test was performed on the trees which were selected according to the results of the preliminary calculations and which are stated in *Table 6*. Trees with axial or cross welds were tested in two directions, radial and tangential, to determine the difference in stiffness caused by these connections. Single standing trees were tested only in the radial direction. In general, all the trees were pulled in the length of 2 metres of their stems. The reason why the distance was measured according to length, not height, is mainly because of the uneven terrain, thus this approach is more reliable.

When all the tools necessary for the pulling test were prepared in the garden, the test itself could be started. For summary, the tools are following (*Figure 70*):

- setup with all necessary bolts
- rope
- weights
- lath
- measuring tape



Figure 70. Tools necessary for the pulling test.

At first, the setup was assembled after the transport and the measuring tape used for determining the deflection was attached to the wooden lath (*Figure 70*). Measuring itself always started with placing the setup in front of the pulled tree, in case of measured radial deflection, or on side, in case of the tangential deflection, and anchoring it to the ground to prevent any possible movement. Then, a rope was tied around a tree at its length of 2 meters. One person standing by the pulled tree held the lath with attached measuring tape. This lath was placed in such a way that 0 on the tape was matching with the closest surface of the tree to the setup. The other end of the lath was placed on the ground. To ensure that the lath is standing vertically, a rope with weight was run down and the lath was placed alongside it. When everything was set, measuring itself could start. The weights were added in accordance with the results from the calculation, thereby accordingly created *Table*

6. The pulled tree started to move when weights were hung on the rope and in the moment when all weights were fixed to the rope, a person standing by the tree with read the number on the measuring tape, respectively the caused deflection. The process was also repeated backwards, 0 on the measuring tape was moved again to the closest surface to the setup and verticality of the lath was checked. When everything was set, the tree was released and the difference between deflected and still tree was read again. This process was repeated twice, sometimes even more times if the results considerably differed. When whole process was finished, the setup was moved to another position and whole measuring started again.



Figure 72. Preparations before the measurement. From left: assembly of the setup after transport, attaching the measuring tape to the lath and preparation of the system of weights.



Figure 71. Measuring of the deflection, before and after.



Figure 73. Pulling test.

Despite the fact that the test was thoroughly prepared, some imperfections appeared during the measuring. In order to make future researches easier and more accurate, the following paragraph describes the things that should be improved or should be a subject to reflection in the future. The list of above mentioned points of attention is stated below and their description follows.

- weights
- used materials
- root control
- measurement accuracy

The weight system consisted of the metal rod on which the weights were hung and whole system was tied to the rope (*Figure 72, Figure 73*). Whereas the manipulation with weights, hanging them on the rod, was not as easy as expected, the maximal weight used during the test was only 36 kg, not planned 50 kg. It was caused mainly by the way how the weights are hung on the pole. Slot in the weight is really small, just slightly bigger than the circumference of the rod and thus the manipulation can become difficult due to heavy weight, especially when some weights had corrosion which was not so significant. However, the main limiting factor was strength of the person controlling the setup, in this case mine.

As stated further, in the chapter devoted to the results of the test (*Table 7*), the deflections were in certain cases very small, so in future, heavier weights should be used during the test. Therefore the system of weights should be adjusted to facilitate manipulation with weights for the person controlling the setup.

Another remark is about the used materials. Whole setup is from timber and under higher load, cracking was heard. Therefore, use of different material, preferably steel, should be considered in the future and thereby appropriate dimensions and connection between the beam and the slab. Also the rope should be chosen properly because the textile one used during the test prolonged itself slightly under heavy load and this also caused sometimes difficulties. Therefore a wire which is underset by some softer material in the contact with a tree could be better an option for the future testing.

Special point of interest is the root behaviour. It should be controlled during the testing whether there is any movement of the roots and taken it into account during the calculations. In this case, it was really difficult to distinguish the movement because the terrain is very uneven and thus more sophisticated system for the root movement control should be designed. Next calculations are performed without taking root movement into account. It could be said that this approach for the calculation of the tree stiffness is rather on the save side because the assumption is that whole deflection is caused only by the bend of a tree, not movement of tree itself even with the roots.

In general, the root behaviour is naturally very important and its movement can endanger whole structure and therefore, it should be considered during the test and then in

the calculations in the future. However, as already said, the root system and its effect to whole structure is topic itself which should be investigated but it is not the main content of this thesis.

Last mention is devoted to measurement accuracy. Two circumstances during the measuring could cause inaccuracies and that is position and stillness of the lath with the measuring tape and parallelism between the rope and the ground. Although, there was an effort to make measurement as accurate as possible, these two factors are not 100% reliable and that is mainly because of the terrain inequality and human factor. This is also the reason why each measurement was provided in total at least 4 times to ensure the credibility of the result. However, these two circumstances may be also subject to reflection for the future researches.

Step 4: Calculation of the mechanical properties

As already mentioned in the previous chapter, the resulting deflections were smaller than expected, sometimes even 2 mm. Despite all mentioned circumstances which could cause inequalities, the results can be considered as reliable. Results of the pulling test and whole calculation including all tables with below mentioned comparisons can be found in *Appendix B*. All main values are mentioned and described in this chapter.

All resulting values, primarily weights and deflections, for selected trees are stated in *Table 7* below. The table is divided into two directions, radial for all tested trees and tangential for interconnected trees.

TREE	RADIAL DIRECTION			TANGENTIAL DIRECTION			LEVEL ARM [m]	WELD
	weight [kg]	force [kN]	deflection [mm]	weight [kg]	force [kN]	Deflection [mm]		
1B	12	0,118	55	-	-	-	1,89	-
3A	24	0,235	5	36	0,353	3	1,78	axial, cross
3B	12	0,118	48	12	0,118	24	1,88	axial
4B	12	0,118	115	-	-	-	1,88	-
6A	36	0,353	8	36	0,353	2	1,79	axial
7	12	0,118	43	-	-	-	1,85	-
9A	12	0,118	52	-	-	-	1,85	-
10A	20	0,196	20	24	0,235	2	1,67	cross
10B	32	0,314	10	-	-	-	1,85	-

Table 7. Results from the pulling test.

The analysis of the results is divided into two parts, part about the single standing trees where the main subject is to determine the modulus of elasticity and part about the

interconnected trees where the main focus is on influence of the connection on stiffness of the structure.

Single standing trees

First part of the calculation is devoted to determination of the modulus of elasticity of the single standing trees. The calculation is based on formula for deflection which was already used for the preliminary calculations. This formula is following:

$$\delta = \frac{1}{3} FL^3 / EI$$

δ ...caused deflection

F ... pulling force

L ... lever arm

E ... modulus of elasticity

I ... moment of inertia

Whereas the outcome from the pulling test is deflection according to certain force, the resulting modulus of elasticity can be calculated as follows:

$$E = \frac{1}{3} FL^3 / I\delta$$

The rope was always tied in the length of 2 meters of a tree. Whereas the trees are not straight but they are under certain angle and sometimes even bent, the height of the pulled spot above the ground is considered as a lever arm. This approach is rather pessimistic because the obtained modulus of elasticity is smaller but this manner is on the side of safety as the modulus of elasticity should not be overestimated.

TREE	FORCE [kN]	DEFLECTION [mm]	LEVER ARM [m]	RADIUS [m]	HEIGHT [m]	MOMENT OF INERTIA [m ⁴]	ELASTICITY MODULUS [MPa]
1B	0,118	55	1,89	0,023	4,4	2,35668E-07	20 439
4B	0,118	115	1,88	0,021	3,6	1,44147E-07	15 729
7	0,118	43	1,85	0,019	3,9	1,01209E-07	57 090
9A	0,118	52	1,85	0,018	3,8	7,66166E-08	62 362
10B	0,314	10	1,85	0,050	5,2	5,03245E-06	13 165

Table 8. Single standing trees, their deflections and resulting modulus of elasticity.

From the results, which are stated in *Table 8*, can be visible that the resulting values are to some extent similar except for the trees 7 and 9A. There are several scenarios which can cause this big difference. As already mentioned, the radius of the trees does not radically differ in the spot where the rope is tied during the pulling test but that does not mean that the difference cannot be caused by the shape. One possibility could be that trees 7 and 9A have proportionally bigger cross-section of the trunk above the ground than the other trees and

therefore their stiffness could be higher. For this reason, *Table 9* with an overview of circumferences by meter of a trunk follows. It also shows reduction of the circumferences along the trunks, in 1 and 2 meters.

TREE	CIRCUMFERENCE AT THE LENGTH OF [mm]			PROPORTIONAL REDUCTION OF THE CIRCUMFERENCE (percentage of cross-section)		
	0 m	1 m	2 m	0m	1 m	2 m
1B	314	200	147	100,0 %	63,7 %	46,8 %
4B	211	157	130	100,0 %	74,4 %	61,6 %
7	242	182	119	100,0 %	75,2 %	49,2 %
9A	189	148	111	100,0 %	78,3 %	58,7 %
10B	626	386	316	100,0 %	61,7 %	50,5 %

Table 9. Overview of the circumferences and their reduction along the trunk.

As can be seen from *Table 9*, trees 7 and 9A reduced their cross-section at 2 meters to its half. In comparison to other trees, this reduction is nothing special so the reason for such difference in the modulus of elasticity can be probably caused by something different.

Another idea is also connected to a tree shape but in this case, to its straightness, or rather its bend, and slope. As visible from *Figure 74* (first and second from the left), tree 7 is very straight without any significant slope, while tree 9A is bent on the side. Shape of the rest of trees is also very different so it hard to find any common feature which could lead to such significant higher stiffness.



Figure 74. Pictures showing shapes of the single standing trees which were tested during the pulling test. From the left: 7, 9A, 1B, 4B, 10B.

Very likely, the increased stiffness of trees 7 and 9A is caused by several factors together. Shape of the trees certainly plays its role, although there is no specific feature which could be pointed out. The truth is that on the tension side of a trunk (permanent

tension, not during the test), there is so-called reaction wood which is stiffer than rest of the cross-section, as already mentioned in the chapter devoted to tree biomechanics. Therefore, if a tree was pulled during the test against this tension wood, more than others, the resulting deflection could be smaller and thus calculated modulus of elasticity higher. For the future researches, resistant drill measurement could be performed as well. This measurement reveals the location of the reaction wood inside the structure which can be useful. Another influencing factor can be roots and their movement or on the other hand firm anchorage. In the end, as visible from the results shown in *Table 8*, the differences in deflections are small but in combination with other values, used in formula for determination of the modulus of elasticity, cause big difference. Even though, the measuring was performed as precisely as possible, some small inaccuracies could occur, mainly because of above mentioned comments to the test process, and could have their influence on the final result.

Whereas the calculated modulus of elasticity is used as a help or reference for determination of as corresponding strength class of wood as possible, and thus defining the maximal strength of the trees which is used for further calculation of the load-bearing capacity, the lowest measured stiffness, respectively modulus of elasticity is used for this assumption. The lowest value is 13,1 GPa and the strength classes for wood with similar modulus of elasticity are following:

- D40: Bending strength 40 MPa, Modulus of elasticity 13,0 GPa
- D45: Bending strength 45 MPa, Modulus of elasticity 13,5 GPa
- C35: Bending strength 35 MPa, Modulus of elasticity 13,0 GPa

Although, the Pavilion is created by ash trees which should be compared to strength classes of deciduous trees, also classes for conifers are used in order to find the most matching class.

According to EN1912:2002, ash wood is comparable to class D40 which properties are mentioned above. As visible, the value of resulting modulus of elasticity from the pulling test relatively corresponds to the value from the tables for ash wood. Even though the strength is not proportional to the modulus of elasticity, it should be mentioned that the smallest resulting modulus of elasticity, based on the pulling test, is still slightly higher than the table value for the strength class D40. However, the table values are determined by testing wood without any defects, such as for example knots or undesirable course of fibres. On the other hand, the value is given for sawn timber which has considerably lower strength than round wood. Therefore, the strength class D40 is used for the following calculations. The value is further reduced due to high moisture content which negatively influences the strength.

This approach is realistic, whereas the class C27 used during the preliminary calculations was very pessimistic.

Interconnected trees

In terms of interconnected trees, the main focus is on the connections between the trees and their influence on the stiffness of a structure. Therefore these trees were pulled in the radial but also in the tangential direction. All the values obtained from the test are stated in *Table 10* below.

TREE	RADIAL DIRECTION		TANGENTIAL DIRECTION		RADIUS [mm]	WELDS
	F [kN]	δ [mm]	F [kN]	δ [mm]		
3A	0,235	5	0,353	3	23	axial welds, cross weld
3B	0,118	48	0,118	24	20	axial welds
6A	0,353	8	0,353	2	52	axial welds
10A	0,196	20	0,235	2	20	cross weld

Table 10. Interconnected trees and their results from the pulling test.

Whereas the same weight was used during the test for both directions for trees 3B and 6A, their stiffness in these directions can be directly compared depending on their radius. As visible from *Table 10*, tree 3B has twice smaller deflection in the tangential direction and tree 6A even four times smaller. This difference is naturally caused by the connection between the trees which positively influence the bend, reduce it, in the direction parallel to the connection.

To describe the influence of connection between the trees more in detail, behaviour of a single standing tree and interconnected is compared in the following *Table 11* and *Table 12*. There are four pairs of trees, always one single standing tree and one tree interconnected with others. The single standing tree is an imaginary tree which has the same geometry as the interconnected tree and the modulus of elasticity of another real single standing tree which has similar geometry as the interconnected one. This imaginary tree is basically the interconnected tree converted into the single standing. Then, the deflection for the force used during the test for the interconnected tree is calculated for the single tree. The formula used for this calculation is the same as the above mentioned:

$$\delta = \frac{1}{3} FL^3 / EI$$

δ ...caused deflection

δ^R for radial and δ^T for tangential direction

F... pulling force

L... lever arm

E... modulus of elasticity

I... moment of inertia

One assumption has to be done and this is that this new created tree has the same modulus of elasticity as another real single standing tree. This single standing tree has been selected

in the preliminary calculations, as stated in *Table 6*. Result from this conversion is clearly visible difference between the behaviour of single standing and interconnected tree with the same geometry and roughly the same modulus of elasticity. The comparison is performed for both directions, radial and tangential, with regard to the existence and type of the connection.

Following *Table 11* describes tree behaviour in the radial direction. Deflection for the single standing imaginary trees is calculated and compared with the real measured deflection of the interconnected trees.

SUPPORT	FORCE F [kN]	MODULUS OF ELASTICITY [MPa]	RADIUS [m]	DEFLECTION δ^R [mm]	RATIO*	WELDS
3A	0,235	-	0,023	0,005	23,8	axial, cross
single 3A		20 439		0,119		-
3B	0,118	-	0,020	0,048	2,3	axial weld
single 3B		20 439		0,102		-
6A	0,353	-	0,052	0,008	1,1	axial weld
single 6A		13 165		0,009		-
10A	0,196	-	0,020	0,020	5,0	cross weld
single 10A		20 439		0,099		-

Table 11. Comparison of the converted single standing and interconnected trees in the radial direction.

* ratio between the deflections of the single and interconnected trees

According to results in *Table 11*, interconnected trees contribute to the higher stiffness in the radial direction. Moreover, trees which are connected by cross welds have smaller deflection in the radial direction in comparison to the trees with axial welds. But still, even their deflection is smaller than could be expected from single standing trees. Whereas the radius of trees 3A, 3B and 10A is similar, the effect of different types of welds can be compared. It is clearly visible that the axial welds contribute less because while using the smallest force, tree 3B has the biggest deflection. On the other hand, cross welds, which are present within trees 3A and 10A, contribute to higher stiffness much more because the used force was higher but deflection much smaller. It is also possible to speculate about the advantage of combination of an axial and cross weld, as can be seen on tree 3A. However, it is not really clear from the numbers how more the combination influences the stiffness in the radial direction. But still, taken into account that tree 3A was pulled by higher force on slightly bigger cross-section, the deflection is still four times smaller than the one for tree 10A, thus the influence of double connection is significant.

The same comparison is provided also for the tangential direction where the trees with welds should show higher stiffness. Following *Table 12* is based on the same principle as the previous one for the radial direction but in this case, one assumption has to be made. Whereas the single standing trees were pulled only in the radial direction, the assumption for

this comparison is that these trees have the same deflection even in the tangential direction. Therefore the following comparison is rather rough, to give an idea about the influence of the connections in this direction. However, the difference in the deflection for the single standing trees in the tangential direction should not be significantly different than in the radial direction.

SUPPORT	FORCE F [kN]	MODULUS OF ELASTICITY [MPa]	RADIUS [m]	DEFLECTION δ^T [mm]	RATIO	WELDS
3A	0,353	-	0,023	0,003	33,0	.axial, cross
single 3A		20 439		0,099		-
3B	0,118	-	0,020	0,024	4,3	axial weld
single 3B		20 439		0,102		-
6A	0,353	-	0,052	0,002	4,5	axial weld
single 6A		13 165		0,009		-
10A	0,235	-	0,020	0,002	107,0	cross weld
single 10A		20 439		0,214		-

Table 12. Comparison of the single standing and interconnected trees in the tangential direction.
* ratio between the deflections of single and interconnected trees

As obvious from the results stated in Table 12, the interconnected trees have naturally much smaller deflection in comparison to single trees. However, this finding is not so surprising because more material is placed in this direction, thereby higher force is necessary for causing the same deflection as a single tree has. Nevertheless, comparison between different types of connections is interesting. Trees with axial welds, which are located above the ground, do not have as radically different deflections as trees with cross welds. However, the difference is still very significant. Interesting fact is that both trees with



axial welds have very similar ratio of the deflection of the real interconnected tree and modelled single tree. Whereas both connections started to be formed at approximately same age of the trees, they are very proportional to their trunks and thus could be really roughly said that, in this case, axial welds can reduce the deflection more or less 4 times (Figure 75).

Figure 75. Axial welds of trees 6 (left) and 3 (right).

Whereas the cross welds are located in the height of approximately 2 meters, framework structure is created from the trees and therefore they are very stiff in this direction. According to *Table 12*, tree 10A can give a feeling that combination of axial and cross welds, which can be found within tree 3A, does not influence the resulting stiffness in the tangential direction but the opposite is true. Tree 10A has very massive cross weld while cross weld of tree 3A is substantially smaller (*Figure 76*). So although, it may not be obvious at first glance, another two solid connections, of tree 3A with its neighbouring tree, also influence the resulting deflection.



Figure 76. Cross welds between trees 9B & 10A (left) and 2 & 3A (right).

According to above mentioned, the presence of welds connecting the trees has a significant influence to overall stiffness of the structure. Tree welds do not effect trees only in the tangential direction, as could be expected, but also in the radial direction. In this case, mainly cross welds radically decrease the deflection. This is primarily caused by their location which is in bigger height, around two meters, in comparison to axial welds which are located above the ground. Speaking about tangential direction, existence of any weld radically decreases the deflection and thus makes the structure stiffer. Again, cross welds have more significant influence than axial welds but even in this case, it is substantially caused by the location higher above the ground. Resulting effect of the interconnection of the trees is also dependant on the size of the joints.

Regarding the future researches, one point of interest could be the influence of size and amount of the joints within one tree to the stiffness. To compare whether structure with more small joints (related to size of a trunk) is in result more resistant to bending than structure with one massive joint located on the ideal position. Another subject for the investigation is the weld itself, its structure, course of fibres and their effect on the stiffness of the weld itself and thus on the structure.

6. CALCULATION OF THE LOAD-BEARING CAPACITY OF THE PAVILION

This chapter is devoted to the main purpose of this project, therefore to the evaluation of the structure. Calculation process is divided into following steps:

- description of the previous calculations
- calculation of permanent and variable loads
- combinations of actions
- calculation of the current load-bearing capacity
- estimation of time when the load-bearing capacity is sufficient

Whole calculation approach with all the main outputs is described in the following text and detailed calculation including all the necessities is given in *Appendix C, D and E*.

6.1. DESCRIPTION OF THE PREVIOUS CALCULATIONS

The first estimation of the load-bearing capacity of trees has been done in 2010 by the designer of the Pavilion. The result from the calculation was that the load-bearing capacity is sufficient in year 2021, thus 10 years from the creation of the structure.

The approach of the calculation was following. Whereas the structure has not existed yet, all the wood characteristics, growth rate and other values had to be taken from the tables. First step of the calculation was to estimate growth rate. According to The Shodor Education Foundation 2002 and their formula for growth of hardwood, a speed was estimated at approximately 500 mm gain in length per year and 20 mm gain in circumference per year. Also wood strength had to be estimated. Estimation was based on the real table values for wood classes. Strength of ash wood was reduced because of the imperfections of live material in comparison to treated timber.

When all the necessary characteristics had been estimated, all the loads influencing the structure were calculated and the most critical scenario was found and applied on a five-year old and ten-year old structure. The result of the calculation was, as already mentioned, that the living structure itself should be able to carry the platform in 10 years from its formation. [9]

As clearly obvious, the calculation contained lot of estimations. Moreover, the composition of the structure has changed, therefore the result of the further calculation could be significantly different and it is not really relevant to compare it to the estimation from 2010.

6.2. CALCULATION OF PERMANENT AND VARIABLE LOADS

All the loads on the structure can be divided into two groups, permanent and variable loads, and their list is following:

- own weight of the trees
- own weight of the platform and the railing
- imposed load
- snow load
- wind load

Calculation of all above mentioned loads is described below and all the details can be found in *Appendix C*.

Own weight of the trees

The weight of the trees is based on the density of fresh, thereby wet, ash wood. These values are in the range of 750 to 1150 kg/m³ [6]. The highest value, thus 1150 kg/m³, was used during the calculations. Whereas each tree has different shape, both length and diameter differs, only load per cubic meter is calculated for now. This value was easily obtained from formula:

$$q_{k,tree} = \rho_{rep} * g$$

$q_{k,tree}$... own weight of tree

ρ_{rep} ... density of live (wet) ash wood

g ... gravitational acceleration

The resulting characteristic load is 11,3 kN/m³. Further in the calculations, the own weight is applied as a linear non-uniform load. Shape of a tree is simplified to a cone shape and the load distribution copies the circumference change of a trunk (*Figure 77*). Such simplified model is very realistic.

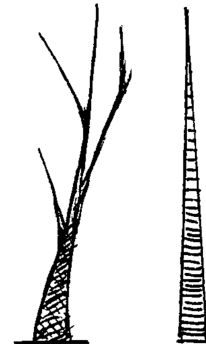


Figure 77. Simplification of tree shape to a cone.

Own weight of the platform and the railing

The load caused by the platform and the railing was counted per square meter. For simplification, load caused by the railing was converted to square meter of platform area.

Calculation itself is similarly like the previous one based on formula:

$$Q_{k,platform} = \rho_{platform} * g * t * A_{platform}$$

$Q_{k,platform}$... own weight of the platform

$\rho_{platform}$... density of material of the platform

g ... gravitational acceleration

t ...thickness of the platform

A_{platform} ... platform area

The weight of the railing is given in Newton per meter, thus the load is counted only by multiplying it by its length. As already mentioned the railing load was converted to the platform area as follows:

$$q_{k,tot} = (Q_{platform} + Q_{railing})/A_{platform}$$

Q_{k,platform} ... own weight of the platform

Q_{k,railing} ... own weight of the railing

A_{platform} ... platform area

The resulting characteristic load is 1,7 kN/m².

Imposed load

Whereas the Living Tree Pavilion is situated in a public place where people can arbitrarily enter the platform, category B for the imposed load was chosen. However, it should be noted that this is not a place where people can congregate because of its small size. Amount of persons entering the platform is currently limited to three by the sign placed on the staircase but it is certainly impossible to rely on it. Thought, people appear there only occasionally and for a short time.

According to NEN-EN 1991-1-1/NB, the value of imposed load for category B is 2,6 kN/m².

Snow load

According to NEN-EN 1991-1-3:2003/NB:2007, is it not necessary to consider any exceptional snow loads in the Netherlands, thus only normal conditions are applicable. The design is used for both, transient and persistent design situation. All the parameters necessary for the calculation were taken from NEN-EN 1991-1-3/NB. The calculation according to NEN-EN 1991-1-3:2003 is following:

$$s = \mu_i * C_e * C_t * s_k$$

s ... snow load

μ_i ... snow load shape coefficient

C_e ... exposure coefficient for the Netherlands

C_t ... thermal coefficient for the Netherlands

s_k ... characteristic value of snow load

The resulting snow load is 0,56 kN/m². Considering tree shape and snow conditions in the Netherlands, snow load acting on the trees can be neglected in the calculations.

Wind load

Whereas, the wind load is dependent on the height of a structure, the calculations were provided for the current length of the tallest tree, thus they are on the safety side. This tree measures 5,59 m and thereby exceeds the entire construction. Whole calculation is based on NEN-EN 1991-1-4/NB, also all the necessary parameters are taken from this norm.

First step of the calculation was to find the peak velocity pressure which is based on following formula:

$$q_p(z) = c_e(z) * q_b,$$

$q_p(z)$... peak velocity pressure
 $c_e(z)$... exposure factor
 q_b ... basic wind pressure

Above mentioned characteristics are dependent on many other parameters which are described in detail in Appendix C where whole calculation can be found.

Peak velocity pressure is just the general pressure caused by wind and must be adjusted, reduced or increased, according to the position of an element within the construction. This adjustment is provided by so-called external and internal pressure coefficients as follows:

$$w_e = C_{pe} * q_p(z)$$

$$w_i = C_{pi} * q_p(z)$$

w_e ... external wind pressure
 C_{pe} ... external pressure coefficient
 w_i ... internal wind pressure
 C_{pi} ... internal pressure coefficient
 $q_p(z)$... peak velocity pressure

The value of coefficients depends on the location of an element, whether it is located on the windward or the leeward side or parallel to the wind direction. Whereas this structure is not a typical building which can be divided into parts according to the norm and be easily calculated depending on the assigned coefficients, the calculation must be slightly adjusted.

Figure 78. Positive and negative pressure. (NEN-EN 1991-1-4:2005)

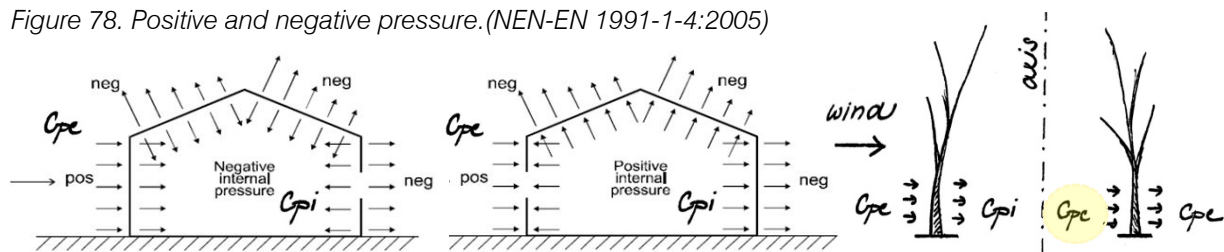


Figure 79. Use of the coefficients for the calculation.

Calculation of the Living Tree Pavilion is based on the calculations from the standard but use of the coefficients is slightly adjusted to match the reality as much as possible. Whereas the internal coefficients are normally used as shown in *Figure 78*, naturally inside the structure, in this calculation the coefficients were used as shown in *Figure 79*. Instead of the internal coefficient on the leeward side inside the building, the external coefficient is used. Reason for this change is the fact that the structure is not tight, that means that the wind can blow through the structure and however its strength gets smaller inside the structure, it is safe to calculate with higher coefficient which the external coefficient is.

Another small adjustment was in the direction parallel to wind. There the maximum external pressure coefficient was uniformly used for the whole side, not only for its part. This decision was made for simplification of the calculation, moreover it is on the side of safety. How the coefficients are used within the structure is shown in *Figure 80* and *Figure 82* (the changes are highlighted) and the resulting pressure is stated in *Figure 81* and *Figure 83*.

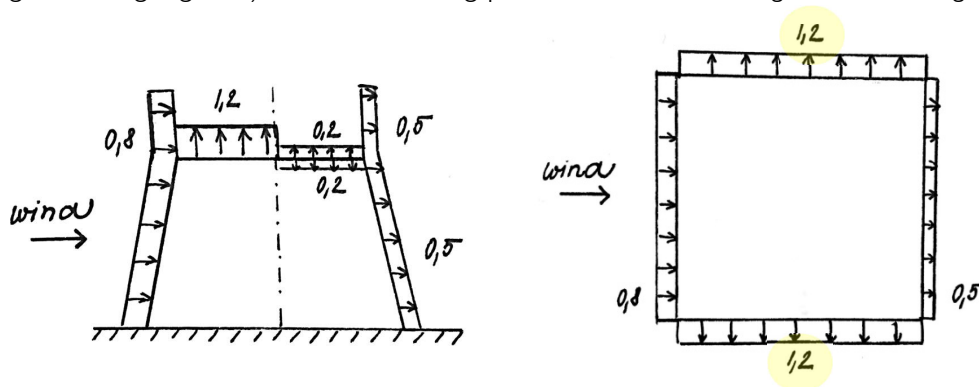


Figure 80. External pressure coefficients shown on the simplified vertical and horizontal schema (from the left).

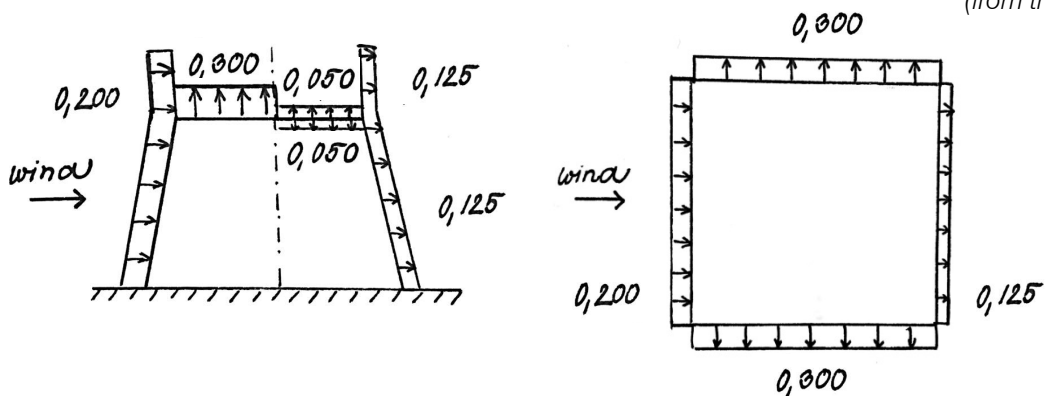


Figure 81. Wind pressure action on the external surfaces shown on the simplified vertical and horizontal schema (from the left).

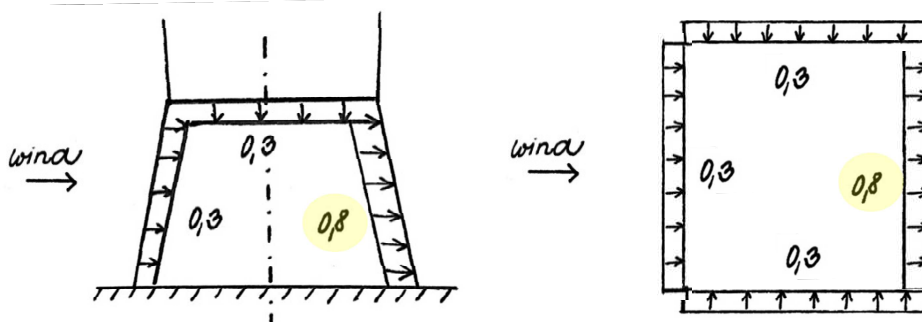


Figure 82. Internal pressure coefficients shown on the simplified vertical and horizontal schema (from the left).

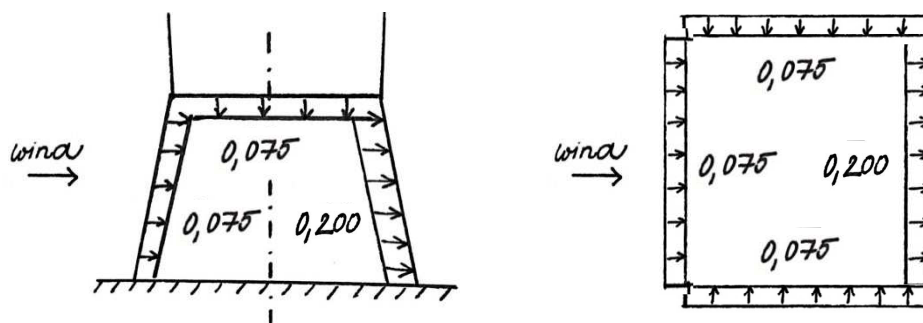


Figure 83. Wind pressure action on the internal surfaces shown on the simplified vertical and horizontal schema (from the left).

As visible from the figures above, shape of the Pavilion is during the calculation for simplification considered as a square, while it is in reality a round. This approach is on the side of safety because the rounded shape does not catch as much wind as a square shape. In general, calculation of the wind load is provided with a pessimistic approach and therefore the resulting effect on the structure should be in reality smaller.

All the characteristic values of loads acting on the structure are for better orientation summarized in following Table 13.

TYPE OF LOAD		CHARACTERISTIC VALUE [kN/m ³]	CHARACTERISTIC VALUE [kN/m ²]	CHARACTERISTIC VALUE [kN]
Own weight of the trees		11,282	-	-
Own weight of the platform		-	1,732	5,893
Own weight of the railing		-	-	8,557
Imposed load for category B		-	2,600	21,691
Snow load		-	0,560	-
Wind load	Trees windward out	-	0,200	-
	Trees windward in	-	0,075	-
	Trees leeward out	-	0,125	-
	Trees leeward in	-	0,200	-
	Trees side out	-	0,300	-
	Trees side in	-	0,075	-
	Platform windward out half	-	0,300	-
	Platform leeward out half	-	0,050	-
	Platform in	-	0,075	-

Table 13. Summary of characteristic values of all loads.

6.3. COMBINATIONS OF ACTIONS

Living Tree Pavilion is verified in accordance with the following:

- life category 3
- consequence class 2
- indicative design working life is 50 years

These criteria were chosen according to the characteristics of the Pavilion and according to the main goal for such types of structures, to use them for variable purposes.

Following two paragraphs are devoted to the description of two design states, ultimate limit state and serviceability state.

Ultimate limit state

Following calculations are provided according to structural ultimate limit state (STR). Whereas the strength of the material governs, loss of static equilibrium (EQU) is not appropriate. Also the behaviour of roots influencing the stability of the structure as a whole, but also the soil under the structure, was not examined, therefore geotechnical ultimate limit state (GEO) is not relevant neither. And fatigue ultimate limit state (FAT) is for this type of structure basically impossible to define at the moment. Thus, only STR ultimate limit state is verified during the calculations, other limit states, such as EQU, GEO and FAT are not really relevant for this calculation.

Combination of actions for persistent and transient design situations are following:

$$\sum \gamma_{G,j} G_{k,j} + \gamma_P P + \gamma_{Q,1} \psi_{0,1} Q_{k,1} + \sum \gamma_{Q,i} \psi_{0,i} Q_{k,i}$$

$$\sum \xi_j \gamma_{G,j} G_{k,j} + \gamma_P P + \gamma_{Q,1} Q_{k,1} + \sum \gamma_{Q,i} \psi_{0,i} Q_{k,i}$$

G_k ... characteristic value of the a permanent action

Q_k ... characteristic value of the a variable action

P ... prestress

(NEN-EN, 1990:2002)

Values of γ factors, concerning the limit static equilibrium of the structure, are:

$\gamma_G = 1,2$ or $1,35$ factor for an unfavourable permanent action

$\gamma_G = 0,9$ factor for a favourable permanent action

$\gamma_Q = 1,5$ factor for a permanent action

(NEN-EN, 1990/NB)

Values of ψ factors for the variable loads are:

$\psi_0 = 0$ snow and wind load

$\psi_0 = 0,5$ imposed loads, category B (offices)

(NEN-EN, 1990/NB)

Finally the combinations of actions for the ultimate limit state of the Pavilion are following:

$$I) \gamma_G G_{k,trees} + \gamma_G G_{k,permanent\ load} + \gamma_Q Q_{k,imposed\ load}$$

$$II) \gamma_G G_{k,trees} + \gamma_G G_{k,permanent\ load} + \gamma_Q Q_{k,snow} + \gamma_Q \psi_{0, imposed\ load} Q_{k,imposed\ load}$$

$$III) \gamma_G G_{k,trees} + \gamma_G G_{k,permanent\ load} + \gamma_Q Q_{k,wind} + \gamma_Q \psi_{0, imposed\ load} Q_{k,imposed\ load}$$

Whereas the wind load acts in different directions on the structure, the combination concerning the wind load has several forms. When the acting force is directed outside the structure, the used value of γ factor for the permanent load is 0,9. Use of the value 1,2 could cause false favourable behaviour. In other case, value 1,2 is used.

Serviceability limit state

Combinations of actions for the serviceability limit state are the same as for the ultimate limit state. The difference is in the value of γ factor which is in this case 1,0, for both, permanent and variable actions.

6.4. CALCULATION OF THE CURRENT LOAD-BEARING CAPACITY

The main goal of whole project of Living Tree Pavilion is to remove the temporary structure, created by the braces, and use only the trees as the load-bearing structure. At the moment, the trees certainly do not have sufficient load-bearing capacity to support the platform at the height of 4 m. Therefore, the following calculations are devoted to determining their current load bearing capacity at the height of 2 m. This height was chosen due to the current geometry of the trees. Circumference of majority of the trees is very small at the height of 4 m, rather only fine branches reach this height, thereby it is unsuitable to determine the load-bearing capacity there. In the height of 2 m, each tree has a reasonable circumference.

Calculation itself consists of two steps, first is modelling the trees in the software SCIA Engineer and second is verification of the load-bearing capacity. Detailed description of the calculation is given in *Appendix D*.

Modelling of the trees in the software SCIA Engineer

In order to determine the load-bearing capacity of each tree of the Pavilion, each tree separately is modelled in the software, also with connections taken into account. Trees are loaded by their own weight according to the circumference, thus by non-constant linear load. Other loads are weight of the platform and the railing, imposed load, snow load and wind load (*Figure 84*). All three above mentioned combinations are used during the simulation. One assumption has been made for modelling the structure and thus that the total weight of the vertical load (platform, railing, imposed load and snow load) is distributed equally between all 16 trees. Therefore each tree is modelled to carry 1/16 of the total value. In reality, this distribution is different according to the stiffness of each support but for simplification of the calculations, the distribution is considered equal. Moreover, main goal of this calculation is to determine the current load-bearing capacity, or rather whether the trees are able to carry the platform in the height of 2 m, therefore this assumption is possible.

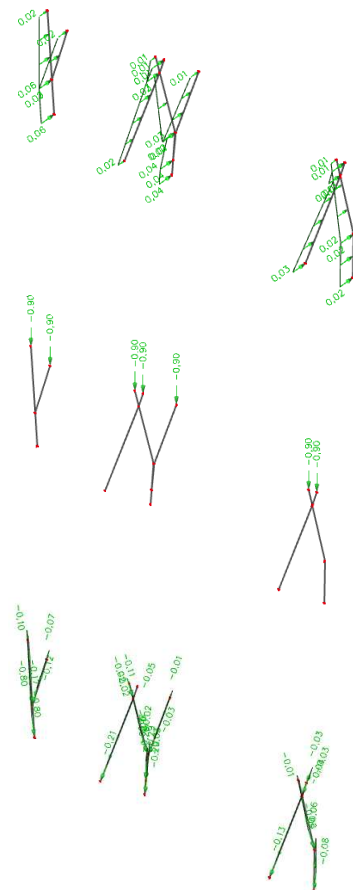


Figure 84. Examples of the modelled elements in the software Scia Engineer.

From the top: wind load, vertical load, own weight.

From the left: support 6, interconnected supports 2 and 3, interconnected supports 9 and 10.

The trees are loaded by wind, by the value calculated for the windward side.

Shape of the trees is simplified. Trees which are in reality more or less direct are modelled direct as well. Bent trees are modelled as a broken line, thus rate of bent of tree is adjusted each meter. The angles, radial and tangential, or rather slope is based on the real measurements provided in the Botanical garden.

The main objective of this simulation is to obtain the data for the following verification, thus to find out the tentative current load-bearing capacity and to give an idea about the state of the structure. Result also serves as a basis for the estimation of time when the structure is strong enough to carry the platform only by itself.

Data obtained from the simulation are stated in *Table 14*.

TREE AND MAXIMAL FORCES	COMBINATION I			COMBINATION II			COMBINATION III		
	N _d	M _d	V _d	N _d	M _d	V _d	N _d	M _d	V _d
1B	3,36	1,24	0,58	2,80	1,02	0,48	2,36	0,89	0,44
2	3,49	2,82	1,06	2,95	2,33	0,87	2,53	1,99	0,76
3A	3,14	2,15	1,26	2,62	1,77	1,04	2,20	1,48	0,88
3B	3,14	1,66	1,01	2,60	1,37	0,83	2,18	1,15	0,70
4A	3,28	0,88	0,42	2,71	0,73	0,34	2,27	0,63	0,32
4B	3,30	0,90	0,42	2,74	0,74	0,35	2,29	0,65	0,32
5A	3,31	0,64	0,31	2,74	0,52	0,25	2,29	0,47	0,24
5B	3,21	1,68	0,76	2,65	1,38	0,63	2,22	1,18	0,55-
6A	3,41	1,33	0,89	2,86	1,10	0,74	2,43	0,95	0,66
6B	3,28	1,10	0,89	2,94	0,91	0,74	2,31	0,77	0,64
7	3,27	1,55	0,70	2,72	1,28	0,58	2,28	1,10	0,52
8	3,21	1,69	0,77	2,66	1,39	0,64	2,22	1,19	0,56
9A	3,22	1,72	0,78	2,67	1,42	0,64	2,23	1,22	0,57
9B	4,29	2,09	0,95	3,59	1,73	0,78	3,04	1,51	0,70
10A	2,62	0,23	0,39	2,18	0,19	0,32	1,85	0,16	0,28
10B	3,8	1,9	0,85	3,26	1,57	0,70	2,82	1,40	0,68

Table 14. Maximal forces acting in the trees, calculated for all combinations which are following:

- I) $\gamma_G G_{k,trees} + \gamma_G G_{k,permanent\ load} + \gamma_Q Q_{k,imposed\ load}$
- II) $\gamma_G G_{k,trees} + \gamma_G G_{k,permanent\ load} + \gamma_Q Q_{k,snow} + \gamma_Q \psi_0, imposed\ load Q_{k,imposed\ load}$
- III) $\gamma_G G_{k,trees} + \gamma_G G_{k,permanent\ load} + \gamma_Q Q_{k,wind} + \gamma_Q \psi_0, imposed\ load Q_{k,imposed\ load}$

Note: Tree 1A is not included in the calculations because its trunk is considerably destroyed and it should be removed, therefore the calculation is provided without it.

Verification of the load-bearing capacity

This chapter is devoted to the description of the approach to the verification of the current state of the structure. Whole calculation is attached as *Appendix D*.

The verification is divided into two parts, verification of the tree trunks and verification of the connections between the trees. Data from the simulation in the software are used as the input value, thus resulting maximal forces from each combination for each tree shown in *Table 14*. These values are compared and the verification is provided always for the most critical value, therefore for the most critical cross-section.

First step of the calculation is to calculate design values of the strength characteristics of the material. Material characteristics are taken from the strength class D40, as was already derived before. Design values are obtained with help of design factors which are taken in accordance with the standard. Material properties, their characteristic and design values can be found in *Table 15*.

MATERIAL PROPERTY		CHARACTERISTIC	DESIGN
Bending strength	$f_{m,rep}$	40 MPa	21,538 MPa
Tension strength parallel to the fibres	$f_{t,0,rep}$	24 MPa	12,923 MPa
Tension strength perpendicular to the fibres	$f_{t,90,rep}$	0,6 MPa	0,420 MPa
Compression strength parallel to the fibres	$f_{c,0,rep}$	26 MPa	14,000 MPa
Compression strength perpendicular to the fibres	$f_{c,90,rep}$	8,3 MPa	4,469 MPa
Shear strength	$f_{v,0,rep}$	4 MPa	2,154 MPa
Modulus of elasticity	$E_{0,05}$	10900 MPa	
Density	ρ_{ash}	1150 kg/m ³	
Design factors:	k_{mod}	0,7	
	γ_m	1,3	
	k_h	1,0	

Table 15. Overview of the material properties and their characteristic and design values.

Verification of the tree trunks

Each tree trunk unity is checked in dependence to above mentioned maximal forces acting within its structure (*Table 14*). There are 4 for conditions controlled:

- Compression stresses parallel to the grain caused by the normal force
- Bending caused by the moment
- Combination of previous two conditions, normal force and moment
- Shear stresses caused by the shear force

The verification is based on the following inequalities.

Compression stresses parallel to the grain caused by the normal force:

$$\sigma_{c,0,d} \leq f_{c,0,d}$$

$$\sigma_{c,0,d} = N_d / A$$

$$\longrightarrow N_d \leq f_{c,0,d} * A$$

$\sigma_{c,0,d}$... compressive stress

$f_{c,0,d}$... compression strength

N_d ... design normal force

A ... area of cross-section

Bending caused by the moment:

$$\sigma_{m,d} \leq f_{m,d}$$

$$\sigma_{m,d} = M_{z,d} / W$$

$$\longrightarrow M_{z,d} \leq f_{m,d} * W$$

$\sigma_{m,d}$... bending stress

$f_{m,d}$... bending strength

$M_{z,d}$... design moment

W ... section modulus

Combination of previous two conditions, normal force and moment:

$$\sigma_{c,0,d} / f_{c,0,d} + \sigma_{m,d} / f_{m,d} \leq 1$$

Shear stresses caused by the shear force:

$$\sigma_{v,d} \leq f_{v,d}$$

$$\sigma_{v,d} = 4/3 * V_d / A$$

$$\longrightarrow V_d \leq 3/4 * f_{v,d} * A$$

$\sigma_{v,d}$... shear stress

$f_{v,d}$... shear strength

V_d ... design shear force

A ... area of cross-section

The results from this check are maximal forces which can act within the structure while keeping the unity. These results are compared to the maximal forces obtained from the simulation in the software. All these values can be found in following *Table 16*.

TREE	REAL VALUES			MAX. ALLOWED			VERIFICATION			
	N_d	M_d	V_d	N_{max}	M_{max}	V_{max}	$N_d < N_{max}$	$M_d < M_{max}$	$M_d + N_d$	$V_d < V_{max}$
1B	3,36	1,24	0,58	23,5	2,11	2,71	•	•	•	•
2	3,49	2,82	1,06	67,6	7,64	7,79	•	•	•	•
3A	3,14	2,15	1,26	24,1	2,75	2,78	•	•	•	•
3B	3,14	1,66	1,01	17,4	0,45	2,01	•	x	x	•
4A	3,28	0,88	0,42	11,8	0,39	1,36	•	x	x	•
4B	3,30	0,90	0,42	18,8	0,64	2,17	•	x	x	•
5A	3,31	0,64	0,31	15,0	0,59	1,74	•	x	x	•
5B	3,21	1,68	0,76	9,6	0,28	1,11	•	x	x	•
6A	3,41	1,33	0,89	118	7,13	13,7	•	•	•	•
6B	3,28	1,10	0,89	80,2	3,95	9,25	•	•	•	•
7	3,27	1,55	0,70	15,7	0,97	1,81	•	x	x	•
8	3,21	1,69	0,77	9,9	0,36	1,14	•	x	x	•
9A	3,22	1,72	0,78	13,7	0,50	1,59	•	x	x	•
9B	4,29	2,09	0,95	43,6	3,93	5,03	•	•	•	•
10A	2,62	0,23	0,39	17,9	1,36	2,07	•	•	•	•
10B	3,8	1,9	0,85	111	16,8	12,8	•	•	•	•
UNIT	kN	kNm	kN	kN	kNm	kN				

Table 16. Overview of the results from the calculation of unity check of the structural elements.

Verification of the connections

All the connections appearing within the structure are verified, therefore axial welds between the trees 3a and 3b, 6a and 6b, in both levels, and cross welds between the trees 2 and 3a, 9b and 10a. Verifying of unity of the connections is checked in dependence on their character, geometry, which has been measured in the garden, naturally on the maximal acting forces. All the controlled conditions are following:

- Compression stresses parallel to the grain caused by the normal force
- Bending caused by the moment
- Combination of previous two conditions, normal force and moment
- Shear stresses caused by the shear force
- Shear stresses caused by the moment
- Compression stresses perpendicular to the grain caused by the normal force
- Compression stresses perpendicular to the grain caused by the moment
- Tension stresses perpendicular to the grain due to the normal force

Inequalities, according to which the calculations are provided, follow. Although, the inequalities for first four points are the same as already mentioned in the previous part about

verification of the stems, they are repeated again due to small changes which occur in the calculations for the connections.

Compression stresses parallel to the grain caused by the normal force:

$$\begin{aligned}\sigma_{c,0,d} &\leq f_{c,0,d} \\ \sigma_{c,0,d} &= N_d / A \\ \longrightarrow N_d &\leq f_{c,0,d} * A\end{aligned}$$

$\sigma_{c,0,d}$... compressive stress
 $f_{c,0,d}$... compression strength
 N_d ... design normal force
 A ... area of cross-section

In this case, area of the cross-section is entire cross-section in the place of connection, therefore area of the weld.

Bending caused by the moment:

$$\begin{aligned}\sigma_{m,d} &\leq f_{m,d} \\ \sigma_{m,d} &= M_d / W \\ \longrightarrow M_d &\leq f_{m,d} * W\end{aligned}$$

$\sigma_{m,d}$... bending stress
 $f_{m,d}$... bending strength
 M_d ... design moment
 W ... section modulus

Whereas, there are two moments, M_y and M_z , the biggest one is considered during the calculation. The moment in connection is transferred mainly by the outer part where the common annual rings are located. Nearly zero forces are transferred by the middle part. Therefore the cross-section is adjusted according to this situation and is calculated as if there is a hole inside.

Combination of previous two conditions, normal force and moment:

$$\sigma_{c,0,d} / f_{c,0,d} + \sigma_{m,d} / f_{m,d} \leq 1$$

Shear stresses caused by the shear force, by the moment:

$$\begin{aligned}\sigma_{v,d} &\leq f_{v,d} \\ \sigma_{v,d} &= 2 * V_d / A \\ \longrightarrow V_d &\leq 1/2 * f_{v,d} * A\end{aligned}$$

$\sigma_{v,d}$... shear stress
 $f_{v,d}$... shear strength
 V_d ... design shear force
 A ... area of cross-section

Also shear stresses are calculated with hollow cross-section, therefore area of the cross-section is different and either formula for the caused shear stress. For the shear force caused by the moment, forces causing this moment are counted and the verification is provided for them.

Compression stresses perpendicular to the grain caused by the normal force or by the moment:

$$\begin{aligned} \sigma_{c,90,d} &\leq f_{c,90,d} \\ \sigma_{c,90,d} &= N_d / A \\ &\longrightarrow N_d \leq f_{c,90,d} * A \end{aligned}$$

$\sigma_{c,90,d}$... compressive stress
 $f_{c,90,d}$... compression strength
 N_d ... design normal force
 A ... area of cross-section

Principle of this check is to find necessary length of the connection in dependence on the width. Therefore the area is calculated as b*h, width and length of the connection.

Tension stresses perpendicular to the grain caused by the normal force:

$$\begin{aligned} \sigma_{t,90,d} &\leq f_{t,90,d} \\ \sigma_{t,90,d} &= N_d / A \\ &\longrightarrow N_d \leq f_{t,90,d} * A \end{aligned}$$

$\sigma_{t,90,d}$... tension stress
 $f_{t,90,d}$... tension strength
 N_d ... design normal force
 A ... area of cross-section

Also for this check, the main principle is to find necessary length of the connection in dependence on the width of the connection.

Results of the calculations based on the above mentioned conditions are stated in following Table 17.

Comparison of the real values with the maximal allowed values according to the control conditions	N [kN]	M[kNm]	RATIO	V [kN]		MINIMAL HEIGHT [m]			
	Compression	Bending	combination of compression and bending	Shear due to shear force	Shear due to moment	Compression perp. due to N	Compression perp. due to M	Tension perp. due to N	
2-3	real value	3,11	0,32	0,10	1,01	2,63	0,012	0,012	0,012
	limit value	174,48	4,11	1	18,32	12,21	0,041	0,031	0,370
	Check	•	•	•	•	•	x	x	x
3-3a	real value	7,12	2,06	0,42	0,84	12,57	0,051	0,051	0,051
	limit value	209,29	5,40	1	21,98	14,65	0,008	0,082	0,092
	Check	•	•	•	•	•	x	x	x
3-3b	real value	7,12	2,06	0,26	0,84	12,57	0,057	0,057	0,057
	limit value	288,4	8,74	1	30,28	20,19	0,007	0,075	0,084
	Check	•	•	•	•	•	x	x	x
6-6a	real value	7,51	2,57	0,087	1,91	7,653	0,210	0,210	0,210
	limit value	709,03	33,70	1	74,45	49,63	0,008	0,020	0,119
	Check	•	•	•	•	•	•	•	•
6-6b	real value	7,51	2,57	0,135	1,91	7,65	0,150	0,150	0,150
	limit value	522,29	21,31	1	54,84	36,56	0,012	0,022	0,108
	Check	•	•	•	•	•	•	•	•
9-10	real value	4,02	0,43	0,338	1,16	3,26	0,075	0,075	0,075
	limit value	87,84	1,47	1	9,22	6,15	0,007	0,006	0,062
	Check	•	•	•	•	•	•	•	•

Table 17. Overview of the verification of the connections.

As visible from the results stated in *Table 16* and *Table 17*, the structure is clearly not able to carry the weight of the platform at 2 meters, therefore definitely not at the height of 4 meters. It is necessary to point out that this statement is based on the assumption that the load is distributed equally between all 16 trees. However, even without this assumption, the structure apparently does not have sufficient load bearing capacity.

Nevertheless, it is necessary to point out that the trees, which were planted in year 2010, thus the oldest ones, are those which load-bearing capacity is at the height of 2 meters sufficient. All those trees, except for tree 10B, are interconnected. Tree 10B is the most massive tree of whole structure, therefore its load-bearing capacity is that high.

Regarding the deflections, it is clearly obvious, from Scia Engineer results, that the interconnected trees have considerably smaller deflections and thus their existence within the structure is really important for the stability of the structure.

At the end, it is necessary to mention some simplifications and assumptions which were used during the calculation of the load-bearing capacity. As mentioned above, shape

of the trees was simplified. Even though, some trees are very direct, they are still slightly curved and therefore inner stresses caused by this curvature should be calculated and verified as well. Regarding the welds, and mainly cross welds, the course of fibres inside the structure is still not really clear and therefore the calculations are not absolutely precise. However, always the worst case scenario was calculated during the verification of the structure, therefore the approach is rather pessimistic.

Nevertheless, as visible from *Table 16* and *Table 17*, the resulting stresses for the verified trees are significantly lower than limiting values. Therefore, even with all above mentioned simplifications, the resulting values cannot that radically change to exceed the limiting values. On the contrary, they are probably able to carry much bigger weight than modelled in the software.

6.5. ESTIMATION OF TIME WHEN THE LOAD-BEARING CAPACITY IS SUFFICIENT

The estimation is based on the verification of the weakest member of the structure. That means that the weakest member is chosen and time needed for obtaining the sufficient load-bearing capacity is calculated. According to the result of this calculation, the assumption of time when the load-bearing capacity of whole structure is sufficient for taking over the load of the platform can be made. As obvious, this estimation is for simplification based on the assumption that the load is distributed equally and therefore, each element has to carry 1/16 of whole vertical load caused by the platform. And therefore the weakest member is calculated.

The weakest tree to be verified has been chosen according to the results obtained from the previous calculations of the current load-bearing capacity (*Table 16*). Naturally, all the interconnected trees are automatically out of the game. From single standing trees, tree 5B was selected as the weakest because its load-bearing capacity is currently the lowest. Tree 5B is shown in *Figure 85* and all important characteristic are stated in *Table 18* below.



Figure 85 (up and down). Pictures of tree 5B, chosen as the weakest tree of the structure.

GEOMETRY		
Circumference in the length of:	0 m	0,161 m
	1 m	0,125 m
	2 m	0,093 m
	3 m	0,072 m
Total length		3,62 m
Total height		3,50 m
Slope		75,53 °



Table 18. Geometry of tree 5B.

To estimate how fast the trees grow, the difference in geometry in 2010 and 2017 is used. Circumference in the length of 1 meter and length of the stem in year 2010 and 2017 are compared and according to the difference, an average growth speed is calculated. This comparison is not provided for all trees but only for the original ones, thus the ones planted in 2011. All information about the geometry and calculated speed can be found in *Table 19*.

TREE	CIRCUMFERENCE IN 1 M		LENGTH OF THE TRUNK		GROWTH SPEED [m/year]	
	year 2010	year 2017	year 2010	year 2017	Circumference	length
2	0,1 m	0,384 m	2,5 m	4,66 m	0,047	0,360
3A	0,1 m	0,282 m	2,5 m	4,48 m	0,030	0,330
6A	0,1 m	0,380 m	2,5 m	5,91 m	0,047	0,568
6B	0,1 m	0,308 m	2,5 m	5,19 m	0,035	0,448
9B	0,1 m	0,326 m	2,5 m	5,09 m	0,038	0,432
10A	0,1 m	0,214 m	2,5 m	4,27 m	0,019	0,295
10B	0,1 m	0,386 m	2,5 m	5,42 m	0,048	0,487

Table 19. Overview of circumferences and lengths in 2010 and 2017 and calculation of growth speed.

Based on the values stated in *Table 19*, average growth speed is calculated, specifically 0,041 m per year in the circumference and 0,411 in the length. It necessary to mention that the average value is calculated without considering growth speed of tree 10A because its speed considerably differs from others, thus could be possible that this tree was not planted in 2010 like others.

According to average values of speed, geometry of tree 5B over time is calculated. The gain of mass is based on the current geometry. These circumferences and lengths can be found in *Table 20*.

TIME [years]	CIRCUMFERENCE IN THE LENGTH OF					LENGTH
	0 m	1 m	2 m	3 m	4 m	
0	0,161 m	0,125 m	0,093 m	0,072 m	-	3,620 m
2	0,242 m	0,206 m	0,174 m	0,153 m	0,061 m	4,443 m
5	0,365 m	0,329 m	0,297 m	0,276 m	0,183 m	5,677 m
6	0,405 m	0,369 m	0,337 m	0,316 m	0,224 m	6,088 m
7	0,446 m	0,410 m	0,378 m	0,357 m	0,265 m	6,499 m
10	0,568 m	0,532 m	0,500 m	0,479 m	0,387 m	7,733 m

Table 20. Overview of circumferences and lengths of tree 5B over time.

To find out whether the tree has sufficient load-bearing capacity in given year, the same approach is used like above, for verification of the tree trunks. First, the tree is modelled in software Scia Engineer, thus the inner stresses acting within the structure are determined for all three combinations. The results for the most unfavourable combination are verified according to maximal allowed stresses calculated in the same way as in the previous

chapter. Also in this case, first combination is the most critical. First, state in 7 years is calculated. The results are positive, thus the load-bearing capacity of the element in 7 years is sufficient. Whereas the maximal allowed stresses are significantly higher than stresses acting within the structure, also calculation for 5 and 6 years is provided. Combination of normal force and bending moment is critical for the state in 5 years and is not verified. On the contrary, state in 6 years fulfils all the requirements, thus the necessary load-bearing capacity comes already in 6 years. All values used during the calculation and their comparison can be found in following *Table 21*.

TIME [years]	REAL VALUES			MAX. ALLOWED				VERIFICATION			
	N_d	M_d	V_d	N_{max}	M_{max}	N+M	V_{max}	$\frac{N_d}{N_{max}}$	$\frac{M_d}{M_{max}}$	$\frac{N+M}{N+M_{max}}$	$\frac{V_d}{V_{max}}$
5	3,61	3,03	0,76	37,40	3,31	1,012	4,32	•	•	x	•
6	3,81	3,03	0,76	55,87	4,55	0,735	6,45	•	•	•	•
7	3,93	3,03	0,76	78,05	6,06	0,550	9,01	•	•	•	•

Table 21. Overview of design and maximum allowed stresses within the structure over time.

Based on the assumption made at the beginning, that load of the platform is distributed equally, thus each element must be able to carry 1/16 of total vertical load, Living Tree Pavilion is able to take over the load in 6 years. Whereas this approach is pessimistic and other trees would probably have much bigger strength and thus take over much bigger load, estimated time could be probably shorter than 6 years coming from the calculation.

It is necessary to mentioned that as for the previous calculation, also for this one, the shape of the tree was simplified. Therefore also stresses caused by the curved shape should be verified. For more detailed estimation, whole structure should be modelled with consideration of the different stiffness of each element, thus the uneven distribution of load is taken into account. In future researches, the stability of the platform itself should become the point of interest.

Nevertheless, the main goal of this calculation was to estimate the approximate year when the load-bearing capacity could be sufficient and that is year 2023.

7. CONCLUSION

Whereas the topic of the living tree structures and their evaluation can seem simple at first sight, the opposite is true. The problematics is really complex and sophisticated. During the investigation of Living Tree Pavilion, lot of new questions have been revealed. Therefore next researches should be carried out.

Main goal of the analysis of the Pavilion was to estimate the time when the load-bearing capacity of the structure is sufficient enough to take over the load of the platform and carry it without any additional supportive construction. Based on the measurements and following calculations, this time was estimated for 6 years. Therefore the structure should be able to become fully load-bearing in 2023.

Each step towards the result was a great benefit for the research of the living structures and mainly for future researches which will be performed on the Pavilion. During all the procedures of measuring, many unexpected situations happened. Thanks to that and all the remarks and suggestions, the future investigation can become easier and mainly more precise and thus give more accurate results.

Speaking about the measuring of the geometry of the structure, whole procedure was carried out manually. For the future researches, other methods should be considered for obtaining as precise date as possible and also for easier work.

The pulling test performed on the Pavilion also revealed lot of matters which can be now made in better quality. However, despite that, the pulling test mainly proved the great effect of the connections to the overall structure. Not only that the connections positively influence the stiffness in the direction along the connection, as could be expected, they also increase the stiffness in the direction perpendicular to the connection. And the effect is significant. It also showed the importance of location of the connection within the structure and importance of its type, whether it as an axial weld or cross weld. Also the question of the effect of size of the connections and their amount has been opened.

According to the pulling test, also modulus of elasticity for trees creating the Pavilion was determined. This resulting modulus of elasticity gives a picture about the stiffness of the trees and about their potential. Surprisingly, the smallest measured value of the modulus of elasticity is around 13 GPa which really correspond to the properties for ash wood.

For evaluation of the structure, the determination of the strength class of the wood corresponding to the trees of the Pavilion had to be done. The resulting class was chosen as class D40. This decision was made based on the standard for an ash tree and the modulus of elasticity was used as a reference. During the verification itself, several assumptions had to be done but also remarks for future researches were given.

Even though, there are still lot of questions regarding the living tree structures, these structures have something to offer for the future. Living Tree Pavilion is a living proof that this

kind of structures has great potential in the field of civil engineering and thus it deserves our attention. Therefore also list of possible points of interests for future researches follows.

Points of interest related specifically to the structure analysis:

- Methods of measurement of the structures
- Investigation of the internal structure of the connections, mainly of the cross-welds
- Influence of the amount and size of the connections and their positioning to overall stiffness, thus whether more smaller connections are more efficient than one massive ideally located or conversely
- Root analysis
- Connection between the living and non-living elements

General topics:

- Human response to the living tree structures
- Maintenance of the structures
- Replacement of the elements
- For the future, water and wind tightness



8. REFERENCES

Books

- [1] MATTHECK, C. *Design in nature: learning from trees*. New York: Springer-Verlag, 1998. ISBN 3540629378.
- [2] BIJEN, Jan. *Durability of engineering structures: design, repair and maintenance*. Cambridge: Woodhead, 2003. ISBN 1855736950.
- [3] GÖTZ K. O. & Mattheck C., *Festigkeitsuntersuchungen an grünen Bäumen mit dem Fractometer III*, Bericht des Forschungszentrums Karlsruhe, 1998.
- [4] JACOBS M. R., *The fiber tension of woody stems with special reference to the genus Eucalyptus*. Commonwealth Forestry Bureau, Bulletin No. 24, Canberra, 1938.
- [5] KUBLER H., *Growth stresses in trees and related wood properties*. Forestry Abstracts, 1987.
- [6] WISELIUS, S.I., *Houtvademecum*, Stichting Centrum Hout Almere, 2005
- [7] COPIJN J., *Bomen laten leven, Bomen in stad en land, hun functie, geschiedenis en verzorging*, De Driehoek, Amsterdam, 1978
- [8] OTTO F.P., *Natürliche Konstruktionen: Formen und Konstruktionen in Natur und Technik und Prozesse ihrer Entstehung*, 1982

Publications

- [9] A.D.W. Nuijten BS, *Master Thesis – Living tree buildings*, TU Delft, 2011

Websites

- [10] Why Do Trees Get Sick and Die? | Owlcation. *Owlcation - Education* [online]. Copyright © 2018 HubPages Inc. and respective owners. Other product and company names shown may be trademarks of their respective owners. HubPages [cit. 19.02.2018]. Available from: <https://owlcation.com/stem/Why-do-trees-die>
- [11] Veneer Specifications. *Haley Bros Home* [online]. Copyright ©2004 [cit. 19.02.2018]. Available from: <http://www.haleybros.com/veneer-specifications.html>

- [12] Mechanická stability stromu a metody jejího zjištění (PDF Download Available). *ResearchGate* | *Share and discover research* [online]. Copyright © 2008 [cit. 19.02.2018]. Available from: https://www.researchgate.net/publication/266135522_mechanicka_stabilita_stromu_a_metody_jejeho_zjistovani
- [13] Baubotanic [online]. Available from: <http://www.baubotanik.org/en/baubotanik/living-structures/>
- [14] Archdaily [online]. Copyright © Ferdinand Ludwig [cit. 19.02.2018]. Available from: <https://www.archdaily.com/775884/baubotanik-the-botanically-inspired-design-system-that-creates-living-buildings>
- [15] Nelson the Tree House [online]. Available from: <https://www.nelsontreehouse.com/blog/2016/9/28/off-tv-photo-tour-orcas-part-2>
- [16] ferdinand ludwig builds hybrids of living nature and technology. *designboom magazine* | your first source for architecture, design & art news [online]. Copyright © 2018 [cit. 19.02.2018]. Available from: <https://www.designboom.com/architecture/egger-ferdinand-ludwig-baubotanik-nature-11-10-2016/>
- [17] Living buildings « Richard Karty. Richard Karty [online]. Available from: <http://richardkarty.org/living-buildings/>
- [18] Archdaily [online]. Available from: <https://www.archdaily.com/16445/yellow-treehouse-restaurant-pacific-environments>
- [19] Tree growth stress and related problems | SpringerLink. *Home - Springer* [online]. Copyright © 2017 Springer International Publishing AG. Part of [cit. 19.02.2018]. Available from: <https://link.springer.com/article/10.1007/s10086-017-1639-y>
- [20] Časopis ŽIVA [online]. Copyright © [cit. 19.02.2018]. Available from: <http://ziva.avcr.cz/files/ziva/pdf/k-hodnoceni-stavu-baze-stromu-a-korenoveho-systemu.pdf>

Regulations

NEN-EN 1990

NEN-EN 1991-1

APPENDIX A

PRELIMINARY CALCULATIONS FOR THE PULLING TEST

MAIN CHARACTERISTICS - ASH WOOD

Bending strength	$f_{m,0,k} =$	110	MPa
Elasticity modulus	$E_k =$	12 800	MPa

in reality, due to the defects only 25% of the strength

Char. estimated bending strength $0,25 \times f_{m,0,k} = 27,5$ MPa $\approx C27$

MAIN CHARACTERISTICS - ESTIMATION ACCORDING TO CLASS C27

Bending strength	$f_{m,0,rep} =$	27	MPa
Density	$\rho_{rep} =$	750 - 1 150	kg/m ³
Tension strength			
- parallel to the fibres	$f_{m,0,rep} =$	16	MPa
- perpendicular to the fibres	$f_{t,90,rep} =$	0,4	MPa
Compression strength			
- parallel to the fibres	$f_{c,0,rep} =$	22	MPa
- perpendicular to the fibres	$f_{c,90,rep} =$	2,6	MPa
Shear strength	$f_{v,0,rep} =$	4	MPa
Elasticity modulus	$E_{rep} =$	7 700	MPa

ESTIMATION OF THE MAXIMAL FORCES

the main idea: $f_{e,d} > \sigma_{m,d}$ ($f_{e,d} = 70\% f_{m,d}$ - elastic area)

formulas:

$$f_{m,d} = (f_{m,k} \cdot k_{mod} \cdot k_h) / \gamma_m$$

$$k_{mod} = 0,7$$

$$k_h = 1$$

$$\gamma_m = 1,3$$

$$\sigma_{m,d} = M_{e,d} / W$$

$$M_{e,d} = F \cdot L$$

$$W = (1/32) \cdot \pi \cdot D^3$$

$$F < f_{e,d} \cdot W / L$$

SUPPORT	CIRCUMFERENCES [mm]			DIAMETER D ₀ [mm]	CHARAKTERISTICS			MAX FORCE F [kN]	
	C ₀ (L=0 m)	C ₁ (L=1 m)	C ₂ (L=2 m)		f _{e,d} [Mpa]	W [mm ³]	L [m]		
1	A	211	154	123	67,20	10,18	29774	2,00	0,15
	B	314	200	147	100,00	10,18	98125	2,00	0,50
2		482	384	246	153,50	10,18	354921	2,00	1,81
3	A	343	282	145	109,24	10,18	127901	2,00	0,65
	B	188	157	125	59,87	10,18	21060	2,00	0,11
4	A	178	129	103	56,69	10,18	17875	2,00	0,09
	B	211	157	130	67,20	10,18	29774	2,00	0,15
5	A	205	154	116	65,29	10,18	27306	2,00	0,14
	B	161	125	93	51,27	10,18	13227	2,00	0,07
6	A	513	380	326	163,38	10,18	427901	2,00	2,18
	B	435	308	268	138,54	10,18	260891	2,00	1,33
7		242	182	119	77,07	10,18	44920	2,00	0,23
8		174	143	94	55,41	10,18	16697	2,00	0,08
9	A	189	148	111	60,19	10,18	21398	2,00	0,11
	B	386	326	198	122,93	10,18	182286	2,00	0,93
10	A	305	214	127	97,13	10,18	89927	2,00	0,46
	B	522	386	316	166,24	10,18	450819	2,00	2,29

ESTIMATION OF THE DEFLECTION

the main idea: estimate the pulling force necessary for 150 mm deflection (in length of 2 meters)

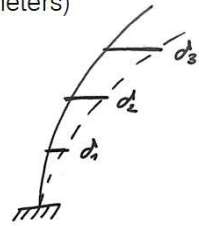
formula:

$$\delta = 1/3 * FL^3 / EI$$

$$\gg F = 3\delta * EI / L^3$$

$$E = 7\,700 \text{ MPa}$$

$$I = (1/4) * \pi * R^4$$

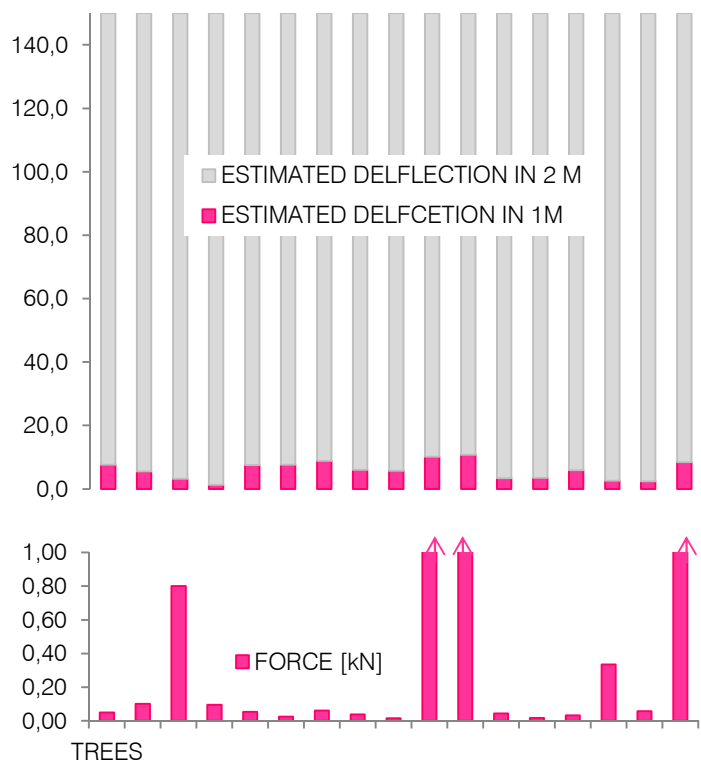


SUPPORT	CIRCUMFERENCES [mm]			DIAMETER [mm]			MOMENT OF INERTIA [mm ⁴]			FORCE [kN] F _{δ2 = 150 mm}
	C ₀	C ₁	C ₂	D ₀	D ₁	D ₂	I ₀	I ₁	I ₂	
1 A	211	154	123	67	49	39	1000371	283866	115518	0,05
B	314	200	147	100	64	47	4906250	807516	235668	0,10
2	482	384	246	154	122	78	27240761	10973773	1848296	0,80
3 A	343	282	145	109	90	46	6985662	3191740	223102	0,10
B	188	157	125	60	50	40	630467	306641	123217	0,05
4 A	178	129	103	57	41	33	506654	139762	56804	0,02
B	211	157	130	67	50	41	1000371	306641	144147	0,06
5 A	205	154	116	65	49	37	891346	283866	91383	0,04
B	161	125	93	51	40	30	339105	123217	37754	0,02
6 A	513	380	326	163	121	104	34954295	10523628	5700349	2,47
B	435	308	268	139	98	85	18071246	4541862	2603576	1,13
7	242	182	119	77	58	38	1730982	553754	101209	0,04
8	174	143	94	55	46	30	462624	211045	39404	0,02
9 A	189	148	111	60	47	35	643989	242146	76617	0,03
B	386	326	198	123	104	63	11204186	5700349	775697	0,34
10 A	305	214	127	97	68	40	4367475	1058489	131294	0,06
B	522	386	316	166	123	101	37472537	11204186	5032449	2,18

estimated deflection

SUPPORT	FORCE		DEFLECTION [mm]	
	[kN]	[kg]	δ ₁	δ ₂
1 A	0,05	5,1	7,6	150
B	0,10	10,4	5,5	150
2	0,80	81,6	3,2	150
3 A	0,10	9,9	1,3	150
B	0,05	5,4	7,5	150
4 A	0,02	2,5	7,6	150
B	0,06	6,4	8,8	150
5 A	0,04	4,0	6,0	150
B	0,02	1,7	5,7	150
6 A	2,47	251,7	10,2	150
B	1,13	115,0	10,7	150
7	0,04	4,5	3,4	150
8	0,02	1,7	3,5	150
9 A	0,03	3,4	5,9	150
B	0,34	34,2	2,6	150
10 A	0,06	5,8	2,3	150
B	2,18	222,2	8,4	150

graph comparing the deflection of the tree with respect to the used force



STRUCTURE OVERVIEW

SUPPORT	CIRCUMFERENCES [cm]			JOINT		MAX PULLING FORCE	
	0 m	1 m	2 m	TYPE	MARKING	F [kN]	NOTES
1 A	21,1	15,4	12,3	NO		0,15	dead
B	31,4	20	14,7	NO		0,50	comparison with 10A
2	48,2	38,4	24,6	CROSS WELD 2-3		1,81	higher root stress
3 A	34,3	28,2	14,5	BOTH		0,65	probably higher force
B	18,8	15,7	12,5	AXIAL WELD 3A, 3B		0,11	higher probability of rupture
4 A	17,8	12,9	10,3	NO		0,09	comparison with 3B
B	21,1	15,7	13	NO		0,15	higher root stress
5 A	20,5	15,4	11,6	NO		0,14	higher root stress
B	16,1	12,5	9,3	NO		0,07	-
6 A	51,3	38	32,6	AXIAL WELD 6A, 6B		2,18	higher probability of rupture
B	43,5	30,8	26,8	AXIAL WELD 6A, 6B		1,33	higher probability of rupture
7	24,2	18,2	11,9	NO		0,23	comparison with 4B
8	17,4	14,3	9,4	NO		0,08	comparison with 3B
9 A	18,9	14,8	11,1	NO		0,11	comparison with 3B
B	38,6	32,6	19,8	CROSS WELD 9-10		0,93	higher root stress
10 A	30,5	21,4	12,7	CROSS WELD 9-10		0,46	higher root stress
B	52,2	38,6	31,6	NO		2,29	comparison with 6A

TREES TO BE PULLED AND THEIR COMPARISON

SUPPORT	PULLING FORCE [kN]			NOTES
	maximal	according to deflection	recommendation	
1B	0,50	0,10	0,20	single
10A	0,46	0,06		cross weld 9 - 10
9A	0,11	0,03	0,10	single
3B	0,11	0,05		axial welds 3
7	0,23	0,04	0,10	single
4B	0,15	0,06		single
10B	2,29	2,18	0,50	single
6A	2,18	2,47		axial welds 6
1B	0,50	0,10	0,20	single
3A	0,65	0,10		axial welds 3, cross weld 2-3

APPENDIX B

RESULTS OF THE PULLING TEST

CHARACTERISTICS OBTAINED FROM THE PULLING TEST

TREE	RADIAL DIRECTION			TANGENTIAL DIRECTION			LEVEL ARM [m]	WELD
	WEIGHT [kg]	FORCE [kN]	DEFLECTION [m]	WEIGHT [kg]	FORCE [kN]	DEFLECTION [m]		
1B	12	0,118	0,055	-	-	-	1,89	-
3A	24	0,235	0,005	36	0,353	0,003	1,78	axial, cross
3B	12	0,118	0,048	12	0,118	0,024	1,88	axial
4B	12	0,118	0,115	-	-	-	1,88	-
6A	36	0,353	0,008	36	0,353	0,002	1,79	axial
7	12	0,118	0,043	-	-	-	1,85	-
9A	12	0,118	0,052	-	-	-	1,85	-
10A	20	0,196	0,020	24	0,235	0,002	1,67	cross
10B	32	0,314	0,010	-	-	-	1,85	-

SINGLE STANDING TREES

CALCULATION OF THE MODULUS OF ELASTICITY

the main idea: elasticity modulus can be calculated according to particular deflection caused by certain weight

formula: $\delta = 1/3 * FL^3 / EI$ (only for not connected trees)

$$\gg E = 1/3 * FL^3 / \delta I$$

$$I = (1/4) * \pi * R^4$$

TREE	FORCE [kN]	DEFLECTION [m]	LEVER ARM [m]	RADIUS [m]	MOMENT OF INERTIA [m ⁴]	ELASTICITY MODULUS	
						[kPa]	[MPa]
1B	0,118	0,055	1,89	0,023	2,35668E-07	20438607,4	20439
4B	0,118	0,115	1,88	0,021	1,44147E-07	15728967,5	15729
7	0,118	0,043	1,85	0,019	1,01209E-07	57089573,8	57090
9A	0,118	0,052	1,85	0,018	7,66166E-08	62361685,3	62362
10B	0,314	0,010	1,85	0,050	5,03245E-06	13165383,2	13165

note: trees with significantly higher modulus of elasticity

COMPARISON OF THE ESTIMATED DEFLECTIONS AND THE REALITY

TREE	ESTIMATED DEFLECTIONS				REAL DEFLECTIONS		PROPORCIONAL COMPARISON
	max elastic deflection		deflection of 150 mm		F [kN]	δ^R [m]	
	F [kN]	δ^R [m]	F [kN]	δ^R [m]			
1B	0,50	0,734	0,10	0,150	0,118	0,055	2,3 x smaller than exp.
4B	0,15	0,364	0,06	0,150	0,118	0,115	2,6 x smaller than exp.
7	0,23	0,782	0,04	0,150	0,118	0,043	10,3 x smaller than exp.
9A	0,11	0,492	0,03	0,150	0,118	0,052	11,3 x smaller than exp.
10B	2,29	0,158	2,18	0,150	0,314	0,010	2,2 x smaller than exp.

note: trees with significantly higher modulus of elasticity

INTERCONNECTED TREES

COMPARISON OF THE DEFLECTION ACCORDING TO THE DIRECTION

TREE	RADIAL DIRECTION		TANGENTIAL DIRECTION		RADIUS	WELDS	NOTE
	F [kN]	δ [m]	F [kN]	δ [m]			
3A	0,235	0,005	0,353	0,003	0,023	axial, cross w.	
3B	0,118	0,048	0,118	0,024	0,020	axial welds	2x smaller deflection
6A	0,353	0,008	0,353	0,002	0,052	axial welds	4x smaller deflection
10A	0,196	0,020	0,235	0,002	0,020	cross weld	

note: whereas the same weight was used, the deflection in both direction can be compared

COMPARISON OF THE ESTIMATED DEFLECTIONS AND THE REALITY - RADIAL DIRECTION

TREE	ESTIMATED DEFLECTIONS				REAL DEFLECTIONS		PROPORCIONAL COMPARISON
	max elastic deflection		deflection of 150 mm		F [kN]	δ^R [m]	
	F [kN]	δ^R [m]	F [kN]	δ^R [m]			
3A	0,65	1,010	0,10	0,150	0,235	0,005	70 x smaller than exp.
3B	0,11	0,301	0,05	0,150	0,118	0,048	6 x smaller than expect.
6A	2,18	0,132	2,47	0,150	0,353	0,008	3 x smaller than expect.
10A	0,46	1,207	0,06	0,150	0,196	0,020	26 x smaller than exp.

note: values of this tree can be compared directly because of the same used weight

note: comparing values are distorted

comparison of other trees is estimated according to assumption that caused deflection is directly proportional to the acting force

-> simplified approach, only to give an idea of the approximate difference, because:

- the deflection is not exactly directly proportional
- lever arm used during the preliminary calculations was 2 m

COMPARISON OF THE ESTIMATED DEFLECTIONS AND THE REALITY - TANGENTIAL DIRECTION

TREE	ESTIMATED DEFLECTIONS				REAL DEFLECTIONS		PROPORCIONAL COMPARISON
	max elastic deflection		deflection of 150 mm		F [kN]	δ^T [m]	
	F [kN]	δ^R [m]	F [kN]	δ^R [m]			
3A	0,65	1,010	0,10	0,150	0,353	0,003	180 x smaller than exp.
3B	0,11	0,301	0,05	0,150	0,118	0,024	13 x smaller than exp.
6A	2,18	0,132	2,47	0,150	0,353	0,002	11 x smaller than exp.
10A	0,46	1,207	0,06	0,150	0,235	0,002	395 x smaller than exp.

note: values of this tree can be compared directly because of the same used weight

note: comparing values are distorted

comparison of other trees is estimated according to assumption that caused deflection is directly proportional to the acting force

- simplified approach, only to give an idea of the approximate difference, because:

- the deflection is not exactly directly proportional
- lever arm used during the preliminary calculations was 2 m

COMPARISON OF PRE-SELECTED PAIRS OF TREES

single standing vs. interconnected tree

RADIAL DIRECTION

APPROACH A

main idea: deflections of the single standing trees are converted to the forces used for the interconnected trees and compared depending on radius of the trees

assumption deflection is directly proportional to the pulling force (for single standing trees only)

SUPPORT	RADIAL DIRECTION		CONVERTED δ^R		WELD	RADIUS [m]	NOTES
	F [kN]	δ^R [m]	F [kN]	δ^R [m]			
1B	0,118	0,055	0,196	0,092	-	0,023	big difference due to cross weld
10A	0,196	0,020		0,020	cross	0,020	
9A	0,118	0,052	0,118	0,052	-	0,018	relatively small difference
3B	0,118	0,048		0,048	axial	0,020	
10B	0,314	0,010	0,353	0,011	-	0,050	relatively small difference
6A	0,353	0,008		0,008	axial	0,052	
1B	0,118	0,055	0,235	0,110	-	0,023	big difference due to double connection
3A	0,235	0,005		0,005	axial, cross	0,023	

APPROACH B

main idea: new tree is created, with geometry of the interconnected tree but with the modulus of elasticity of the single standing tree of the similar shape

deflection of this new tree is calculated, for the same force as used during pulling the interconnected tree

assumption modulus of elasticity of the material is the same for interconnected and similar single standing tree

SUPPORT	FORCE [kN]	RADIUS [m]	ELASTICITY MOD. [MPa]	I [mm ⁴]	LEVER ARM [m]	δ^R [m]	CONNECTIONS
single 10A	0,196	0,020	20439	125600	1,67	0,119	-
10A			-			0,020	cross
single 3B	0,118	0,020	20439	125600	1,88	0,102	-
3B			-			0,048	axial
single 6A	0,353	0,052	13165	5739619	1,79	0,009	-
6A			-			0,008	axial
single 3A	0,235	0,023	20439	219675	1,78	0,099	-
3A			-			0,005	axial, cross

TANGENTIAL DIRECTION

APPROACH A

calculation based on the same idea as previous

- note:
- single standing trees were pulled only in the radial direction
 - > assumption that the deflection of the single standing trees is the same in the tangential direction
 - > in reality, the deflection would differ, therefore the comparison is only rough

SUPPORT	TANGENTIAL DIRECT.		CONVERTED δ^T		WELD	RADIUS [m]	NOTES
	F [kN]	δ^T [m]	F [kN]	δ^T [m]			
1B	0,118	0,055	0,235	0,110	-	0,023	extreme difference due to cross weld
10A	0,235	0,002		0,002	cross	0,020	
9A	0,118	0,052	0,118	0,052	-	0,018	big difference
3B	0,118	0,024		0,024	axial	0,020	
10B	0,314	0,010	0,353	0,011	-	0,050	big difference
6A	0,353	0,002		0,002	axial	0,052	
1B	0,118	0,055	0,353	0,165	-	0,023	extreme difference due to double connection
3A	0,353	0,003		0,003	axial, cross	0,023	

APPROACH B

main idea: new tree is created, with geometry of the interconnected tree but with the modulus of elasticity of the single standing tree of the similar shape

deflection of this new tree is calculated, for the same force as used during pulling the interconnected tree

assumption modulus of elasticity of the material is the same for interconnected and similar single standing tree

SUPPORT	FORCE [kN]	RADIUS [m]	ELASTICITY MOD. [MPa]	I [mm ⁴]	LEVER ARM [m]	δ^T [m]	CONNECTIONS
single 10A	0,353	0,020	20438,607	125600	1,67	0,214	-
10A						0,003	cross
single 3B	0,118	0,020	20438,607	125600	1,88	0,102	-
3B						0,024	axial
single 6A	0,353	0,052	13165,383	5739619	1,79	0,009	-
6A						0,002	axial
single 3A	0,235	0,023	20438,607	219675	1,78	0,099	-
3A						0,002	axial, cross

APPENDIX C

CALCULATION OF PERMANENT AND VARIABLE LOADS

OWN WEIGHT OF THE TREES

Density (according to class)	$\rho_{\text{rep}} = 1150$	kg/m ³	
Load from trees	$q_k = \rho_{\text{rep}} * g$	N/m ³	g ... gravitational acceleration
	$q_k = 11282$	N/m ³	9,81 m/s ²
	$q_k = 11,282$	kN/m ³	

OWN WEIGHT OF THE PLATFORM AND THE RAILING

THE PLATFORM

Geometry	$r_{\text{out}} = 1,850$	m	
	$r_{\text{in}} = 0,875$	m	
	$A = 8,343$	m ²	
	$t = 0,090$	m	t ... 3 boards with of 0,03 m
Material characteristics for Robinia wood			
- density	$\rho = 800$	kg/m ³	
Load of the platform	$Q_k = \rho_{\text{rep}} * g * A * t$	N	
	$Q_k = 5893$	N	
	$Q_k = 5,893$	kN	

THE RAILING

Geometry	$L_{\text{out}} = 11,618$	m	
	$L_{\text{in}} = 5,495$	m	
	$L_{\text{tot}} = 17,113$	m	
Characteristics of the railing			
- load per its meter	$q_k = 500$	N/m	
Load of the railing	$Q_k = q_k * L_{\text{tot}}$	N	
	$Q_k = 8557$	N	
	$Q_k = 8,557$	kN	

TOTAL LOAD

Total load	$Q_{k,\text{tot}} = 14,449$	kN	(load of the railing for simplification divided into area of the platform)
	$q_{k,\text{tot}} = Q_{\text{tot}}/A$	kN/m ²	
	$q_{k,\text{tot}} = 1,732$	kN/m ²	

IMPOSED LOAD

Category B

Characteristic value of a uniformly distributed load according to NEN-EN 1991-1-1/NB

$$q_k = 2,600 \text{ kN/m}^2$$
$$Q_k = q_k * A \text{ kN}$$
$$Q_k = 21,691 \text{ kN}$$

SNOW LOAD

Snow load for the persistent and transient design situation according to NEN-EN 1991-1-3:2003

$$s = \mu * C_e * C_t * s_k$$
$$s = 0,560 \text{ kN/m}^2$$

Shape coefficient	$\mu =$	0,8	
Exposure coefficient	$C_e =$	0,7	(NEN-EN 1991-1-1/NB)
Thermal coefficient	$C_t =$	1,0	(NEN-EN 1991-1-1/NB)
Characteristic value of snow load	$s_k =$	1,0	kN/m ² (NEN-EN 1991-1-1/NB)

WIND LOAD

PEAK VELOCITY PRESSURE

Basic wind velocity	$v_b = C_{dir} * C_{season} * v_{b,0}$		
	$v_b =$	27,0	m/s
Direction factor	$C_{dir} =$	1,0	(NEN-EN 1991-1-4/NB)
Season factor	$C_{season} =$	1,0	(NEN-EN 1991-1-4/NB)
Fundamental value of the basic wind velocity (area II)	$v_{b,0} =$	27,0	m/s (NEN-EN 1991-1-4/NB)
Wind velocity according to height	$v_m(z) = c_r(z) * c_0(z) * v_b$		
	$v_m(z) =$	10,46	m/s
Ortopgraphy factor	$c_0(z) =$	1,0	
Roughness factor	$c_r(z) = k_r * \ln(z/z_0)$		applicable when $z_{min} < z < z_{max}$
	$c_r(z) =$	0,39	$z < z_{min}$ then: $z = z_{min}$
Height of a tree	$z =$	5,590	m
Roughness length	$z_0 =$	0,5	m (NEN-EN 1991-1-4/NB)
Minimal length	$z_{min} =$	7,0	m (NEN-EN 1991-1-4/NB)
Maximal length	$z_{max} =$	200,0	m (NEN-EN 1991-1-4/NB)
- all the used values are for the terrain category III - city area			
Terrain factor	$k_r = 0,19 * (z_0 * 0,05)^{0,07}$		
	$k_r =$	0,15	
Turbulence intensity	$I_v = k_l / (c_0(z) * \ln(z/z_0))$		
	$I_v =$	0,38	
Turbulence factor	$k_l =$	1,0	
Peak velocity pressure	$q_p(z) = c_e(z) * q_b$		
	$q_p(z) = (1 + 7I_v(z)) * 0,5 * \rho * v_m(z)^2$		
	$q_p(z) =$	249,6	N/m ²
	$q_p(z) =$	0,25	kN/m ²
Air density	$\rho =$	1,25	kg/m ³

EXTERNAL STRESSES

General formula for the load caused by the wind force acting on external surfaces:

$$w_e = q_p(z) * c_{pe} \quad \begin{array}{l} q_p(z) \dots \text{peak velocity pressure} \\ c_{pe} \dots \text{external pressure coefficient} \end{array}$$

Wind pressure on trees

External pressure coefficients:

- windward side	$C_{pe,windward} =$	0,8	(according to h/d)
- leeward side	$C_{pe,leeward} =$	-0,5	
- maximum, parallel to wind	$C_{pe,max} =$	-1,2	

External wind pressure:

- windward side
- leeward side
- maximum, parallel to wind

$$\begin{aligned} W_{e,\text{windward}} &= 0,200 \text{ kN/m}^2 \\ W_{e,\text{leeward}} &= -0,125 \text{ kN/m}^2 \\ W_{e,\text{max}} &= -0,300 \text{ kN/m}^2 \end{aligned}$$

Wind pressure on the platform

External pressure coefficients:

- windward side (half of the platform) $C_{pe,\text{windward}} = -1,2$ (parapetes - according to h_p/h)
- leeward side (half of the platform) $C_{pe,\text{leeward}} = \pm 0,2$

External wind pressure:

- windward side
- leeward side

$$\begin{aligned} W_{e,\text{windward}} &= -0,300 \text{ kN/m}^2 \\ W_{e,\text{leeward}} &= \pm 0,05 \text{ kN/m}^2 \end{aligned}$$

INTERNAL STRESSES

General formula for the load caused by the wind force acting on external surfaces:

$$W_i = q_p(z) * C_{pi}$$

$q_p(z) \dots$ peak velocity pressure
 $C_{pi} \dots$ internal pressure coefficient

Internal pressure coefficients:

- positive pressure $C_{pi,\text{positive}} = 0,2$ (according to h/d)
- negative pressure $C_{pi,\text{negative}} = -0,3$

Internal wind pressure:

- positive pressure
- negative pressure

$$\begin{aligned} W_{i,\text{positive}} &= 0,050 \text{ kN/m}^2 \\ W_{i,\text{negative}} &= -0,075 \text{ kN/m}^2 \end{aligned}$$

APPENDIX D

CALCULATION OF THE CURRENT LOAD-BEARING
CAPACITY

PRINCIPLES USED FOR EVALUATION OF THE ELEMENTS

Normal force:

$$\sigma_{c,0,d} \leq f_{c,0,d}$$

$$\sigma_{c,0,d} = N_d/A$$

$$f_{c,0,d} = f_{c,0,k} * k_{mod} / \gamma_m$$

Moment:

$$\sigma_{m,d} \leq f_{m,d}$$

$$\sigma_{m,d} = M_{z,d}/W_z$$

$$f_{m,d} = f_{m,0,k} * k_{mod} * k_h / \gamma_m$$

$$\sigma_{c,0,d}/f_{c,0,d} + \sigma_{m,d}/f_{m,d} \leq 1$$

Shear force:

$$\sigma_{v,d} \leq f_{v,d}$$

$$\sigma_{v,d} = 4/3 V_d/A$$

$$f_{v,d} = f_{v,k} * k_{mod} / \gamma_m$$

Tensile stresses
perpendicular to the grain

$$\sigma_{t,90,d} < k_{dis} * k_{vol} * f_{t,90,d}$$

$$\sigma_{t,90,d} = 6k_p * M_{ap,d}/(bh_{ap}^2)$$

$$f_{t,90,d} = f_{t,90,rep} * k_{mod} * k_h / \gamma_m$$

DESIGN VALUES OF STRENGTH

Compression strength parallel to the fibres

$$f_{c,0,d} = f_{c,0,k} * k_{mod} / \gamma_m$$

$$f_{c,0,d} = 14,000 \text{ MPa}$$

$$f_{c,0,k} = 26,00 \text{ MPa} \quad (\text{strength class C30})$$

$$k_{mod} = 0,70$$

$$\gamma_m = 1,30$$

Compression strength perpendicular to the fibres

$$f_{c,90,d} = f_{c,90,k} * k_{mod} / \gamma_m$$

$$f_{c,90,d} = 4,469 \text{ MPa}$$

$$f_{c,90,k} = 8,30 \text{ MPa} \quad (\text{strength class C30})$$

$$k_{mod} = 0,70$$

$$\gamma_m = 1,30$$

Bending strength

$$f_{m,d} = f_{m,0,k} * k_{mod} * k_h / \gamma_m$$

$$f_{m,d} = 21,538 \text{ MPa}$$

$$f_{m,k} = 40,00 \text{ MPa} \quad (\text{strength class C30})$$

$$k_{mod} = 0,70$$

$$k_h = 1,00$$

$$\gamma_m = 1,30$$

Shear strength

$$f_{v,d} = f_{v,k} * k_{mod} / \gamma_m$$

$$f_{v,d} = 2,154 \text{ MPa}$$

$$f_{v,k} = 4,00 \text{ MPa} \quad (\text{strength class C30})$$

$$k_{mod} = 0,70$$

$$\gamma_m = 1,30$$

Tension strength perpendicular to the fibres

$$f_{t,90,d} = f_{t,90,rep} * k_{mod} * k_h / \gamma_m$$

$$f_{t,90,d} = 0,420 \text{ MPa}$$

$$f_{t,90,rep} = 0,60 \text{ MPa} \quad (\text{strength class C30})$$

$$k_{mod} = 0,70$$

$$k_h = 1,00$$

$$\gamma_m = 1,30$$

UNITY CHECK FOR TREES

TREE 1B

Geometry

$$\text{Radius} \quad r_{min} = 0,0231 \text{ m} \quad r_{max} = 0,0500 \text{ m}$$

$$\text{Area of the cross-section} \quad A_{min} = 0,0016755 \text{ m}^2 \quad A_{max} = 0,00785 \text{ m}^2$$

$$\text{Sectional modulus} \quad W_{min} = 9,676E-06 \text{ m}^3 \quad W_{max} = 9,813E-05 \text{ m}^3$$

$$W = \pi r^3/4$$

The maximum forces from the software:

	I. Combination	II. Combination	III. Combination
$N_{max} =$	3,36 kN	2,80 kN	2,36 kN
$M_{max} =$	1,24 kNm	1,02 kNm	0,89 kNm
$V_{max} =$	0,58 kN	0,48 kN	0,44 kN

I) Normal force

$$\sigma_{c,0,d} \leq f_{c,0,d}$$

$$\sigma_{c,0,d} = N_d/A$$

$$\rightarrow N_d \leq f_{c,0,d} * A$$

$$N_d \leq 23,457 \text{ kN}$$

$$f_{c,0,d} = 14,000 \text{ MPa}$$

II) Moment

$$\sigma_{m,d} \leq f_{m,d}$$

$$\sigma_{m,d} = M_{z,d}/W_z$$

$$\rightarrow M_{z,d} \leq f_{m,d} * W_z$$

$$M_{z,d} \leq 2,113 \text{ kNm}$$

$$f_{m,d} = 21,538 \text{ MPa}$$

III) Combination of moment and normal force

$$\sigma_{c,0,d}/f_{c,0,d} + \sigma_{m,d}/f_{m,d} \leq 1$$

$$0,617 \leq 1$$

IV) Shear force

$$\sigma_{v,d} \leq f_{v,d}$$

$$\sigma_{v,d} = 4/3 V_d/A$$

$$\rightarrow V_d \leq 3/4 f_{v,d} * A$$

$$V_d \leq 2,707 \text{ kNm}$$

$$f_{v,d} = 2,154 \text{ MPa}$$

Check:

I) Normal force

$$3,36 < 23,457$$

$$N_{max} < \text{limit value of normal force}$$

verified - N_{max} smaller

II) Moment

$$1,24 < 2,113$$

$$M_{max} < \text{limit value of moment}$$

verified - M_{max} smaller

III) Combination M and N

$$0,817 < 1,000$$

$$\text{combination} < 1,000$$

verified - combination smaller than 1

IV) Shear force

$$0,58 < 2,707$$

$$V_{\max} < \text{limit value of shear force}$$

verified - V_{\max} smaller

Note: following trees are checked on the same basis as tree 1B

TREE 2

Geometry

Radius	$r_{\min} = 0,0392 \text{ m}$	$r_{\max} = 0,0768 \text{ m}$
Area of the cross-section	$A_{\min} = 0,004825 \text{ m}^2$	$A_{\max} = 0,0184964 \text{ m}^2$
Sectional modulus	$W_{\min} = 4,729\text{E-}05 \text{ m}^3$	$W_{\max} = 0,0003549 \text{ m}^3$

The maximum forces from the software:

	I. Combination	II. Combination	III. Combination
$N_{\max} =$	3,49 kN	2,95 kN	2,53 kN
$M_{\max} =$	2,82 kNm	2,33 kNm	1,99 kNm
$V_{\max} =$	1,06 kN	0,87 kN	0,76 kN

I) Normal force

$$N_d \leq f_{c,0,d} * A$$

$$N_d \leq 67,551 \text{ kN}$$

$$f_{c,0,d} = 14,000 \text{ MPa}$$

verified - N_{\max} smaller

II) Moment

$$M_{z,d} \leq f_{m,d} * W_z$$

$$M_{z,d} \leq 7,644 \text{ kNm}$$

$$f_{m,d} = 21,538 \text{ MPa}$$

verified - M_{\max} smaller

III) Combination of moment and normal force

$$\sigma_{c,0,d} / f_{c,0,d} + \sigma_{m,d} / f_{m,d} \leq 1$$

$$0,421 < 1$$

verified - combination smaller than 1

IV) Shear force

$$V_d \leq 3/4 f_{v,d} * A$$

$$V_d \leq 7,794 \text{ kNm}$$

$$f_{v,d} = 2,154$$

verified - V_{\max} smaller

CONNECTION BETWEEN THE TREES 2 AND 3

Geometry of the connection

Total radius	$r_{6A} = 0,063 \text{ m}$
Area of the cross-section	$A_{\text{real},6A} = 0,0124627 \text{ m}^2$
Sectional modulus	$W_{6A} = 0,000191 \text{ m}^3$
(hole in the middle of the connection considered)	
Adjusted area of the section	$A_{\text{hole},6A} = 0,011341 \text{ m}^3$
(hole in the middle of the connection considered)	
Height of the connection	$h_{6A} = 0,012 \text{ m}$
Width of the connection	$b_{6A} = 0,013 \text{ m}$

The maximum forces from the software:

	I. Combination	II. Combination	III. Combination
$N_{\max} =$	3,11 kN	2,57 kN	2,14 kN
$M_{\max} =$	0,32 kNm	0,26 kNm	0,22 kNm
$V_{\max} =$	1,01 kN	0,83 kN	0,70 kN

I) Normal force

(real A used)

$$N_d \leq f_{c,0,d} * A_{\text{real}}$$

$$N_d \leq 174,477 \text{ kN}$$

$$f_{c,0,d} = 14,000 \text{ MPa}$$

verified - N_{\max} smaller

II) Moment

$M_{z,d} \leq f_{m,d} * W_z$	$f_{m,d} = 21,538 \text{ MPa}$
$M_{z,d} \leq 4,114 \text{ kNm}$	verified - M_{max}

III) Combination of moment and normal force

$\sigma_{c,0,d} / f_{c,0,d} + \sigma_{m,d} / f_{m,d} \leq 1$	verified - combination smaller than 1
0,096 < 1	

IV) Shear force (adjusted A used)

$V_d \leq 3/4 f_{v,d} * A_{hole}$	$f_{v,d} = 2,154 \text{ MPa}$
$V_d \leq 18,320 \text{ kN}$	verified - V_{max} smaller

V) Shear stresses due to the moment

$V_d \leq 0,5 f_{v,d} * A_{hole}$	$V_d = 2 * M_{max} / L + N$
$V_d \leq 12,213 \text{ kN}$	$V_d = 2,629 \text{ kN}$
	verified - V_{max} smaller

VI) Compression stresses perpendicular to the grain
- due to normal force

$h_d \geq N_h / f_{c,90,d} * b$	$N_h = N * \cos \alpha$
$h_d > 0,041 \text{ m}$	$f_{c,90,d} = 4,469 \text{ MPa}$
	not verified - h smaller

- due to moment

$h_d \geq N / f_{c,90,d} * b$	$N = 2 * M_{max} / L$
$h_d > 0,031 \text{ m}$	$N = 1,83 \text{ kN}$
	not verified - h smaller

VII) Tension stresses perpendicular to the grain
- due to normal force

$h_d \geq N_h / f_{t,90,d} * b$	$f_{t,90,d} = 0,420 \text{ MPa}$
$h_d > 0,370 \text{ m}$	not verified - h smaller

TREES 3A AND 3B CONNECTED TOGETHER
TREE 3A ABOVE THE CONNECTION

Geometry above the connection:

Radius	$r_{min} = 0,0234 \text{ m}$	$r_{max} = 0,0546 \text{ m}$
Area of the cross-section	$A_{min} = 0,0017193 \text{ m}^2$	$A_{max} = 0,0093608 \text{ m}^2$
Sectional modulus	$W_{min} = 1,006E-05 \text{ m}^3$	$W_{max} = 0,0001278 \text{ m}^3$

The maximum forces from the software:

	I. Combination	II. Combination	III. Combination
$N_{max} =$	3,14 kN	2,62 kN	2,20 kN
$M_{max} =$	2,15 kNm	1,77 kNm	1,48 kNm
$V_{max} =$	1,26 kN	1,04 kN	0,88 kN

I) Normal force

$N_d \leq f_{c,0,d} * A$	$f_{c,0,d} = 14,000 \text{ MPa}$
$N_d \leq 24,071 \text{ kN}$	verified - N_{max} smaller

II) Moment

$M_{z,d} \leq f_{m,d} * W_z$	$f_{m,d} = 21,538 \text{ MPa}$
$M_{z,d} \leq 2,752 \text{ kNm}$	verified - M_{max} smaller

III) Combination of moment and normal force

$\sigma_{c,0,d} / f_{c,0,d} + \sigma_{m,d} / f_{m,d} \leq 1$	verified - combination smaller than 1
0,912 < 1	

III) Shear force

$V_d \leq 3/4 f_{v,d} * A$	$f_{v,d} = 2,154$
$V_d \leq 2,777 \text{ kNm}$	verified - V_{max} smaller

TREE 3B ABOVE THE CONNECTION

Geometry above the connection:

Radius	$r_{min} = 0,0199 \text{ m}$	$r_{max} = 0,02995 \text{ m}$
Area of the cross-section	$A_{min} = 0,0012435 \text{ m}^2$	$A_{max} = 0,0028166 \text{ m}^2$
Sectional modulus	$W_{min} = 6,186E-06 \text{ m}^3$	$W_{max} = 2,109E-05 \text{ m}^3$

The maximum forces from the software:

	I. Combination	II. Combination	III. Combination
$N_{max} =$	3,14 kN	2,60 kN	2,18 kN
$M_{max} =$	1,66 kNm	1,37 kNm	1,15 kNm
$V_{max} =$	1,01 kN	0,83 kN	0,70 kN

I) Normal force

$N_d \leq f_{c,0,d} * A$	$f_{c,0,d} = 14,000 \text{ MPa}$
$N_d \leq 17,409 \text{ kN}$	verified - N_{max} smaller

II) Moment

$M_{z,d} \leq f_{m,d} * W_z$	$f_{m,d} = 21,538 \text{ MPa}$
$M_{z,d} \leq 0,454 \text{ kNm}$	not verified - M_{max} bigger

III) Shear force

$V_d \leq 3/4 f_{v,d} * A$	$f_{v,d} = 2,154$
$V_d \leq 2,009 \text{ kNm}$	verified - V_{max} smaller

CONNECTION A - ABOVE THE GROUND

Geometry of the connection

Total radius	$r_{6A} = 0,069 \text{ m}$
Area of the cross-section	$A_{real,6A} = 0,0149495 \text{ m}^2$
Sectional modulus	$W_{6A} = 0,0002509 \text{ m}^3$
(hole in the middle of the connection considered)	
Adjusted area of the section	$A_{hole,6A} = 0,0136041 \text{ m}^2$
(hole in the middle of the connection considered)	
Height of the connection	$h_{6A} = 0,051 \text{ m}$
Width of the connection	$b_{6A} = 0,032 \text{ m}$

The maximum forces from the software:

	I. Combination	II. Combination	III. Combination
$N_{max} =$	7,12 kN	5,99 kN	5,10 kN
$M_{max} =$	2,06 kNm	1,71 kNm	1,57 kNm
$V_{max} =$	0,84 kN	0,71 kN	1,51 kN

I) Normal force
(real A used)

$N_d \leq f_{c,0,d} * A_{real}$	$f_{c,0,d} = 14,000 \text{ MPa}$
$N_d \leq 209,294 \text{ kN}$	verified - N_{max} smaller

II) Moment

$M_{z,d} \leq f_{m,d} * W_z$	$f_{m,d} = 21,538 \text{ MPa}$
$M_{z,d} \leq 5,404 \text{ kNm}$	verified - M_{max} smaller

III) Combination of moment and normal force

$\sigma_{c,0,d} / f_{c,0,d} + \sigma_{m,d} / f_{m,d} \leq 1$	
0,415 < 1	verified - combination smaller than 1

IV) Shear force
(adjusted A used)

$$V_d \leq 3/4 f_{v,d} * A_{hole}$$

$$V_d \leq 21,976 \text{ kN}$$

$f_{v,d} = 2,154 \text{ MPa}$
verified - V_{max} smaller

V) Shear stresses due to the moment

$$V_d \leq 0,5 f_{v,d} * A_{hole}$$

$$V_d \leq 14,651 \text{ kN}$$

$V_d = 2 * M_{max} / L + N$
 $V_d = 12,571 \text{ kN}$
verified - V_{max} smaller

VI) Compression stresses perpendicular to the grain
- due to normal force

$$h_d \geq N_h / f_{c,90,d} * b$$

$$h_d > 0,008 \text{ m}$$

$N_h = N * \cos \alpha$
 $f_{c,90,d} = 4,469 \text{ MPa}$
verified - h bigger

- due to moment

$$h_d \geq N / f_{c,90,d} * b$$

$$h_d > 0,082 \text{ m}$$

$N = 2 * M_{max} / L$
 $N = 11,77 \text{ kN}$
not verified - h smaller

VII) Tension stresses perpendicular to the grain
- due to normal force

$$h_d \geq N_h / f_{t,90,d} * b$$

$$h_d > 0,092 \text{ m}$$

$f_{t,90,d} = 0,420 \text{ MPa}$
not verified - h smaller

CONNECTION B - ABOVE THE CONNECTION A

Geometry of the connection

Total radius	$r_{6B} = 0,081 \text{ m}$
Area of the cross-section	$A_{real,6B} = 0,0206015 \text{ m}^2$
Sectional modulus (hole in the middle of the connection considered)	$W_{6B} = 0,0004059 \text{ m}^3$
Adjusted area of the section (hole in the middle of the connection considered)	$A_{hole,6B} = 0,0187474 \text{ m}^2$
Height of the connection	$h_{6B} = 0,057 \text{ m}$
Width of the connection	$b_{6A} = 0,035 \text{ m}$

The maximum forces from the software:

	I. Combination	II. Combination	III. Combination
$N_{max} =$	7,12 kN	5,99 kN	5,10 kN
$M_{max} =$	2,06 kNm	1,71 kNm	1,57 kNm
$V_{max} =$	0,84 kN	0,71 kN	1,51 kN

I) Normal force
(real A used)

$$N_d \leq f_{c,0,d} * A_{real}$$

$$N_d \leq 288,422 \text{ kN}$$

$f_{c,0,d} = 14,000 \text{ MPa}$
verified - N_{max} smaller

II) Moment

$$M_{z,d} \leq f_{m,d} * W_z$$

$$M_{z,d} \leq 8,743 \text{ kNm}$$

$f_{m,d} = 21,538 \text{ MPa}$
verified - M_{max} smaller

III) Combination of moment and normal force

$$\sigma_{c,0,d} / f_{c,0,d} + \sigma_{m,d} / f_{m,d} \leq 1$$

$$0,260 < 1$$

verified - combination smaller than 1

IV) Shear force
(adjusted A used)

$$V_d \leq 3/4 f_{v,d} * A_{hole}$$

$$V_d \leq 30,284 \text{ kN}$$

$f_{v,d} = 2,154 \text{ MPa}$
verified - V_{max} smaller

V) Shear stresses due to the moment

$$V_d \leq 0,5 f_{v,d} * A_{\text{hole}}$$

$$V_d \leq 20,190 \text{ kN}$$

$$V_d = 2 * M_{\text{max}} / L + N$$

$$V_d = 12,571 \text{ kN}$$

verified - V_{max} smaller

VI) Compression stresses perpendicular to the grain

- due to normal force

$$h_d \geq N_h / f_{c,90,d} * b$$

$$h_d > 0,007 \text{ m}$$

$$N_h = N * \cos \alpha$$

$$f_{c,90,d} = 4,469 \text{ MPa}$$

verified - h bigger

- due to moment

$$h_d \geq N / f_{c,90,d} * b$$

$$h_d > 0,075 \text{ m}$$

$$N = 2 * M_{\text{max}} / L$$

$$N = 11,77 \text{ kN}$$

not verified - h smaller

VII) Tension stresses perpendicular to the grain

- due to normal force

$$h_d \geq N_h / f_{t,90,d} * b$$

$$h_d > 0,084 \text{ m}$$

$$f_{t,90,d} = 0,420 \text{ MPa}$$

not verified - h smaller

TREE 4A

Geometry

Radius	$r_{\text{min}} = 0,0164 \text{ m}$	$r_{\text{max}} = 0,0284 \text{ m}$
Area of the cross-section	$A_{\text{min}} = 0,0008445 \text{ m}^2$	$A_{\text{max}} = 0,0025326 \text{ m}^2$
Sectional modulus	$W_{\text{min}} = 3,463\text{E-}06 \text{ m}^3$	$W_{\text{max}} = 1,798\text{E-}05 \text{ m}^3$

The maximum forces from the software:

	I. Combination	II. Combination	III. Combination
$N_{\text{max}} =$	3,28 kN	2,71 kN	2,27 kN
$M_{\text{max}} =$	0,88 kNm	0,73 kNm	0,63 kNm
$V_{\text{max}} =$	0,42 kN	0,34 kN	0,32 kN

I) Normal force

$$N_d \leq f_{c,0,d} * A$$

$$N_d \leq 11,823 \text{ kN}$$

$$f_{c,0,d} = 14,000 \text{ MPa}$$

verified - N_{max} smaller

I) Moment

$$M_{z,d} \leq f_{m,d} * W_z$$

$$M_{z,d} \leq 0,387 \text{ kNm}$$

$$f_{m,d} = 21,538 \text{ MPa}$$

not verified - M_{max} bigger

I) Shear force

$$V_d \leq 3/4 f_{v,d} * A$$

$$V_d \leq 1,364 \text{ kNm}$$

$$f_{v,d} = 2,154 \text{ MPa}$$

verified - V_{max} smaller

TREE 4B

Geometry

Radius	$r_{\text{min}} = 0,0207 \text{ m}$	$r_{\text{max}} = 0,0336 \text{ m}$
Area of the cross-section	$A_{\text{min}} = 0,0013455 \text{ m}^2$	$A_{\text{max}} = 0,0035449 \text{ m}^2$
Sectional modulus	$W_{\text{min}} = 6,963\text{E-}06 \text{ m}^3$	$W_{\text{max}} = 2,978\text{E-}05 \text{ m}^3$

The maximum forces from the software:

	I. Combination	II. Combination	III. Combination
$N_{\text{max}} =$	3,30 kN	2,74 kN	2,29 kN
$M_{\text{max}} =$	0,90 kNm	0,74 kNm	0,65 kNm
$V_{\text{max}} =$	0,42 kN	0,35 kN	0,32 kN

I) Normal force	$N_d \leq f_{c,0,d} * A$ $N_d \leq 18,836 \text{ kN}$	$f_{c,0,d} = 14,000 \text{ MPa}$ verified - N_{max} smaller
II) Moment	$M_{z,d} \leq f_{m,d} * W_z$ $M_{z,d} \leq 0,641 \text{ kNm}$	$f_{m,d} = 21,538 \text{ MPa}$ not verified - M_{max} bigger
IV) Shear force	$V_d \leq 3/4 f_{v,d} * A$ $V_d \leq 2,173 \text{ kNm}$	$f_{v,d} = 2,154 \text{ MPa}$ verified - V_{max} smaller

TREE 5A

Geometry

Radius	$r_{min} = 0,0185 \text{ m}$	$r_{max} = 0,0326 \text{ m}$
Area of the cross-section	$A_{min} = 0,0010747 \text{ m}^2$	$A_{max} = 0,0033371 \text{ m}^2$
Sectional modulus	$W_{min} = 4,97E-06 \text{ m}^3$	$W_{max} = 2,72E-05 \text{ m}^3$

The maximum forces from the software:

	I. Combination	II. Combination	III. Combination
$N_{max} =$	3,31 kN	2,74 kN	2,29 kN
$M_{max} =$	0,64 kNm	0,52 kNm	0,47 kNm
$V_{max} =$	0,31 kN	0,25 kN	0,24 kN

I) Normal force	$N_d \leq f_{c,0,d} * A$ $N_d \leq 15,045 \text{ kN}$	$f_{c,0,d} = 14,000 \text{ MPa}$ verified - N_{max} smaller
I) Moment	$M_{z,d} \leq f_{m,d} * W_z$ $M_{z,d} \leq 0,586 \text{ kNm}$	$f_{m,d} = 21,538$ not verified - M_{max} bigger
I) Shear force	$V_d \leq 3/4 f_{v,d} * A$ $V_d \leq 1,736 \text{ kNm}$	$f_{v,d} = 2,154 \text{ MPa}$ verified - V_{max} smaller

TREE 5B

Geometry

Radius	$r_{min} = 0,0148 \text{ m}$	$r_{max} = 0,0256 \text{ m}$
Area of the cross-section	$A_{min} = 0,0006878 \text{ m}^2$	$A_{max} = 0,0020578 \text{ m}^2$
Sectional modulus	$W_{min} = 2,545E-06 \text{ m}^3$	$W_{max} = 1,317E-05 \text{ m}^3$

The maximum forces from the software:

	I. Combination	II. Combination	III. Combination
$N_{max} =$	3,21 kN	2,65 kN	2,22 kN
$M_{max} =$	1,68 kNm	1,38 kNm	1,18 kNm
$V_{max} =$	0,76 kN	0,63 kN	0,55 kN

I) Normal force	$N_d \leq f_{c,0,d} * A$ $N_d \leq 9,629 \text{ kN}$	$f_{c,0,d} = 14,000 \text{ MPa}$ verified - N_{max} smaller
II) Moment	$M_{z,d} \leq f_{m,d} * W_z$ $M_{z,d} \leq 0,284 \text{ kNm}$	$f_{m,d} = 21,538$ not verified - M_{max} bigger

III) Shear force

$$V_d \leq 3/4 f_{v,d} * A$$

$$V_d \leq 1,111 \text{ kNm}$$

$$f_{v,d} = 2,154 \text{ MPa}$$

verified - V_{max} smaller

TREES 6A AND 6B CONNECTED TOGETHER

TREE 6A ABOVE THE CONNECTION

Geometry above the connection

Radius	$r_{min} = 0,0519 \text{ m}$	$r_{max} = 0,075 \text{ m}$
Area of the cross-section	$A_{min} = 0,0084579 \text{ m}^2$	$A_{max} = 0,0176625 \text{ m}^2$
Sectional modulus	$W_{min} = 0,0001097 \text{ m}^3$	$W_{max} = 0,0003312 \text{ m}^3$

The maximum forces from the software:

	I. Combination	II. Combination	III. Combination
$N_{max} =$	3,41 kN	2,86 kN	2,43 kN
$M_{max} =$	1,33 kNm	1,10 kNm	0,95 kNm
$V_{max} =$	0,89 kN	0,74 kN	0,66 kN

I) Normal force

$$N_d \leq f_{c,0,d} * A$$

$$N_d \leq 118,411 \text{ kN}$$

$$f_{c,0,d} = 14,000 \text{ MPa}$$

verified - N_{max} smaller

II) Moment

$$M_{z,d} \leq f_{m,d} * W_z$$

$$M_{z,d} \leq 7,133 \text{ kNm}$$

$$f_{m,d} = 21,538 \text{ MPa}$$

verified - M_{max} smaller

III) Combination of moment and normal force

$$\sigma_{c,0,d} / f_{c,0,d} + \sigma_{m,d} / f_{m,d} \leq 1$$

$$0,215 < 1$$

verified - combination smaller than 1

IV) Shear force

$$V_d \leq 3/4 f_{v,d} * A$$

$$V_d \leq 13,663 \text{ kNm}$$

$$f_{v,d} = 2,154 \text{ MPa}$$

verified - V_{max} smaller

TREE 6B ABOVE THE CONNECTION

Geometry above the connection

Radius	$r_{min} = 0,0427 \text{ m}$	$r_{max} = 0,0616 \text{ m}$
Area of the cross-section	$A_{min} = 0,0057251 \text{ m}^2$	$A_{max} = 0,0119149 \text{ m}^2$
Sectional modulus	$W_{min} = 6,112E-05 \text{ m}^3$	$W_{max} = 0,0001835 \text{ m}^3$

The maximum forces from the software:

	I. Combination	II. Combination	III. Combination
$N_{max} =$	3,28 kN	2,94 kN	2,31 kN
$M_{max} =$	1,10 kNm	0,91 kNm	0,77 kNm
$V_{max} =$	0,89 kN	0,74 kN	0,64 kN

I) Normal force

$$N_d \leq f_{c,0,d} * A$$

$$N_d \leq 80,152 \text{ kN}$$

$$f_{c,0,d} = 14,000 \text{ MPa}$$

verified - N_{max} smaller

II) Moment

$$M_{z,d} \leq f_{m,d} * W_z$$

$$M_{z,d} \leq 3,952 \text{ kNm}$$

$$f_{m,d} = 21,538 \text{ MPa}$$

verified - M_{max} smaller

III) Combination of moment and normal force

$$\sigma_{c,0,d} / f_{c,0,d} + \sigma_{m,d} / f_{m,d} \leq 1$$

$$0,319 < 1$$

verified - combination smaller than 1

IV) Shear force

$$V_d \leq 3/4 f_{v,d} * A$$

$$V_d \leq 9,248 \text{ kNm}$$

$f_{v,d} = 2,154 \text{ MPa}$
verified - V_{max} smaller

CONNECTION A - ABOVE THE GROUND

Geometry of the connection

Total radius $r_{6A} = 0,127 \text{ m}$
 Area of the cross-section $A_{real,6A} = 0,0506451 \text{ m}^2$
 Sectional modulus $W_{6A} = 0,0015646 \text{ m}^3$
 (hole in the middle of the connection considered)
 Adjusted area of the section $A_{hole,6A} = 0,046087 \text{ m}^3$
 (hole in the middle of the connection considered)
 Height of the connection $h_{6A} = 0,21 \text{ m}$
 Width of the connection $b_{6A} = 0,075 \text{ m}$

The maximum forces from the software:

	I. Combination	II. Combination	III. Combination
$N_{max} =$	7,51 kN	6,41 kN	5,55 kN
$M_{max} =$	2,57 kNm	2,15 kNm	1,93 kNm
$V_{max} =$	1,91 kN	1,63 kN	1,51 kN

I) Normal force (real A used)

$$N_d \leq f_{c,0,d} * A_{real}$$

$$N_d \leq 709,031 \text{ kN}$$

$f_{c,0,d} = 14,000 \text{ MPa}$
verified - N_{max} smaller

II) Moment

$$M_{z,d} \leq f_{m,d} * W_z$$

$$M_{z,d} \leq 33,698 \text{ kNm}$$

$f_{m,d} = 21,538 \text{ MPa}$
verified - M_{max} smaller

III) Combination of moment and normal force

$$\sigma_{c,0,d} / f_{c,0,d} + \sigma_{m,d} / f_{m,d} \leq 1$$

$$0,087 < 1$$

verified - combination smaller than 1

IV) Shear force (adjusted A used)

$$V_d \leq 3/4 f_{v,d} * A_{hole}$$

$$V_d \leq 74,448 \text{ kN}$$

$f_{v,d} = 2,154 \text{ MPa}$
verified - V_{max} smaller

V) Shear stresses due to the moment

$$V_d \leq 0,5 f_{v,d} * A_{hole}$$

$$V_d \leq 49,632 \text{ kN}$$

$V_d = 2 * M_{max} / L + N$
 $V_d = 7,653 \text{ kN}$
 verified - V_{max} smaller

VI) Compression stresses perpendicular to the grain

- due to normal force

$$h_d \geq N_h / f_{c,90,d} * b$$

$$h_d > 0,008 \text{ m}$$

$N_h = N * \cos \alpha$
 $f_{c,90,d} = 4,469 \text{ MPa}$
 verified - h bigger

- due to moment

$$h_d \geq N / f_{c,90,d} * b$$

$$h_d > 0,020 \text{ m}$$

$N = 2 * M_{max} / L$
 $N = 6,85 \text{ kN}$
 verified - h bigger

VII) Tension stresses perpendicular to the grain

- due to normal force

$$h_d \geq N_h / f_{t,90,d} * b$$

$$h_d > 0,119 \text{ m}$$

$f_{t,90,d} = 0,420 \text{ MPa}$
 verified - h bigger

CONNECTION B - ABOVE THE CONNECTION A

Geometry of the connection

Total radius	$r_{6B} = 0,109 \text{ m}$
Area of the cross-section	$A_{\text{real},6B} = 0,0373063 \text{ m}^2$
Sectional modulus (hole in the middle of the connection considered)	$W_{6B} = 0,0009891 \text{ m}^3$
Adjusted area of the section (hole in the middle of the connection considered)	$A_{\text{hole},6B} = 0,0339488 \text{ m}^2$
Height of the connection	$h_{6B} = 0,15 \text{ m}$
Width of the connection	$b_{6A} = 0,07 \text{ m}$

The maximum forces from the software:

	I. Combination	II. Combination	III. Combination
$N_{\text{max}} =$	7,51 kN	6,41 kN	5,55 kN
$M_{\text{max}} =$	2,57 kNm	2,15 kNm	1,93 kNm
$V_{\text{max}} =$	1,91 kN	1,63 kN	1,51 kN

I) Normal force (real A used)	$N_d \leq f_{c,0,d} * A_{\text{real}}$ $N_d \leq 522,289 \text{ kN}$	$f_{c,0,d} = 14,000 \text{ MPa}$ verified - N_{max} smaller
II) Moment	$M_{z,d} \leq f_{m,d} * W_z$ $M_{z,d} \leq 21,305 \text{ kNm}$	$f_{m,d} = 21,538 \text{ MPa}$ verified - M_{max} smaller
III) Combination of moment and normal force	$\sigma_{c,0,d} / f_{c,0,d} + \sigma_{m,d} / f_{m,d} \leq 1$ $0,135 < 1$	verified - combination smaller than 1
IV) Shear force (adjusted A used)	$V_d \leq 3/4 f_{v,d} * A_{\text{hole}}$ $V_d \leq 54,840 \text{ kN}$	$f_{v,d} = 2,154 \text{ MPa}$ verified - V_{max} smaller
V) Shear stresses due to the moment	$V_d \leq 0,5 f_{v,d} * A_{\text{hole}}$ $V_d \leq 36,560 \text{ kN}$	$V_d = 2 * M_{\text{max}} / L + N$ $V_d = 7,653 \text{ kN}$ verified - V_{max} smaller
VI) Compression stresses perpendicular to the grain		
- due to normal force	$h_d \geq N_h / f_{c,90,d} * b$ $h_d > 0,012 \text{ m}$	$N_h = N * \cos \alpha$ $f_{c,90,d} = 4,469 \text{ MPa}$ verified - h bigger
- due to moment	$h_d \geq N / f_{c,90,d} * b$ $h_d > 0,022 \text{ m}$	$N = 2 * M_{\text{max}} / L$ $N = 6,85 \text{ kN}$ verified - h bigger
VII) Tension stresses perpendicular to the grain		
- due to normal force	$h_d \geq N_h / f_{t,90,d} * b$ $h_d > 0,108 \text{ m}$	$f_{t,90,d} = 0,420 \text{ MPa}$ verified - h bigger

TREE 7

Geometry

Radius	$r_{\min} = 0,0189 \text{ m}$	$r_{\max} = 0,0385 \text{ m}$
Area of the cross-section	$A_{\min} = 0,0011216 \text{ m}^2$	$A_{\max} = 0,0046543 \text{ m}^2$
Sectional modulus	$W_{\min} = 5,3\text{E-}06 \text{ m}^3$	$W_{\max} = 4,48\text{E-}05 \text{ m}^3$

The maximum forces from the software:

	I. Combination	II. Combination	III. Combination
$N_{\max} =$	3,27 kN	2,72 kN	2,28 kN
$M_{\max} =$	1,55 kNm	1,28 kNm	1,10 kNm
$V_{\max} =$	0,70 kN	0,58 kN	0,52 kN

I) Normal force	$N_d \leq f_{c,0,d} * A$ $N_d \leq 15,703 \text{ kN}$	$f_{c,0,d} = 14,000 \text{ MPa}$ verified - N_{\max} smaller
II) Moment	$M_{z,d} \leq f_{m,d} * W_z$ $M_{z,d} \leq 0,965 \text{ kNm}$	$f_{m,d} = 21,538$ not verified - M_{\max} bigger
III) Shear force	$V_d \leq 3/4 f_{v,d} * A$ $V_d \leq 1,812 \text{ kNm}$	$f_{v,d} = 2,154 \text{ MPa}$ verified - V_{\max} smaller

TREE 8

Geometry

Radius	$r_{\min} = 0,0150 \text{ m}$	$r_{\max} = 0,0277 \text{ m}$
Area of the cross-section	$A_{\min} = 0,0007065 \text{ m}^2$	$A_{\max} = 0,0024093 \text{ m}^2$
Sectional modulus	$W_{\min} = 2,649\text{E-}06 \text{ m}^3$	$W_{\max} = 1,668\text{E-}05 \text{ m}^3$

The maximum forces from the software:

	I. Combination	II. Combination	III. Combination
$N_{\max} =$	3,21 kN	2,66 kN	2,22 kN
$M_{\max} =$	1,69 kNm	1,39 kNm	1,19 kNm
$V_{\max} =$	0,77 kN	0,64 kN	0,56 kN

I) Normal force	$N_d \leq f_{c,0,d} * A$ $N_d \leq 9,891 \text{ kN}$	$f_{c,0,d} = 14,000 \text{ MPa}$ verified - N_{\max} smaller
II) Moment	$M_{z,d} \leq f_{m,d} * W_z$ $M_{z,d} \leq 0,359 \text{ kNm}$	$f_{m,d} = 21,538$ not verified - M_{\max} bigger
III) Shear force	$V_d \leq 3/4 f_{v,d} * A$ $V_d \leq 1,141 \text{ kNm}$	$f_{v,d} = 2,154 \text{ MPa}$ verified - V_{\max} smaller

TREE 9A

Geometry

Radius	$r_{\min} = 0,0177 \text{ m}$	$r_{\max} = 0,031 \text{ m}$
Area of the cross-section	$A_{\min} = 0,0009837 \text{ m}^2$	$A_{\max} = 0,0030175 \text{ m}^2$
Sectional modulus	$W_{\min} = 4,353\text{E-}06 \text{ m}^3$	$W_{\max} = 2,339\text{E-}05 \text{ m}^3$

The maximum forces from the software:

	I. Combination	II. Combination	III. Combination
$N_{max} =$	3,22 kN	2,67 kN	2,23 kN
$M_{max} =$	1,72 kNm	1,42 kNm	1,22 kNm
$V_{max} =$	0,78 kN	0,64 kN	0,57 kN

I) Normal force	$N_d \leq f_{c,0,d} * A$ $N_d \leq 13,772 \text{ kN}$	$f_{c,0,d} = 14,000 \text{ MPa}$ verified - N_{max} smaller
I) Moment	$M_{z,d} \leq f_{m,d} * W_z$ $M_{z,d} \leq 0,504 \text{ kNm}$	$f_{m,d} = 21,538 \text{ MPa}$ not verified - M_{max} bigger
I) Shear force	$V_d \leq 3/4 f_{v,d} * A$ $V_d \leq 1,589 \text{ kNm}$	$f_{v,d} = 2,154 \text{ MPa}$ verified - V_{max} smaller

TREE 9B

Geometry

Radius	$r_{min} = 0,0315 \text{ m}$	$r_{max} = 0,0615 \text{ m}$
Area of the cross-section	$A_{min} = 0,0031157 \text{ m}^2$	$A_{max} = 0,0118763 \text{ m}^2$
Sectional modulus	$W_{min} = 2,454E-05 \text{ m}^3$	$W_{max} = 0,0001826 \text{ m}^3$

The maximum forces from the software:

	I. Combination	II. Combination	III. Combination
$N_{max} =$	4,29 kN	3,59 kN	3,04 kN
$M_{max} =$	2,09 kNm	1,73 kNm	1,51 kNm
$V_{max} =$	0,95 kN	0,78 kN	0,70 kN

I) Normal force	$N_d \leq f_{c,0,d} * A$ $N_d \leq 43,619 \text{ kN}$	$f_{c,0,d} = 14,000 \text{ MPa}$ verified - N_{max} smaller
II) Moment	$M_{z,d} \leq f_{m,d} * W_z$ $M_{z,d} \leq 3,933 \text{ kNm}$	$f_{m,d} = 21,538 \text{ MPa}$ verified - M_{max} smaller
III) Combination of moment and normal force	$\sigma_{c,0,d} / f_{c,0,d} + \sigma_{m,d} / f_{m,d} \leq 1$ 0,630 < 1	verified - combination smaller than 1
IV) Shear force	$V_d \leq 3/4 f_{v,d} * A$ $V_d \leq 5,033 \text{ kNm}$	$f_{v,d} = 2,154 \text{ MPa}$ verified - V_{max} smaller

CONNECTION BETWEEN THE TREES 9 AND 10

Geometry of the connection

Total radius	$r_{6A} = 0,0447 \text{ m}$
Area of the cross-section	$A_{real,6A} = 0,006274 \text{ m}^2$
Sectional modulus (hole in the middle of the connection considered)	$W_{6A} = 6,822E-05 \text{ m}^3$
Adjusted area of the section (hole in the middle of the connection considered)	$A_{hole,6A} = 0,0057093 \text{ m}^2$
Height of the connection	$h_{6A} = 0,075 \text{ m}$
Width of the connection	$b_{6A} = 0,085 \text{ m}$

The maximum forces from the software:

	I. Combination	II. Combination	III. Combination
$N_{max} =$	4,02 kN	3,02 kN	2,77 kN
$M_{max} =$	0,43 kNm	0,35 kNm	0,29 kNm
$V_{max} =$	1,16 kN	0,96 kN	0,80 kN

I) Normal force
(real A used)

$$N_d \leq f_{c,0,d} * A_{real}$$

$$N_d \leq 87,836 \text{ kN}$$

$f_{c,0,d} = 14,000 \text{ MPa}$
verified - N_{max} smaller

II) Moment

$$M_{z,d} \leq f_{m,d} * W_z$$

$$M_{z,d} \leq 1,469 \text{ kNm}$$

$f_{m,d} = 21,538 \text{ MPa}$
verified - M_{max} smaller

III) Combination of moment and normal force

$$\sigma_{c,0,d} / f_{c,0,d} + \sigma_{m,d} / f_{m,d} \leq 1$$

$$0,338 < 1$$

verified - combination smaller than 1

IV) Shear force
(adjusted A used)

$$V_d \leq 3/4 f_{v,d} * A_{hole}$$

$$V_d \leq 9,223 \text{ kN}$$

$f_{v,d} = 2,154 \text{ MPa}$
verified - V_{max} smaller

V) Shear stresses due to the moment

$$V_d \leq 0,5 f_{v,d} * A_{hole}$$

$$V_d \leq 6,149 \text{ kN}$$

$V_d = 2 * M_{max} / L + N$
 $V_d = 3,257 \text{ kN}$
verified - V_{max} smaller

VI) Compression stresses perpendicular to the grain

- due to normal force

$$h_d \geq N_h / f_{c,90,d} * b$$

$$h_d > 0,007 \text{ m}$$

$N_h = N * \cos \alpha$
 $f_{c,90,d} = 4,469 \text{ MPa}$
verified - h bigger

- due to moment

$$h_d \geq N / f_{c,90,d} * b$$

$$h_d > 0,006 \text{ m}$$

$N = 2 * M_{max} / L$
 $N = 2,46 \text{ kN}$
verified - h bigger

VII) Tension stresses perpendicular to the grain

- due to normal force

$$h_d \geq N_h / f_{t,90,d} * b$$

$$h_d > 0,062 \text{ m}$$

$f_{t,90,d} = 0,420 \text{ MPa}$
verified - h bigger

TREE 10A

Geometry

Radius	$r_{min} = 0,0202 \text{ m}$	$r_{max} = 0,0486 \text{ m}$
Area of the cross-section	$A_{min} = 0,0012812 \text{ m}^2$	$A_{max} = 0,0074166 \text{ m}^2$
Sectional modulus	$W_{min} = 6,47E-06 \text{ m}^3$	$W_{max} = 9,011E-05 \text{ m}^3$

The maximum forces from the software:

	I. Combination	II. Combination	III. Combination
$N_{max} =$	2,62 kN	2,18 kN	1,85 kN
$M_{max} =$	0,23 kNm	0,19 kNm	0,16 kNm
$V_{max} =$	0,39 kN	0,32 kN	0,28 kN

I) Normal force	$N_d \leq f_{c,0,d} * A$ $N_d \leq 17,937 \text{ kN}$	$f_{c,0,d} = 14,000 \text{ MPa}$ verified - N_{max} smaller
II) Moment	$M_{z,d} \leq f_{m,d} * W_z$ $M_{z,d} \leq 1,359 \text{ kNm}$	$f_{m,d} = 21,538 \text{ MPa}$ verified - M_{max} smaller
III) Combination of moment and normal force	$\sigma_{c,0,d} / f_{c,0,d} + \sigma_{m,d} / f_{m,d} \leq 1$ $0,315 < 1$	verified - combination smaller than 1
I) Shear force	$V_d \leq 3/4 f_{v,d} * A$ $V_d \leq 2,070 \text{ kNm}$	$f_{v,d} = 2,154 \text{ MPa}$ verified - V_{max} smaller

TREE 10B

Geometry

Radius	$r_{min} = 0,0503 \text{ m}$	$r_{max} = 0,0997 \text{ m}$
Area of the cross-section	$A_{min} = 0,0079445 \text{ m}^2$	$A_{max} = 0,0312119 \text{ m}^2$
Sectional modulus	$W_{min} = 9,99E-05 \text{ m}^3$	$W_{max} = 0,000778 \text{ m}^3$

The maximum forces from the software:

	I. Combination	II. Combination	III. Combination
$N_{max} =$	3,8 kN	3,26 kN	2,82 kN
$M_{max} =$	1,9 kNm	1,57 kNm	1,40 kNm
$V_{max} =$	0,85 kN	0,70 kN	0,68 kN

I) Normal force	$N_d \leq f_{c,0,d} * A$ $N_d \leq 111,223 \text{ kN}$	$f_{c,0,d} = 14,000 \text{ MPa}$ verified - N_{max} smaller
II) Moment	$M_{z,d} \leq f_{m,d} * W_z$ $M_{z,d} \leq 16,756 \text{ kNm}$	$f_{m,d} = 21,538$ verified - M_{max} smaller
III) Combination of moment and normal force	$\sigma_{c,0,d} / f_{c,0,d} + \sigma_{m,d} / f_{m,d} \leq 1$ $0,122 < 1$	verified - combination smaller than 1
IV) Shear force	$V_d \leq 3/4 f_{v,d} * A$ $V_d \leq 12,833 \text{ kNm}$	$f_{v,d} = 2,154 \text{ MPa}$ verified - V_{max} smaller

APPENDIX E

CALCULATION OF THE LOAD-BEARING CAPACITY
OVER TIME

CURRENT GEOMETRY OF TREE 5B

Circumference of the trunk in the length of:

0 m	$C_0 =$	0,161	m
1 m	$C_1 =$	0,125	m
2 m	$C_2 =$	0,093	m
3 m	$C_3 =$	0,072	m
Total length	$L =$	3,62	m
Total height	$h =$	3,5	m
Slope	$a =$	75,53	°

CALCULATION OF GROWTH SPEED

Overview of geometry in 2010 and 2017

TREE	CIRCUMFERENCE AT 1 M [m]		LENGTH OF A TRUNK [m]		GROWTH SPEED [m/year]	
	year 2010	year 2017	year 2010	year 2017	circumference	length
2	0,1	0,384	2,5	4,66	0,047	0,360
3A	0,1	0,282	2,5	4,48	0,030	0,330
6A	0,1	0,380	2,5	5,91	0,047	0,568
6B	0,1	0,308	2,5	5,19	0,035	0,448
9B	0,1	0,326	2,5	5,09	0,038	0,432
10A	0,1	0,214	2,5	4,27	0,019	0,295
10B	0,1	0,386	2,5	5,42	0,048	0,487
AVERAGE VALUE					0,041	0,411

GEOMETRY OF TREE 5B OVER TIME

TIME [years]	CIRCUMFERENCE IN THE LENGTH OF					LENGTH [m]
	0 M [m]	1 M [m]	2 M [m]	3 M [m]	4 M [m]	
0	0,161	0,125	0,093	0,072	-	3,620
2	0,242	0,206	0,174	0,153	0,061	4,443
5	0,365	0,329	0,297	0,276	0,183	5,677
6	0,405	0,369	0,337	0,316	0,224	6,088
7	0,446	0,410	0,378	0,357	0,265	6,499
10	0,568	0,532	0,500	0,479	0,387	7,733

VERIFICATION OF LOAD-BEARING CAPACITY OF TREE 5B OVER TIME

IN 7 YEARS

Geometry

Radius	$r_{\min} =$	0,0421	m	$r_{\max} =$	0,0710	m
Area of the cross-section	$A_{\min} =$	0,0055748	m ²	$A_{\max} =$	0,01584	m ²
Sectional modulus	$W_{\min} =$	0,0000587	m ³	$W_{\max} =$	0,00028	m ³

The maximum forces from the software:

	I. Combination	II. Combination	III. Combination
$N_{\max} =$	3,93 kN	3,37 kN	2,94 kN
$M_{\max} =$	3,03 kNm	2,50 kNm	2,48 kNm
$V_{\max} =$	0,76 kN	0,63 kN	0,69 kN

I) Normal force

$$N_d \leq f_{c,0,d} * A$$

$$N_d \leq 78,047 \text{ kN}$$

$f_{c,0,d} = 14,000 \text{ MPa}$
 VERIFIED - $N_{\max} < 78,047 \text{ kN}$

II) Moment

$$M_{z,d} \leq f_{m,d} * W_z$$

$$M_{z,d} \leq 6,058 \text{ kNm}$$

$f_{m,d} = 21,538 \text{ MPa}$
 VERIFIED - $M_{\max} < 6,058 \text{ kNm}$

III) Combination of moment and normal force

$$\sigma_{c,0,d} / f_{c,0,d} + \sigma_{m,d} / f_{m,d} \leq 1$$

$$0,550 \leq 1$$

VERIFIED

IV) Shear force

$$V_d \leq 3/4 f_{v,d} * A$$

$$V_d \leq 9,006 \text{ kNm}$$

$f_{v,d} = 2,154 \text{ MPa}$
 VERIFIED - $V_{\max} < 9,006 \text{ kN}$

STATE AFTER 7 YEARS VERIFIED

IN 5 YEARS

Geometry

Radius	$r_{\min} = 0,0292 \text{ m}$	$r_{\max} = 0,0581 \text{ m}$
Area of the cross-section	$A_{\min} = 0,0026712 \text{ m}^2$	$A_{\max} = 0,01058 \text{ m}^2$
Sectional modulus	$W_{\min} = 0,0000195 \text{ m}^3$	$W_{\max} = 0,00015 \text{ m}^3$

The maximum forces from the software:

	I. Combination	II. Combination	III. Combination
$N_{\max} =$	3,61 kN	3,06 kN	2,62 kN
$M_{\max} =$	3,03 kNm	2,50 kNm	2,34 kNm
$V_{\max} =$	0,76 kN	0,63 kN	0,64 kN

I) Normal force

$$N_d \leq f_{c,0,d} * A$$

$$N_d \leq 37,397 \text{ kN}$$

$f_{c,0,d} = 14,000 \text{ MPa}$
 VERIFIED - $N_{\max} < 37,397 \text{ kN}$

II) Moment

$$M_{z,d} \leq f_{m,d} * W_z$$

$$M_{z,d} \leq 3,309 \text{ kNm}$$

$f_{m,d} = 21,538 \text{ MPa}$
 VERIFIED - $M_{\max} < 3,309 \text{ kNm}$

III) Combination of moment and normal force

$$\sigma_{c,0,d} / f_{c,0,d} + \sigma_{m,d} / f_{m,d} \leq 1$$

$$1,012 > 1$$

NOT VERIFIED

IV) Shear force

$$V_d \leq 3/4 f_{v,d} * A$$

$$V_d \leq 4,315 \text{ kNm}$$

$f_{v,d} = 2,154 \text{ MPa}$
 VERIFIED - $V_{\max} < 4,315 \text{ kN}$

STATE AFTER 5 YEARS NOT VERIFIED

IN 6 YEARS

Geometry

Radius	$r_{\min} = 0,0357$	m	$r_{\max} = 0,0645$	m
Area of the cross-section	$A_{\min} = 0,0039909$	m ²	$A_{\max} = 0,01308$	m ²
Sectional modulus	$W_{\min} = 0,0000356$	m ³	$W_{\max} = 0,00021$	m ³

The maximum forces from the software:

	I. Combination	II. Combination	III. Combination
$N_{\max} =$	3,81 kN	3,25 kN	2,82 kN
$M_{\max} =$	3,03 kNm	2,50 kNm	2,42 kNm
$V_{\max} =$	0,76 kN	0,63 kN	0,67 kN

I) Normal force

$$N_d \leq f_{c,0,d} \cdot A$$

$$N_d \leq 55,873 \text{ kN}$$

$f_{c,0,d} = 14,000 \text{ MPa}$
 VERIFIED - $N_{\max} < 55,873 \text{ kN}$

II) Moment

$$M_{z,d} \leq f_{m,d} \cdot W_z$$

$$M_{z,d} \leq 4,546 \text{ kNm}$$

$f_{m,d} = 21,538 \text{ MPa}$
 VERIFIED - $M_{\max} < 4,546 \text{ kNm}$

III) Combination of moment and normal force

$$\sigma_{c,0,d} / f_{c,0,d} + \sigma_{m,d} / f_{m,d} \leq 1$$

$$0,735 \leq 1$$

VERIFIED

IV) Shear force

$$V_d \leq 3/4 f_{v,d} \cdot A$$

$$V_d \leq 6,447 \text{ kNm}$$

$f_{v,d} = 2,154 \text{ MPa}$
 VERIFIED - $V_{\max} > 6,447 \text{ kN}$

STATE AFTER 6 YEARS VERIFIED